UNIVERSITY OF LIVERPOOL
School of Environmental Sciences
Electroanalytical laboratory

SPECIATION OF TRACE METALS AND METALLOIDS IN NATURAL WATERS USING THE VIBRATING GOLD MICROWIRE ELECTRODE

Doctoral Thesis

Kristopher Bryant Gibbon-Walsh

Supervisors:

Professor C.M.G van den Berg
Doctor P. Salaun

In loving memory of

Norman Otway Knight Gibbon

(1918 – 2008)

"Beauty is truth, truth beauty

that is all Ye know on earth, and all ye need to know."

- John Keats, Ode to the Grecian Urn.

Ohana means family.

Family means nobody gets left behind, or forgotten.

- Lilo & Stitch

ACKNOWLEDGEMENTS

Firstly I would like to thank my supervisors Professor C. M.G van den Berg and Dr. Pascal Salaün for their patience, support, critique and in the end their friendship. It was the barbeques and lunches that saw me through. I would also like to acknowledge the natural environmental research council (N.E.R.C) for financially supporting this studentship.

Thank you to Paula Houghton, Carmel Pinnington, Anu Thompson, Lindsay Davies and Janet Thistlethwaite for all your help and support.

To Professor John McArthur, the inhabitants of Joypur, Ardevok, and Moyna for access to their wells, Azizul Fakir for assistance with local liaison and Bapi for his driving, translation and friendship.

To Professor Jorge Feldman and Dr. Kalle Uroic for their help with the spectroscopic analysis of groundwater samples

Personally I would like to thank Tom Hawkins, Ian Woollard, Russell Tipping, Loz Blackman, Isa Kristiansen, Peter Deaves and especially Emily Oliver for all your unfailing listening, support and inspiration – I'm incredibly lucky to have you guys.

To my parents Alison Gibbon and Michael Walsh, thank you for always being there for me, it did not go unnoticed and I could not have done this without you. Finally I would like to thank my late Granddad, Norman Gibbon, who always believed in me and supported me no matter what; I hope you are still looking over my shoulder

ABSTRACT

This work reports the use of the vibrating gold microwire electrode, with new methods developed for the speciation of Zn, Cu, Mn and As at natural levels in waters of neutral pH.

Trace metals and metalloids can be distributed as different species in the environment, which can control mobility, toxicity and bioavailability and in turn depends on many complex factors. Analysis of this distribution (speciation) can provide an understanding of the relationship between such elements and their relationship with organisms in marine environments and humans through contaminated drinking water supplies.

Such speciation can be analysed using a vibrating gold microwire electrode (VGME), which is easily prepared and maintained at minimal cost. High sensitivity is found for trace metals: Mn; Cu and Zn; and the metalloid As, resulting from a very low diffusion layer (~0.8 μm for a 5μm gold wire) means that they can be measured at trace levels in natural waters. This combined with the VGME's portability, reliability and stability for long term measurement (repeated measurements over several days) and its capability to distinguish between distinct forms of the above trace elements mean that speciation methods could be successfully developed and validated in natural waters, with no, or minimal sample preparation. Such methods made it possible to analyse speciation on-site, which decreases the potential problems inherent in maintaining sample speciation during storage.

Contamination of groundwater with As is a major health risk through contamination of drinking and irrigation water supplies. In geochemically reducing conditions As is mostly present as As^{III}, which is why a method that uses cathodic stripping voltammetry (CSV) to determine reactive As^{III} was developed. The As^{III} is detected after adsorptive deposition of $As(OH)_3^0$, followed by a potential scan to measure the reduction current from As^{III} to As^0. The method is suitable for waters of pH 7–12. The CSV method was successfully applied to groundwaters from Severn Trent, UK, however speciation using this method is severely hampered by high levels of iron and manganese. Experiments showed that the interference is eliminated by addition of EDTA, making it possible to determine the arsenic speciation on-site by CSV in West Bengal, India.

The VGME is also used to detect nanomolar levels of dissolved Mn by anodic stripping chronopotentiometry (ASC) and sub-nanomolar levels of dissolved Zn by anodic stripping voltammetry (ASV) in neutral pH seawater. The limits of detection for Mn (1.4 nM) and for Zn (0.3 nM) in seawater with a 300 s plating time, are better than achieved using other non-mercury based electrodes and nearly as good as a mercury film electrode for Zn.

Deposition of Mn at the VGME was further utilised to catalyse the reduction of As^V to As^{III}, enabling for the first time the direct electrochemical determination of As^V in natural waters of neutral pH including seawater by ASV using a manganese coated gold microwire electrode. Direct electrochemical determination of As^V in neutral pH waters is impossible due to its electro-inactivity. Therefore Mn is added to excess (~1 μM Mn) to the water leading to a Mn coating during the deposition of As^V on the electrode, when depositing at -1.3 V. The detection limit was 0.2 nM As^V using a deposition time of 180 s.

Speciation of Cu is determined without the need for sample preparation, using scanned stripping techniques for the first time at natural levels in seawater. A desorption potential (-1.2 V) and a conditioning interval between scans make the VGME suitable for on-site and potentially in-situ copper speciation. The resulting pseudopolarograms are analysed using an experimentally constructed 'chelate scale' to determine the strength of copper ligand interactions in real seawater samples.

JOURNAL PUBLICATIONS OCCURING IN THIS THESIS (after only text formatting):

- K. Gibbon-Walsh, P. Salaün, and C.M.G. van den Berg, *Arsenic speciation in natural waters by cathodic stripping voltammetry.* Analytica Chimica Acta, 2010. **662**(1): p. 1-8.
- K. Gibbon-Walsh, P. Salaün, M.K. Uroic, J. Feldmann, J.M. McArthur, C.M.G. van den Berg, *Voltammetric determination of arsenic in high iron and manganese groundwaters*, Talanta, 2011, doi:10.1016/j.talanta.2011.06.038
- K. Gibbon-Walsh, P. Salaün, and C.M.G. van den Berg, *Determination of manganese and zinc in coastal waters by anodic stripping voltammetry with a vibrating gold microwire electrode.* Environmental Chemistry, 2011: Accepted
- K. Gibbon-Walsh, P. Salaün, and C.M.G. van den Berg, *Arsenic speciation on the manganese coated gold microwire electrode.* Analytica Chimica Acta, 2011: Accepted
- K. Gibbon-Walsh, P. Salaün, and C.M.G. van den Berg, *Scanned stripping voltammetry of Cu and Zn at a solid gold vibrated microwire electrode*. 2011: In preparation for Marine Chemistry

JOURNAL PUBLICATIONS TO WHICH I HAVE CONTRIBUTED (not included in this thesis):

- P. Salaün, K. Gibbon-Walsh, and C.M.G. van den Berg, B*eyond the hydrogen wave: new frontier in the detection of trace elements by stripping voltammetry.* Analytical Chemistry, 2011. **83**(10): p. 3848-3856.

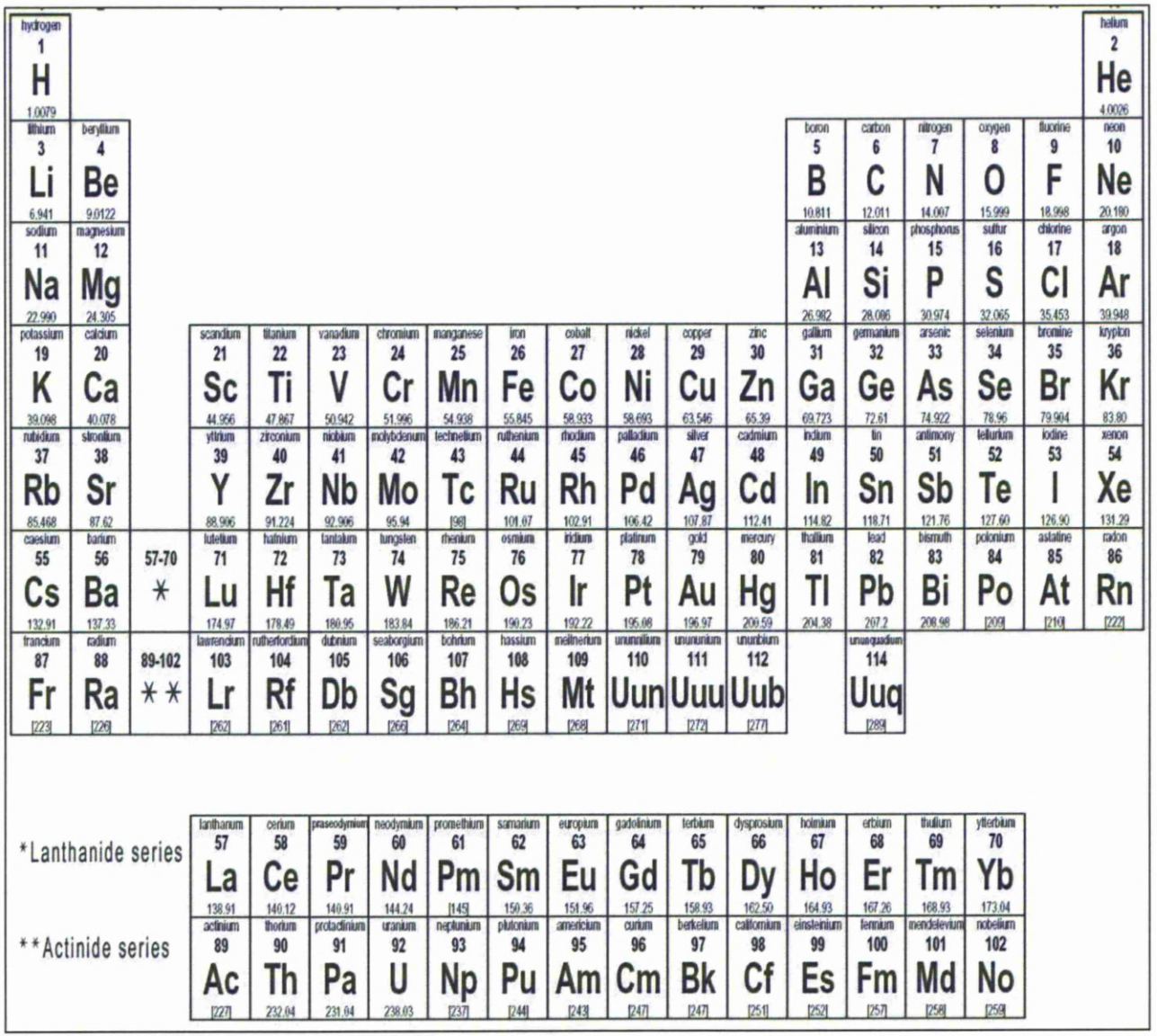
hydrogen 1 H 1.0079
helium 2 He 4.0026
lithium 3 Li 6.941
beryllium 4 Be 9.0122
boron 5 B 10.811
carbon 6 C 12.011
nitrogen 7 N 14.007
oxygen 8 O 15.999
fluorine 9 F 18.998
neon 10 Ne 20.180
sodium 11 Na 22.990
magnesium 12 Mg 24.305
aluminium 13 Al 26.982
silicon 14 Si 28.086
phosphorus 15 P 30.974
sulfur 16 S 32.065
chlorine 17 Cl 35.453
argon 18 Ar 39.948
potassium 19 K 39.098
calcium 20 Ca 40.078
scandium 21 Sc 44.956
titanium 22 Ti 47.867
vanadium 23 V 50.942
chromium 24 Cr 51.996
manganese 25 Mn 54.938
iron 26 Fe 55.845
cobalt 27 Co 58.933
nickel 28 Ni 58.693
copper 29 Cu 63.546
zinc 30 Zn 65.39
gallium 31 Ga 69.723
germanium 32 Ge 72.61
arsenic 33 As 74.922
selenium 34 Se 78.96
bromine 35 Br 79.904
krypton 36 Kr 83.80
rubidium 37 Rb 85.468
strontium 38 Sr 87.62
yttrium 39 Y 88.906
zirconium 40 Zr 91.224
niobium 41 Nb 92.906
molybdenum 42 Mo 95.94
technetium 43 Tc [98]
ruthenium 44 Ru 101.07
rhodium 45 Rh 102.91
palladium 46 Pd 106.42
silver 47 Ag 107.87
cadmium 48 Cd 112.41
indium 49 In 114.82
tin 50 Sn 118.71
antimony 51 Sb 121.76
tellurium 52 Te 127.60
iodine 53 I 126.90
xenon 54 Xe 131.29
caesium 55 Cs 132.91
barium 56 Ba 137.33
57-70 *
lutetium 71 Lu 174.97
hafnium 72 Hf 178.49
tantalum 73 Ta 180.95
tungsten 74 W 183.84
rhenium 75 Re 186.21
osmium 76 Os 190.23
iridium 77 Ir 192.22
platinum 78 Pt 195.08
gold 79 Au 196.97
mercury 80 Hg 200.59
thallium 81 Tl 204.38
lead 82 Pb 207.2
bismuth 83 Bi 208.98
polonium 84 Po [209]
astatine 85 At [210]
radon 86 Rn [222]
francium 87 Fr [223]
radium 88 Ra
89-102 **
lawrencium 103 Lr [262]
rutherfordium 104 Rf [261]
dubnium 105 Db [262]
seaborgium 106 Sg [266]
bohrium 107 Bh [264]
hassium 108 Hs [265]
meitnerium 109 Mt [268]
ununnilium 110 Uun [271]
unununium 111 Uuu [272]
ununbium 112 Uub [277]
ununquadium 114 Uuq [289]
*Lanthanide series
lanthanum 57 La 138.91
cerium 58 Ce 140.12
praseodymium 59 Pr 140.91
neodymium 60 Nd 144.24
promethium 61 Pm [145]
samarium 62 Sm 150.36
europium 63 Eu 151.96
gadolinium 64 Gd 157.25
terbium 65 Tb 158.93
dysprosium 66 Dy 162.50
holmium 67 Ho 164.93
erbium 68 Er 167.26
thulium 69 Tm 168.93
ytterbium 70 Yb 173.04
**Actinide series
actinium 89 Ac [227]
thorium 90 Th 232.04
protactinium 91 Pa 231.04
uranium 92 U 238.03
neptunium 93 Np [237]
plutonium 94 Pu [244]
americium 95 Am [243]
curium 96 Cm [247]
berkelium 97 Bk [247]
californium 98 Cf [251]
einsteinium 99 Es [252]
fermium 100 Fm [257]
mendelevium 101 Md [258]
nobelium 102 No [259]

Acronyms

AAS	Atomic Absorption Spectroscopy
AE	Auxiliary electrode
ASV	Anodic Stripping Voltammetry
CSV	Cathodic stripping voltammetry
CLE-AdSV	competing ligand exchange-adsorptive stripping voltammetry
DET	Diffusive equilibrium in thin films
DGT	Diffusive gradients in thin films
DMT	Donnan membrane technique
EDTA	Ethylenediaminetetraacetic acid
HEPES	4-(2-Hydroxyethyl)piperazine-1-ethanesulfonic acid
HMDE	Hanging mercury drop electrode
ICP-MS	Inductively coupled plasma mass spectroscopy
ISE	Ion selective electrode
GC	Gas chromatography
GF-AAS	Graphite furnace atomic absorption spectroscopy
GIME	Gel-integrated microelectrode
L	Ligand
LC	Liquid chromatography
LoD	Limit of detection
LS	Linear sweep
M	Metal
ML	Metal ligand complex
MQ	Milli-Q water
PLM	Permeation liquid membrane
RE	Reference electrode
SC	Stripping chronoamperometry
SEM	Scanning electron microscope
SSV	Scanned stripping voltammetry
SSC	Scanned stripping chronoamperometry
SW	Square wave
UV-SW	Ultraviolet digested seawater
VGME	Vibrating gold microwire electrode
WE	Working electrode
WHO	World health organisation

δ	Diffusion layer
σ	Standard deviation

Subscripts

R	reactive fraction concentration
Inorg	inorganic fraction concentration
T	total concentration
acc / dep	accumulation / deposition
des	desorption
equ	equilibrium

Mathemetical symbols

A	Surface area
C	concentration
D	Diffusion coefficient
E	Potential (volts)
F	Faraday constant
i	Current
i_d	Diffusion limited current
J	Flux
K*	Thermodynamic stability constant
M	Molarity (moles/ Litre)
t	time
V	Volume
V	Hydrodynamic velocity

m	milli (10^{-3})
µ	micro (10^{-6})
n	nano (10^{-9})
p	pico (10^{-12})
ppb	parts per billion
ppm	parts per million

CONTENTS

MOTIVATIONS

Mercury has been and continues to be the electrode material of choice in many electroanalytical laboratories due to its inherent advantages in terms of reproducibility and its large analytical range resulting from its high hydrogen over-potential. However, its use is subject to controversy caused by its high toxicity and so its routine use is limited to well trained experimenters in laboratory conditions.

Solid electrodes are an alternative for trace metal and organic analysis and have a number of important advantages, including less exposure to mercury, but also its application to on-site and/or in-situ analysis. On-site and in-situ in this context means measurements carried out at the sampling site or directly in the water column respectively. This work aims to continue the development of stripping techniques on the vibrating gold microwire electrode (VGME) for the detection and speciation of trace metals and metalloids in natural waters, with a view to exploiting such advantages. The VGME simply refers to a gold microwire (here defined as a wire with diameter ≤ 25 µm) used in connection with a vibrating device, such as those encountered in mobile phones. The vibrator is attached to the electrode which itself vibrates while the solution remains stagnant, in contrast to more usual stirring methods (the solution is stirred while the electrode is stagnant).

The sensitivity of stripping techniques on the VGME and its easy preparation and maintenance mean that it can be applied for trace metal speciation at natural levels in real systems with as little alteration of the sample as possible. This goal has significant advantages, not least the applicability of such methods for future in-situ analysis. The electroanalytical methods detailed in this thesis are developed at natural pH, with no or minimal reagent additions, to preserve as much as possible the original speciation.

Specifically this thesis presents the development, optimisation and validation of electroanalytical methods using the VGME for:

1) The speciation of arsenic in freshwater; this is particularly important when considering human impact and removal technologies which are highly dependent on the chemical forms;
2) The speciation and detection of metals and metalloids in seawater at trace levels. These include micronutrients such as Cu, Mn, Zn and toxic species such as As and Sb or again Cu depending on its concentration levels and chemical speciation.

All developed methods have been validated in real samples and for each method, a wide range of potential interferences have been assessed. Experimental problems facing solid electrodes, such as stability, reproducibility and surface fouling are also addressed. The limitation of such complications is crucial if such electrodes are to be used successfully for long term monitoring and in-situ analysis.

1

Chapter 1
AN INTRODUCTION

1. INTRODUCTION

1.1. Trace metals in natural waters

As their name suggests, trace metals generally occur at low levels (nanomolar (nM) and sub nM) in natural waters. However this is not always the case, in fresh water there are many examples of trace metals occurring at much higher levels (micromolar (μM) /milimolar (mM)), well exceeding common levels either through natural [1], or anthropogenic inputs [2]. Depending on the metal this can lead to a large burden on the environment and the capability of the ecosystem or human population to cope with such elevated levels. Hence the importance of accurate and reliable monitoring of trace metals in these environments to clarify the extent and nature of the pollution and thus improve strategies for remediation and mitigation [3]. In this thesis, As speciation in the groundwaters of West Bengal (India) is investigated using methods developed on the VGME.

Methods are also developed on the VGME for the speciation of Mn, Zn, As and Cu in seawater, where total trace metal distributions are well documented and are in the order of nM or less in the open ocean [4, 5]. Trace metals occur in marine environments through a combination of riverine, benthic and atmospheric inputs [6]. In aquatic environments Mn, Zn and Cu act as micronutrients which are essential for biological processes, and so deficiencies of these metals may limit the oceanic plankton production [7]. In contrast, As is non-essential, having no known biological importance, but can be toxic to marine phytoplankton, marine invertebrates and fish [8]. Varying forms of these metals in the complex seawater substrate means metal-ligand interactions create a more complicated scenario, because distinct chemical forms of a metal may assume very distinct roles in terms of mobility, potential bioavailability and toxicity [9]. Thus, to fully assess the physiochemical behaviour of a sample and therefore its potential effect on the environment, these individual species must be distinguished and ideally individually identified by some considered measurement. [10].

1.1.1. Speciation of trace metals in seawater

Speciation describes the distribution of an element over its physicochemical forms. This includes redox speciation which relates to an element's oxidation state, for example arsenic can vary between the oxidation states of +V, +III, 0 and –III [11]. Equation (1) shows a redox equilibrium between arsenite (As^{III}) and arsenate (As^{V}) in solution, the balance of such an equilibrium being dependent on the solution's pH and Eh.

$$As^{III}(OH)_3^{0}(aq) + 2e^- \rightleftharpoons HAs^{V}O_4^{2-}(aq) \quad (1)$$

Trace metal speciation also includes various metal-ligand complexes (ML)[10] between a metal (M) and a ligand (L). Equation (2) describes such an equilibrium between a hydrated copper ion and an unknown L in solution. The affinity of L for Cu will define the balance of the equilibrium, i.e. if Cu has a high affinity for L then the equilibrium will thermodynamically favour CuL (aq), whereas if there is a weak affinity then Cu^{2+}(aq) would be favoured. Importantly there is also a kinetic consideration, taking into account the rates of both association and dissociation of the complex.

$$Cu^{2+}(aq) + L(aq) \rightleftharpoons CuL(aq) \quad (2)$$

Natural waters such as lake or sea water are chemically heterogeneous containing many chemical constituents (figure 1) and creating a very complex matrix with many different ligands [12]. A wide variety of metal species exist within a natural system, all with differing mobility, bioavailability and resulting toxicity. The identification of each of them is simply not feasible. Instead, separation of different classes of these metal species can be made based on their physico-chemical behaviour, e.g. oxidation state, kinetic rates, diffusion rate or size. The speciation of a metal affects its behaviour, (although recent studies of the bioactive metals Cu [13] and Ni [14] have shown the potentially important role of hydrophobic, neutral complexes) the bioavailability of a metal is generally greatly increased when the metal occurs in the free ionic form[15] and greatly reduced when complexed to strong ligands [16]. Such ligands can be produced by phytoplankton [17] as a possible defence mechanism to reduce associated toxicity by reducing the potential bioavailability and thus potential

toxicity of specific metal [18]. Therefore complexation by natural (Humic acids, Fulvic acids) ligands may buffer the system with respect to the bioactivity of a given metal [19].

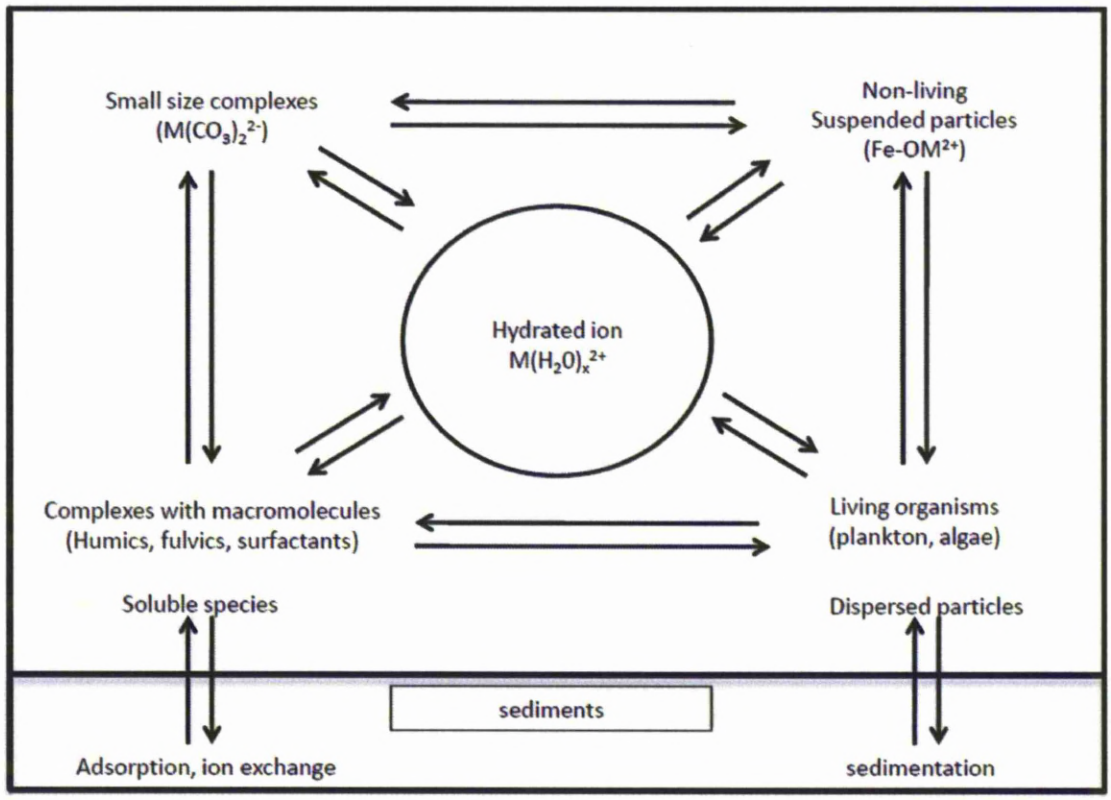

Figure 1. Schematic representation of the reactions of a metal ion, M, with different types of aquatic system constituents [20].

1.1.1.1 Biogenic trace metals (Cu, Zn and Mn) in seawater

The biogenic trace metals, Cu, Zn and Mn, are essential micronutrients, serving as cofactors in a number of enzymes important for algal physiology [6]. The speciation of these trace metals in seawater is characterised by the +II oxidation state and substantial involvement in organic complexation [9].

Cu exists mainly as Cu^{II}, but can also exist as the chloride complexed Cu^{I} in surface waters [21]. Cu^{II} is very strongly complexed with up to 99 % bound to organic matter [22, 23] and this is important as Cu bioavailability and toxicity is related to its free metal ion concentration and the potentially labile

complexes [24]. In seawater, dissolved copper plays the role of both a micronutrient (required for optimal growth) and a toxicant (impeding growth) to phytoplankton and other microorganisms depending on its concentration [25]. At high Cu concentrations (below the 10 nM typically found in seawater [26]), this crucial component of respiratory proteins and oxidases can cause reduction in cell division rates for phytoplankton [27, 28]. Cu toxicity is also dependent on the microorganism, with cyanobacteria being especially sensitive [29].

Zn exists dominantly as Zn^{II} and like Cu, is also strongly complexed by organic matter [9] as even in the open ocean organically bound Zn accounts for 98 % of the total metal concentration [30]. Zn is a cofactor for many important enzymic processes required for bacteria and phytoplankton in the ocean[31] and also crucial in nutrient uptake mechanisms for CO_2 [32] and phosphate [33]. Like Cu, at high concentrations Zn is toxic to phytoplankton [34] and bacteria [35], but at near ambient seawater concentrations Zn can be biolimiting for phytoplankton growth [34, 36], again depending on the free metal ion and potentially labile complex concentration [37].The toxicity of both Cu and Zn in seawater has been related to possible antagonisms with Mn nutrition [38, 39].

Mn exists in the ocean principally in two redox states: the weakly complexed Mn^{II} [40] (mainly as the free hydrated Mn^{2+}) and as Mn^{IV} (as the highly insoluble $MnO_2(s)$). Thus for Mn, its redox state has a big effect on its dissolved distribution in seawater and this is in turn significant for other elements through the role of $MnO_2(s)$ as a site of metal sorption and co-precipitation [9]. Mn is a very important micronutrient, occurring as a cofactor in the enzyme responsible for the oxidation of water to O_2 during photosynthesis [41]. Thermodynamically, an oxygenated ocean at a pH of 8 should lead to the insoluble Mn^{IV} species, however dissolved Mn ocean profiles reveal that the surface waters contain high levels of soluble Mn^{II}. A portion of the soluble Mn is from direct dissolution of dust which contains Mn in its +II oxidation state [42], where slow oxidation to the +IV state allows Mn to stay dissolved in the order of days. However, Mn should still oxidize over time and precipitate out of the surface ocean [6]. This oxidation is prevented by photo-reduction of Mn to

the soluble +II state in the presence of organic material [43], resulting in a large concentration of Mn in the surface water which is available for biological use.

1.1.1.2 Non essential, toxic trace metals (As) in seawater

In seawater As occurs predominately in its +V oxidation state as the thermodynamically stable $HAsO_4^{2-}$, but in the upper water column it can also exist as arsenite in the form $As(OH)_3^0$. The $HAsO_4^{2-}$ anion closely resembles the corresponding species formed by phosphorus, HPO_4^{2-}, which unlike As is an important nutrient [44]. It is this similarity that makes it difficult for organisms to distinguish between them and is thought to be one of the reasons for arsenics toxicity to phytoplankton [45]. However, the presence of arsenite at high arsenic/phosphate ratios in surface waters suggests that the reduction of As^V is due to arsenic detoxification by plankton [46]. Organisms also mediate the methylation of arsenate giving the organic species methylarsonate (MMA) and dimethylarsinate (DMA) [47], which are found to generally contribute only a minor fraction (nM levels) [48]. More refractory organic As fractions have also been found in estuarine waters [49].

1.1.2. Occurrence and speciation of As in groundwaters, West Bengal, India

Arsenic is ubiquitous within the environment and as well as occurring in seawater it can also be mobilised to groundwater via several mechanisms, which depend on local environmental conditions [50]. Long term exposure to arsenic in drinking water has been identified as a cause of skin legions [51] as well as large numbers of bladder, lung, kidney and skin cancers [52]. Increased awareness of the potential risks of chronic exposure to As through ingestion has meant the national Indian drinking water limit, which has remained at 50 parts per billion ((ppb) or approximately 0.7μM) of As has now been deemed unsafe by the world health organisation (WHO). Consequentially a provisional guideline value of 10 ppb (0.13μM) has been advised for As in drinking water since 1993 [53], however to date, only 1st world countries have lowered their drink water limits for As due to the cost and current impracticality of their rigorous implementation (to the detriment of human health of an already burdened population) in poorer countries, such as India and Bangladesh [54].

Though As pollution is a truly global problem [54], the most documented case (due to the population affected) is in the ground waters of large areas of West Bengal and Bangladesh [55] which are heavily enriched with As, mobilised through the reductive dissolution from iron oxyhydroxides (FeOOH) under reducing conditions [56]. These conditions are driven by the decomposition of organic matter also present [57] with the resulting As pollution having been described by WHO as 'the largest poisoning of a population in history' [58].

In this region, tube wells were installed with intentions to give communities access to clean drinking water, thus reducing diarrhoea and infant mortality associated with polluted surface water [59]. One of the biggest difficulties regarding mitigation is the complex spatial variation of As concentrations across the region [59] (locally controlled by paleosols [60] and other geochemical factors [61]), combined with the sheer number of shallow tube wells [62]. The most popular, practical and economic mitigation solution has been to dig deeper wells [54], where water is known to be less contaminated by As, however recently doubts have been cast on such an approach due to leaching of arsenic into deeper aquifers [63]. Hence there remains an urgent need for the arsenic-contaminated wells, both shallow (15-50 m) and deep (>100 m), to be identified as soon as possible and for appropriate action to be taken [64], with rapid, accurate and reliable monitoring being one of the main goals of the mitigation strategies [3].

Speciation is no longer thought to be an important factor for human health in chronic dosage by direct ingestion (unlike acute dosage), as it is now widely reported that inorganic pentavalent arsenate is mostly reduced to trivalent arsenite in the blood stream before entering the cells and being further metabolised [65]. However it is still essential to determine the speciation of arsenic in groundwater for:

i. remediation purposes and implementation of the most adapted arsenic removal technologies which rely on this information [66];

ii. to better understand and predict arsenic biouptake and potential bioaccumulation in plants such as rice [67], consumption of which risks human health [68];

iii. better understanding of the mobility of arsenic in the groundwater system, allowing for improvement of predictions regarding its occurrence in space and time.

1.2. Analytical methods for the speciation of trace metals in natural waters

Speciation of trace metals is more challenging than the determination of total metal content due to

- Difficulties in isolating the compounds of interest from complex matrices;
- Difficulties in interpretation of the signal which is the resultant of a variety of different species with different diffusion co-efficents;
- Speciation techniques disturbing the equilibria between various chemical species;
- Few analytical procedures existing with the necessary sensitivity for ultra-trace level speciation (sub or low nM levels);
- Many analytical procedures necessitate the alteration of the original speciation (e.g. spectroscopic techniques such as atomic absorption spectroscopy (AAS), inductively coupled plasma-mass spectrometry (ICP-MS));
- The varied matrix affecting the choice of technique [9].

As the chemistry of trace metal species is diverse, so consequently are the separation and detection methods used. The main criteria for choosing the appropriate methodology are the stability of the species and the nature and complexity of the environmental sample. Since most species are not thermodynamically stable, but only kinetically stabilised the analysis time becomes a significant parameter for the determination of the complex species [69].

Trace metals are determined by fairly robust analytical methodologies that may involve extraction and chromatography. The timescale of these separation methods must be substantially smaller than the half-life of the species in the new chemical environment encountered during the separation and

sample preparation steps. However the speciation analysis of transition metals such as copper (which form relatively fast-equilibrating complexes with inorganic or natural organic ligands) requires faster separation and detection systems. This means that the technique measurement time (separation + analysis time) must be in accordance with the dissociation kinetics of the complex under scrutiny [69]. Figure 2 summarises the applicability and the retrievable information about a species of some important analytical techniques for the detection of trace metals. Figure 2 shows that electrochemical detection with a measurement time of milliseconds, rather than minutes is the preferred technique for fast equilibrating species.

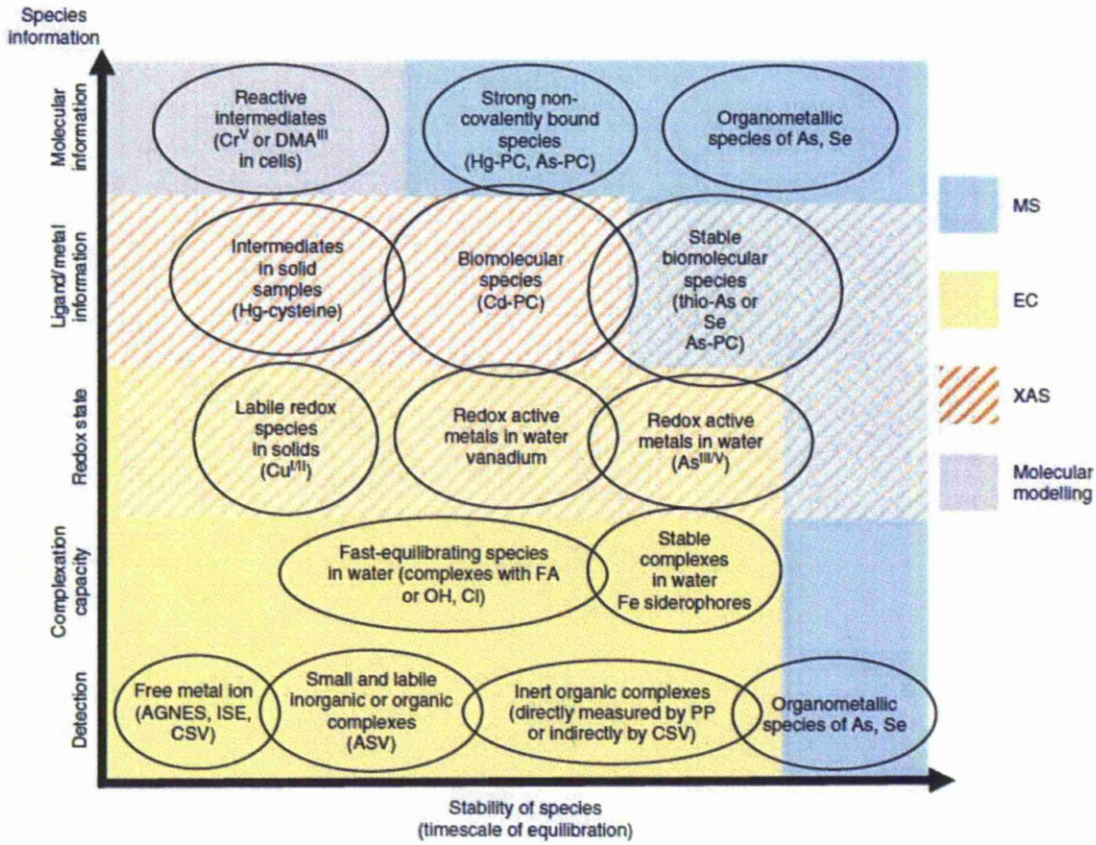

Figure 2. The applicability analytical techniques; mass spectrometry (MS); X-ray absorption spectrometry (XAS); electrochemical (EC) to different types of elemental species in dependence of their stability [69].

Difficulty in the determination of the biologically important free metal ion in environmental samples (due to very low concentrations and of the presence of interferences) means that there are a limited number of methods with the required selectivity and detection limit required.

It should also be noted that, the development of highly sensitive and partially specific analytical techniques occurred in tandem with the equally important advances made in using clean techniques in water sample collection and in sample processing during analysis [6]. The cleaning procedures for sampling used during this thesis are presented in annex V.

1.2.1 Spectroscopic methods

The development of elemental speciation analysis started in the early 1980s with the introduction of methodologies based on the hyphenation of different chromatographic techniques to several kinds of elemental detectors [70]. Spectroscopic techniques such as graphite furnace atomic absorption spectroscopy (GF-AAS), inductively coupled plasma mass spectroscopy (ICP-MS) and neutron activation analysis (NAA) have very low detection limits and have been widely used for the determination of total concentrations of trace metals [71, 72]. For speciation to be achieved separation techniques must be incorporated prior to detection; commonly chromatographic methods such as high performance liquid chromatography (HPLC) and gas chromatography (GC) are used. The application of such hyphenated techniques, HPLC and GC with ICP-MS [69, 73] and X-ray absorption spectroscopy [69], have recently been reviewed within the context of trace metal speciation in environmental samples, including natural waters. There are also important non-chromatographic spectrometric methods for speciation analysis, which rely on extraction or derivatization and have also been extensively reviewed [74]. For arsenic, separation of redox species can be made with hydride generation [75] by altering the sample pH.

These techniques are very powerful tools for the speciation of several important trace metals, with capability for multi-element analysis. However, several considerations should be made when choosing the most appropriate technique, such as timescale of the complex and the type of matrix

[69]. For example in seawater the large chloride interference means that a reaction cell becomes necessary when using the ICP-MS [76].

However, speciation measurements made after separation and extraction procedures significantly increase the risk of contaminations or chemical species modification during sample storage or sample handling and dramatically increase the cost of analyses. This is a major barrier for application of routine speciation measurements on large sample sets [77]. More detailed descriptions of the applications of these laboratory based techniques and their limitations can be found in the literature [9, 69, 78-81] and references therein.

The information gathered about trace metal speciation by spectrometric techniques can be complimentary to that derived by other methods [69], such as the electrochemical ones developed and applied as part of this thesis.

1.2.2 Dynamic versus equilibrium methods

Table 1 summarises the kinetic features of selected dynamic sensors and the characteristics of some equilibrium-based sensors. Such techniques have an important advantage over spectroscopic ones, in their potential application to in-situ measurement [80].

Dynamic techniques are based on detection of metal fluxes i.e. metal accumulated over a given period. When accumulation (uptake) proceeds at a sensor, a gradient of concentration is created within a so-called diffusion layer (δ) (Figure 3). The size of this δ is dependent on the rate of uptake by the sensor and on the hydrodynamic conditions at its surface. When the uptake is very fast (high consumption at the sensor), the metal concentration at the surface of the sensor ($[M]_{x=0}$) is zero. The gradient of concentration at the surface of the electrode is given by $([M]_{x=\delta} - [M]_{x=0})/\delta$, where δ is the size of the diffusion layer and $[M]_{x=\delta}$ equals the metal bulk concentration C^b. The diffusion time is the time required to diffuse through this δ. The latter can be present at the surface of the working electrode (voltammetry), at the surface of the complexing resin (DGT: Diffusive Gradient in thin

Films), or at the surface of the organic impregnated membrane on the source solution side (PLM: Permeation Liquid Membrane). The accumulation time is the time, over which the metal ion is accumulated at the sensor, e.g. at the mercury microelectrodes for the gel-integrated microelectrode (GIME); at the resin (DGT); or at the receiving/ strip solutions (DMT: Donnan Membrane Technique, PLM). The signal resulting from the accumulation step represents an integration of all fluctuations in the test medium and thus provides an average value for this time period [82].

In contrast, equilibrium methods enable the measurement of equilibrium concentrations of solutes if left in place for sufficient time, as dissolved constituents diffuse across the interface until the sampling medium has the same composition as the external waters [91]. The diffusive equilibrium in thin films (DET) and DMT fractionate species by size/charge (using a porous membrane) rather than lability as equilibrium is reached. Ion selective electrodes (ISE) partition the test ion between an ionic hydrophobic liquid or membrane and the test solution; competing ligand exchange-adsorptive stripping voltammetry (CLE-AdSV) involves an exchange reaction in the bulk test solution with an added ligand [80]; and AGNES (Absence of Gradients and Nernstian Equilibrium Stripping) partition the test ion between the solution and the mercury electrodes upon application of a well defined accumulation potential.

The dynamic factors of non-equilibrium methods must be understood for the correct interpretation of the analytical data. For most techniques the analytical signal corresponds to the free metal ion concentration. This concentration is dictated by the metal complexes lability, which indicates the contribution to this concentration from the metal complexes involved in a surface reaction. The overall flux of metal to the analytical interface results from the coupled diffusion and inter-conversion rate between M and its various complexes in the diffusion layer [82], summarised in figure 3.

Table 1. Modified summary of the important characteristics of dynamic and equilibrium methods [82] and important references.

Method	Physiochemical basis	Characteristic diffusion length	Species measured	Analysis time (s)	Ref
Dynamic techniques					
Voltammetries + chronoamperometries	Diffusion in test medium	Macroelectrode, δ_s (10^{-5} m)	Free metal + dynamic complexes	10^2-10^3	[83]
		Microelectrode, r_0 (10^{-6} m)			[84, 85]
		Vibrating microwire, δ_s (10^{-6} m)		10^1-10^3	[48]
Pseudopolarography/ scanned stripping techniques	Diffusion in test medium	Microelectrode, r_0 (10^{-6} m)	Free metal + dynamic complexes + reducible complexes	10^3-10^4	[86]
GIME	Radial diffusion in gel	Microelectrode, r_0 (1-3 x 10^{-4} m)	Free metal + dynamic penetrating complexes	10^2-10^3	[87]
DGT	Planar diffusion in gel	Gel layer thickness, δ_g (0.4-2 x 10^{-3} m)	Free metal + dynamic penetrating complexes	10^3-10^4	[88]
PLM	Planar diffusion in sample and membrane	Diffusion layer thickness, δ_s (1-10 x 10^{-5} m)	Free metal +dynamic complexes	10^3-10^4	[89]
		Membrane thickness, δ_m (1-10 x 10^{-5} m)	Free metal ion		
Equilibrium techniques					
ISE	Equilibrium or steady-state membrane potential	Na	Free metal ion	1 to 10	[90]
DET	Equilibrium gel	Na	All penetrating species	10^5	[91]
PLM	Equilibrium source/acceptor	Na	Free metal ion	10^4	[89]
DMT	Equilibrium source/acceptor	Na	Free metal +part of cationic penetrating complexes	10^5	[92]
CLE-AdSV	Equilibrium with ML_{ad} in sample	Na	Free metal + complexes weaker then ML_{ad}	10^2-10^3	[93]

Inert complexes represent a simpler case: they dissociate so slowly that they do not contribute significantly to the flux (although this is not the case for scanned stripping techniques, where the inert complexes themselves may in some cases be reduced if the deposition potential is low enough [94]). On the contrary, labile metal complexes are characterized by a frequent inter-conversion between the free metal and the complex during their transport through the diffusion layer, leading to a contribution to the resulting measured current, due to this dissociation [82]. Since lability changes drastically with time and spatial scales (both related through the diffusion coefficient), each type of non-equilibrium techniques for speciation analysis has its own characteristic kinetic window, and accordingly measures a dynamic fraction of metal species.

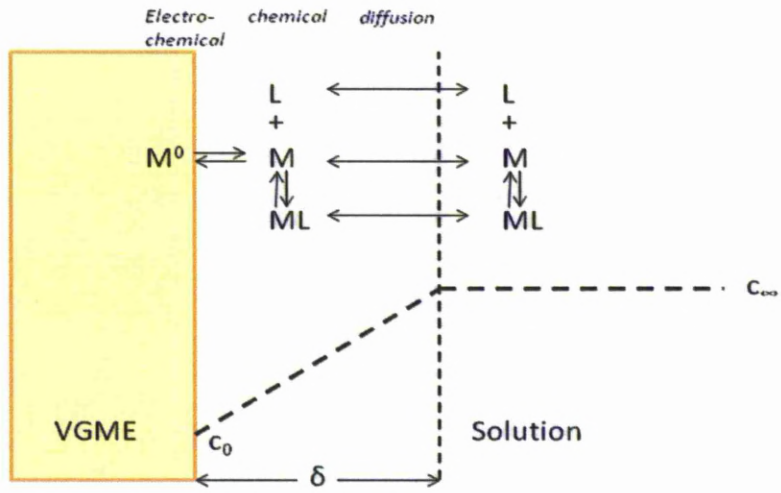

Figure 3. Diffusion layer (concentration gradient at VGME) and processes of a metal (M),ligand (L) and ML influencing voltammetric current [78, 95].

Dynamic and equilibrium methods have been reviewed [80, 82] and give different information about the complexation of trace metals in solution [82]. Collaborative approaches could allow greater understanding of the predictive relationships between the speciation of an element and its potential bioavailability [82]. The current suite of analytical techniques, spanning a range of kinetic windows, and the generic dynamic framework for interpretation of their signals lays the foundations for a sophisticated quantitative approach to metal speciation and bioavailability.

1.2.3 Electroanalytical stripping techniques for trace metal speciation in natural waters

There are two types of stripping technique that can be used for trace metal analysis: voltammetric and chronopotentiometric. Voltammetric techniques are based on the recording of the current, *i*, which flows between the working electrode (WE) and an auxiliary electrode (AE), due to the reduction or oxidation of the metal, as a function of the potential (E) imposed on the WE and expressed with respect to that of a reference electrode (RE). In chronopotentiometry, $E=f(t)$ curves are recorded under a controlled current (i) [96]. In both cases the current is a flux (of electrons) and depends on dynamic processes in a solution, which contains the solvent (water), an electrolyte and the metal that will undergo the redox reaction at the electrode surface [78].

The electrolyte concentration must be sufficient as the current flows in solution though ion transport. This is one of the advantages of electroanalytical techniques over spectroscopic techniques such as ICP-MS, which cannot be used without dilution or analyte extraction [97] in saline samples. Whereas voltammetric analysis can be applied, where high salinity in the solution may be seen as an advantage, in serving the role of a natural electrolyte [98] reducing problems of migration. Although this is mostly irrelevant for microelectrodes.

1.3. Electrochemical principles

General principles of voltammetric and chronoamperometric techniques have been detailed previously [78, 94-96] and so in this section, only the principles relevant to the VGME, within the context of this thesis are discussed.

1.3.1 Electrode processes

Electrode processes are heterogeneous and take place at the interfacial region between electrode and solution [95]. The majority of the examples dealt with in this thesis involve stripping techniques,

where a metal is first reduced and then accumulated at the surface of the electrode during the so-called deposition step, with a set potential, as shown for Cu^{II} in equation (3).

$$Cu^{2+}(aq) + 2e^{-}(electrode) \longrightarrow Cu^{0}(electrode) \quad (3)$$

For this reduction to occur there is a minimum energy that the transferable electrons from the electrode must have, this corresponds to a sufficiently negative deposition potential (E_{dep}). Then assuming that the electron transfer is not limiting the flux of species, J (mol cm^{-2} s^{-1}), to the electrode can be described by the Nernst-Planck equation (Equation (4)) [99]:

$$J(x,t) = -D\frac{\partial C(x,t)}{\partial x} - \frac{zFDC}{RT}\frac{\partial \phi(x,t)}{\partial x} + C(x,t)V(x,t) \quad (4)$$

where D is the diffusion coefficient (cm^2 s^{-1}), C is the concentration (mol cm^{-3}), F is the Faraday constant (96,500 C mol^{-1}), x the distance from the electrode (cm), ϕ the potential (V), z the charge of the metal, t time (s) and V (x, t) the hydrodynamic velocity (in the x direction). The first, second and third term of equation (4) represents the diffusion (gradient of concentration), migration (gradient of potential) and convection components of the flux (J), respectively. Under normal conditions, the migration current is diminished by the presence or additions of an electrolyte that suppress the migration field at the surface of the electrode. Figure 3 shows the diffusion layer (δ), whose size is dependent on the species (diffusion coefficient); on the hydrodynamic conditions at the vicinity of the electrode surface; and on the density (kinematic viscosity) of the media. To achieve a high diffusion flux (or diffusion current), the diffusion layer should be as small as possible as indicated by equation (5) which correlates the flux (or current) to the diffusion layer size for a technique within steady state conditions.

$$i_d = nFAJ = \frac{nFAD(C^b - C^0)}{\delta} \quad (5)$$

where i_d is the diffusion current (A), J is the diffusion flux (mol cm^{-2} s^{-1}), C^b and C^0 are the concentration in the bulk and at the surface of the electrode respectively (mol cm^{-3}) and δ is the diffusion layer size (cm). When the deposition potential is made sufficiently negative, $C^0 = 0$ and i_d

corresponds to the diffusion limited current. There are many ways to decrease the size of the diffusion layer: efficient stirring of the solution, rotation of the electrode (rotating disc electrode RDE), use of ultrasound, heating of the solution, fall of mercury (dropping mercury electrode) or by vibrating the electrode (as with the VGME).

1.1.1.3 Stripping analysis

Stripping analysis is a general term that encompasses a family of electroanalytical techniques that pre-concentrate the analyte on the surface of the working electrode prior to its detection. This accumulation step is responsible for its high sensitivity compared to direct reduction/oxidation methods [100].

Because of this accumulation step and the use of pulsed voltammetric techniques (such as square wave and differential pulse), extremely low detection limits (10^{-10}–10^{-12} M) can be achieved. The methods are usually multi-elemental, are powerful tools for speciation studies at natural levels and are in addition suitable for on-site and in situ applications [77].

Stripping methods are sufficiently sensitive for trace metal analysis in natural waters including seawater [78]. The metal is accumulated at the surface of the working electrode (WE) during the deposition step and followed by a measurement, made by 'stripping' the metal off. In anodic stripping voltammetry (ASV) and stripping chronopotentiomentry (SC) the metal is reduced during the deposition step and oxidised during the stripping step [96]. Different voltammetric modes exist, as E is varied with time (t) by using different wave forms [77]. Linear sweep (Chapter 2), square wave (Chapter 3 -6) and stripping chronoampotentiometry (Chapter 4) are all applied to the VGME in this thesis, where their relevance depends on the metal, matrix studied and interferences.

1.1.1.4 Scanned stripping techniques

Scanned stripping techniques (formally known as pseudopolarography on mercury-based electrodes [101]) are used to gain speciation information about the strength of ML complexes in natural waters.

Waves are generated through a series of independent ASV experiments at increasingly negative potentials [86]. From these scanned stripping voltammograms (SSV), half wave potentials ($E_{1/2}$) and limiting currents are extracted. A typical scanned stripping voltammogram will display one or more sigmoidally shaped waves. The most anodic wave usually corresponds to the free + labile complexes (often considered as inorganic or small organic complexes). More cathodic waves represent the direct reduction of the inert complexes (ML) itself. The fundamental difference between the labile wave and the inert wave is that no dissociation of the metal prior to its reduction is required in the latter case. The position and shape of each of these waves is dependent upon the binding strength of the ML complex and upon the reversibility of the chemical and electron transfer processes at the electrode [94]. Such data is shown for the HMDE in figure 4A, with $E_{1/2}$ shifting to more negative potentials with stronger metal-ligand interactions.

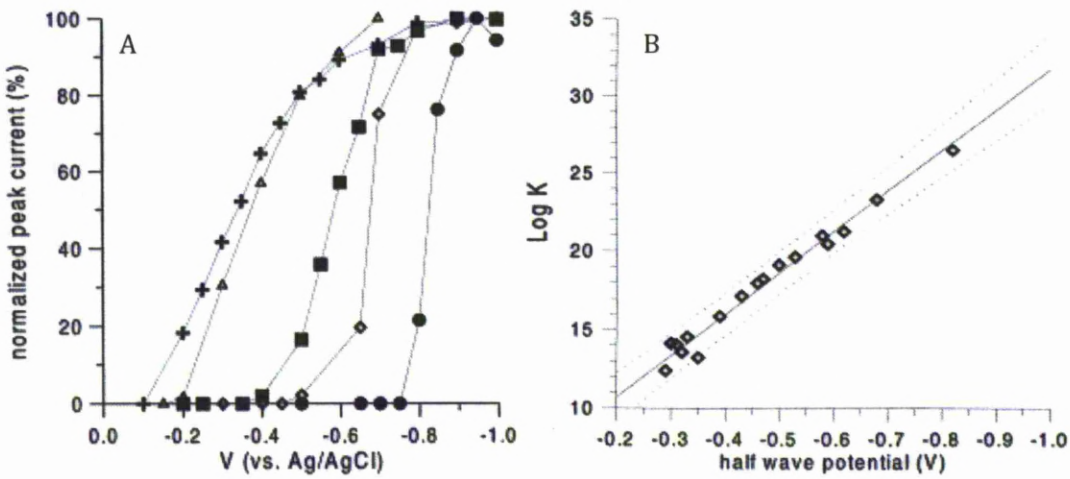

Figure 4. A) Pseudopolarograms of Cu(II) amine complexes. (circles) Cyclam; (diamonds) cyclen; (squares) trien; (triangles) cyclododecane; (crosses) cyclononane. The shift in $E_{1/2}$ corresponds to the strength of the M-L complex **B)** Plot of thermodynamic stability constants (log K^*_i) vs. half-wave potentials ($E_{1/2}'$) for the complexation of Cu(II) in seawater with selected organic ligands at pH≈8.0 [102].

This data can be used to determine thermodynamic stability constants for classes of ligand in real water samples from an empirical model ligand data scale (known as the "chelate scale"), an example of which is shown in figure 4B [19, 102].

The development of scanned stripping techniques on the VGME is described in chapters 6 for Cu^{II} complexes in seawater. The VGME has one of the lowest diffusion layer thickness (< 1 μM for a 5 μm gold wire) ensuring a high diffusion flux and low detection limit. This enabled us to use SSV for Cu (and to a lesser extent Zn) speciation studies in sea water samples at the natural levels encountered in Liverpool Bay. This is the first time a solid electrode (non-mercury) has been used for such application and this has only been possible due to the high stability and reproducibility of the VGME measurement.

1.3.2 Solid electrodes

The ideal working electrode should offer effective pre-concentration, a thermodynamically possible redox reaction of the target metal, reproducible and renewable surface, and a low background current over a wide potential range [78]. The choice of electrode material is dependent on its potential window, shown in figure 5 for Silver (Ag), gold (Au), carbon (C) and mercury (Hg) electrodes. This window is limited on the negative side by the reduction current of cations from the electrolyte (e.g. sodium (Na^+)) or water (to H^+/H_2O) and on the positive potential side by the oxidation of the electrode material itself [78].

Historically Hg has been the electrode material of choice, as it possesses a very high over-potential for hydrogen evolution in aqueous solution [95] meaning it has a large negative potential window combined with a low capacitive current. The hanging mercury drop electrode (HMDE) has a mechanical regeneration of the electrode surface between scans and thus a reproducible surface and a reproducible area [95] with no memory effects, i.e. the last measurement does not affect the next one. Hg can also be deposited as a film on solid electrodes, such as metals (Ag, platinum (Pt), iridium (Ir)), including non-toxic amalgam electrodes [103, 104] and glassy carbon electrodes [105]. However the toxicity of mercury and a limited anodic potential range are still an inconvenience [100].

Bismuth (Bi) has become an environmentally friendly, alternative electrode material to mercury throughout the last ten years [106], with films deposited on substrates like C [107, 108]. Bi electrodes have been used to detect a range of trace metals such as, Zn [89], Mn [109] cobalt (Co) [110], cadmium (Cd) [110], lead (Pb) [111], As [112] and more recently Sb [113] by stripping techniques.

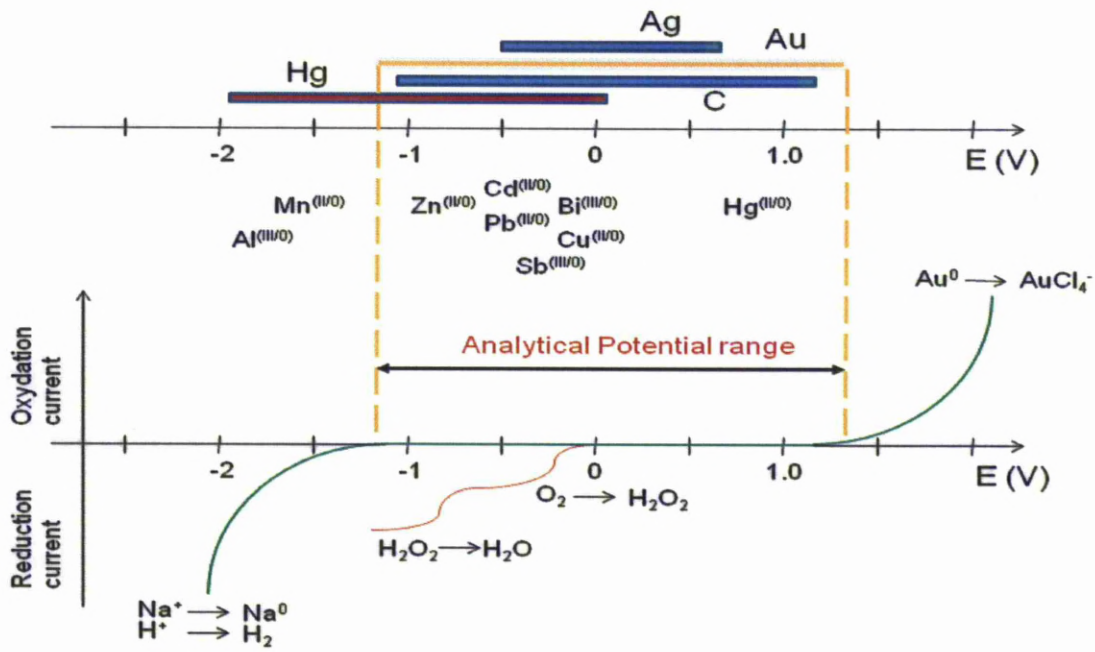

Figure 5. Polarisation ranges of Ag, Au, C and Hg electrodes and the oxido-reduction potentials of selected trace elements [78].

Carbon itself is also commonly used due to its various conducting forms and high surface activity, although this leads to its electrodes being susceptible to: poisoning by organic compounds and pH it also means that purposeful surface modification is possible, making it one of the most flexible electrode substrates, especially for the analysis of organic compounds. Electrodes include glassy carbon [114], carbon nanotubes [115, 116], carbon paste [117], carbon fibers [118] and doped-diamond [119]. Carbon substrates are often modified with metal coating or doping for trace metal analysis [108, 120].

Solid metal electrodes, such as Au and Ag have a high conductivity that results in low background currents, which can increase sensitivity and reproducibility [95] and with redox potentials more positive than the oxidation of Hg (figure 5), they can be applied to the speciation of other trace metals not accessible to mercury or open new analytical opportunities.. The positive shift in redox potentials is due to under potential deposition (UPD) [121]. UPD processes can be seen in chapters 5-6of this thesis which shows, for example, Zn giving a peak at -0.55 V on the VGME versus -0.98 V on the HMDE. This is caused by interactions between the metal being analysed and the electrode substrate [122].

Au with a larger potential window than Ag is the most widely used solid metal electrode for trace metal analysis, determining electropositive elements, selenium (Se) and Cu as well as Hg, As and Sb which are difficult to measure on Hg based electrodes [95].

There are many methods of fabricating electrodes from such substrates, by deposition of nanoparticles [123], screen printing [124] or creating amalgams [103] to name just a few, but in this thesis a bare gold wire is used due to its easy fabrication and manipulation as well as its relatively low cost [125].

1.1.1.5 Microelectrode vs macroelectrode

Microelectrodes have become increasingly important in electroanalytical analysis, with their applications for seawater [126] and other natural samples [127, 128] reviewed. However, the use of the term "microelectrode" can still be confusing [127]. Wang et al described microelectrodes as 'an electrode with at least one dimension not greater than 25 μm' [129], which would include the microwire electrodes studied in this thesis. However, theoretically a true microelectrode can be described as 'an electrode where, $1/r >> 1/\delta$ and can be distinguished by its behaviour as it should be independent of stirring conditions' [78]. In that case, the size of the electrode would need to reach very low dimensions, in the order of nm range.

This growing attention owes to microelectrodes reduced capacitive current and increased mass transport rate [127] leading them to exhibit excellent signal-to-noise characteristics, which allow them to be used for trace concentrations, in solutions of low ionic strengths which is not achievable at larger macroelectrodes [77].

The shape of the diffusion layer can take slightly different forms for varied electrode sizes and geometries. For instance, in stagnant solutions, δ of a disc macroelectrode ($r > 2$ mm[78]) moves very quickly far out into the solution thus decreasing the flux towards the electrode, to the extent that the current would decrease to almost a zero value. To avoid such effect, the solution is stirred or the electrode is rotated to decrease and fix the diffusion layer size. Under these conditions, diffusion from the bulk of solution where concentration is constant to the electrode surface is nearly all linear in nature, in a direction perpendicular to the electrode surface. The electron flux (current), *i*, for a macroelectrode is given in that case by equation (6) [78]:

$$i = \frac{nFADC}{\delta} \tag{6}$$

Equation (6) shows that the electron flux at a macroelectrode is primarily dependent on δ, which in turn depends on hydrodynamic conditions this is because for a macroelectrode $1/r \ll 1/\delta$ [78].

For microelectrodes, the flux per unit time and area is greater than for large electrodes because the region from which electroactive species diffuses to the surface is in essence not limited to one dimension. For a disc microelectrode, it will be hemispherical in shape[78] with a diffusion layer size directly related to radius of the microelectrode. The current, *i*, for such a microelectrode is given by equation (7) [78]:

$$i = \frac{nFADC}{r} \tag{7}$$

Equation (7) shows that the electron flux at a microelectrode should be independent of both time and stirring conditions as $1/r \gg 1/\delta$ [78].

High mass transport obtained by radial diffusion at microelectrodes makes natural convection less problematic [130] and thus could make stirring superfluous during the pre-concentration step [131]. However, as said earlier, the size of the electrode would need to be very small (nm scale) which would lead to other problems of noise due to the low currents involved. The wire is a good compromise: its diameter can be as low as 5 µm which assures a cylindrical shape of the diffusion layer (2 D diffusion) while the third dimension (length) assures a high current can be easily recorded. The electron flux, *i*, for a microwire electrode is given by equation (8) [125]:

$$I(t) = 2\pi n l F D C_b \left\{ \frac{e^{-0.1\sqrt{\frac{\pi Dt}{r^2}}}}{\sqrt{\frac{\pi Dt}{r^2}}} + \left[\ln\left(5.2945 + 1.4986\sqrt{\frac{\pi Dt}{r^2}} \right) \right]^{-1} \right\} \quad (8)$$

In contrast to a disc microelectrode (spherical diffusion), the current for the microwire is not independent of time but tends to decrease due to a loss of diffusion dimension (length). Although this current is predicted to decrease, a steady state current is in practice obtained due to natural convections. For instance at a 5 µm electrode wire, it was found that the steady state current in stagnant solutions was corresponding to a diffusion layer size of ~ 12 µm, which is already relatively low [125]. This was reduced to 2 µm by standard stirring [125] and to below 1 µm using a vibrating device [99]. The wire electrodes can therefore be exploited experimentally in much the same way that steady-state currents are exploited at disk electrodes [132]. However it can be difficult and time consuming to make reproducible microdisk electrodes due to the need for polishing. In comparison the microwire electrode produces greater absolute currents due to a larger surface area and they are easier to make and maintain as they require no mechanical surface preparation prior to or during use [125] which was the major motivation for using the gold microwire as an electrode material.

The current density (per unit of electrode surface) increases with decreasing diameter of the wire electrode, indicating that small-diameter electrodes should have greater specific sensitivity although the absolute current will be smaller than that of a larger electrode [125]. However a compromise

must then be made between sensitivity and cost, ease of fabrication and robustness of the microwires with smaller wires being more expensive, harder to make and less robust. In this thesis 25, 10 and 5 µM gold microwires were all used depending on the experimental circumstances. For example, when the sensor had to be robust for on-site As speciation in West Bengal and considering the relatively high concentrations (chapter 3), the 25 µM wire was used. Whereas for Cu pseudopolarography (chapter 6), where detection limits and experimental time were of importance, the 5 µM wire was used.

1.1.1.6 The vibrating gold microwire electrode (VGME)

The VGME shown in figure 6A is fabricated in a similar manner, as before [132, 133], however the fitting was adapted to facilitate tip replacement and vibration. The gold microwire was fitted within a 100-µL polypropylene pipette tip. This tip was then fitted onto a 1 mL polypropylene pipette tip, which had a vibrator incorporated and a connecting electrical cable protruding ~ 1 cm at the bottom, which made contact with the working electrode (WE). The vibrator was driven by a 1.5 V power supply (home-built converter of 5 V to 1.5 V). A step-by-step guide to the electrode fabrication can be found in annex I. The advantage of such a system is the ease to replace the electrode when needed which takes just a few seconds. The VGME is part of a voltammetric cell also containing an auxiliary electrode (AE) and a reference electrode (RE) shown in figure 6B.

The hydrodynamic modulation caused by the attached vibrator improves the sensitivity of the technique by reducing the diffusion layer thickness, thus increasing the analyte flux to the surface of the electrode. Typical convection (stirring) methods have been reviewed [134, 135] and include moving the solution to the electrode surface using a magnetic stirrer [136], a rotating disk electrode (RDE) [137], pumping of the solution to the electrode [138], a pumped wall-jet system [139], ultrasound [140], low-frequency sound [141], microwaves [142], or by using a heated wire electrode [143].

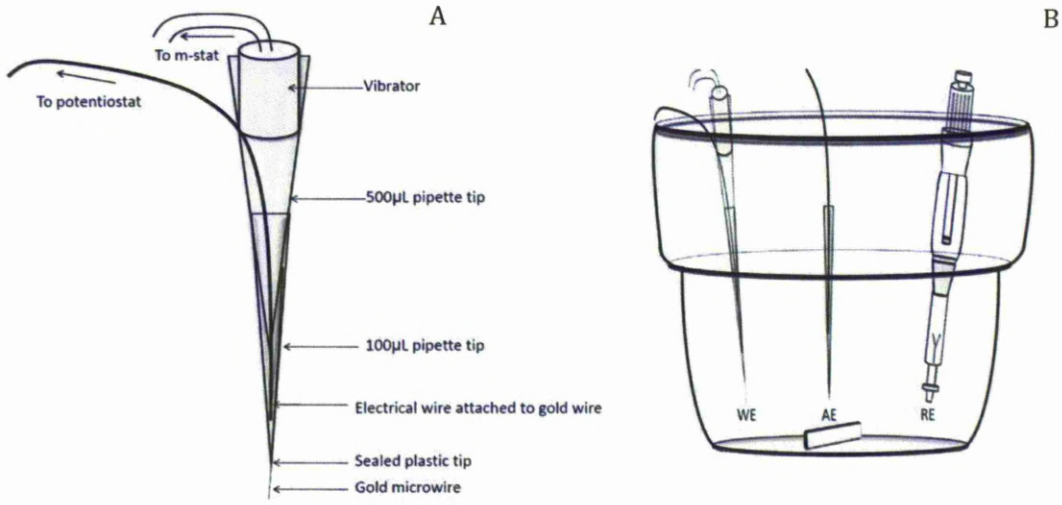

Figure 6. A) Detachable gold microwire electrode attached to vibrating device **B)** General electrochemical cell setup

In this work, a vibrator is attached to the electrode [144]. This vibrator consists in a small rotor similar to the ones found in mobile phones. To assess the efficiency of the vibration in increasing the diffusion flux, the diffusion layer size under diffusion limited conditions was calculated at the different wire diameters, as previously shown [125, 144]. To do so, the length of the electrode is first calculated by fitting the diffusion limited chronoamperommetric current obtained in a 10 mM ferrycyanide solution (electrolyte 0.5 M KCl, E_{dep} = -0.3 V *vs* Ag/AgCl) to the theoretical predictions given by equation (8). The diffusion layer is then calculated from equation (6) by measuring the diffusion limited current under vibrated conditions. Typical values of diffusion layers obtained at 5, 10 and 25 µm electrodes were 0.83, 1.22 and 2.35 µm respectively [99]. These diffusion layer sizes are amongst the lowest ever reported, thanks to the 200 Hz vibration frequency.

Equation (9) is a modified version of the Levich equation and correlates δ with the rotation rate of a rotating disc electrode (RDE) under laminar flow conditions for a reversible system [99]:

$$\delta = 1.61\, D^{1/3}(\pi.f/30)^{-1/2}\, \upsilon^{1/6} \qquad (9)$$

where f is the rotation rate per minute (rpm) and υ is the kinematic viscosity ($cm2.s^{-1}$). It can be calculated that the diffusion layer obtained at the 5 µm electrodes (0.83 µm) would only be achieved

with a rotation rate of ~280,000 rpm which is unattainable experimentally. A standard rotation rate is 10,000 rpm giving a δ of ~ 4.4 μm, i.e. 5 times higher than those obtained at the 10 μm wire electrodes. Such low diffusion layer sizes result in low detection limits by:

i) providing high fluxes of metal towards the electrode during the deposition step

ii) providing well defined hydrodynamic conditions at the vicinity of the electrode which improves the analytical reproducibility [144, 145] when compared to standard stirring.

The vibrating element of the VGME is robust, requires very little power and can be used on-site and in-situ [144]. Overall the combination of the vibrator and the gold microwire electrode provides a simple but very sensitive and relatively robust technique that has been previously used to measure Cu in-situ [144], the speciation of As both in laboratory and in on-site conditions [48] and Sb [99]. The vibrator also adds an advantage over stirring in the solution, in that it can reduce the need for an equilibrium time between deposition and scanning (stagnant solution), thus controlling not giving time for the diffusion layer to expand and thus the operational lability of the metal complexes in solution to alter.

SUMMARY OF METHODS DEVELOPED AND THEIR APPLICATIONS

All methods developed for the electrochemical speciation of trace metals in natural waters in this thesis use the VGME and are conducted at natural pH with minimal sample pre-treatment.

Chapters 2 and 3 focus on the speciation of As in groundwaters, with a on-site field validation of the method in West Bengal. Chapter 2 presents the cathodic stripping voltammetry (CSV) method developed to determine reactive As^{III}, in the presence of oxygen. The As speciation protocol involves measuring reactive As^{III} by CSV at the original pH and acidification to pH 1 to determine inorganic As^{III} + As^{V} by anodic stripping voltammetry (ASV). Total dissolved As is determined by ASV after UV-digestion at pH 1. Chapter 3 details the on-site speciation of inorganic arsenic in groundwater samples in West Bengal. As^{III} was determined on site, immediately upon sampling. This has only been possible after additions of EDTA to remove the interference from high levels of Fe^{II} and Mn^{II} that are commonly found in these reducing waters. EDTA was used to chelate the Fe^{II} and Mn^{II} interference and storage and speciation was assessed by stripping voltammetry, in combination with liquid chromatography mass spectrometry (LCMS) and ICP-MS.

Chapters 4 to 6 look at the development of methods for analysis and speciation of trace metals in seawater. Chapter 4 also deals with As, but this time its speciation in seawater, in the presence of Mn, As^{V} is determined by electrochemistry at natural pH for the first time. Chapter 5 shows the determination of Mn and Zn in seawater. Chapter 6 focuses on the pseudopolarography of Cu and Zn for the first time on a solid, non-mercury electrode, using natural concentrations in seawater samples due to the improved sensitivity of the VGME. Speciation analysis of As, Mn, Zn and Cu was successfully conducted in seawater samples collected from Liverpool Bay (Irish Sea).

References

[1] T.R. Chowdhury, G.K. Basu, B.K. Mandal, B.K. Biswas, G. Samanta, U.K. Chowdhury, C.R. Chanda, D. Lodh, S. Lal Roy, K.C. Saha, S. Roy, S. Kabir, Q. Quamruzzaman, D. Chakraborti, Nature, 401 (1999) 545.

[2] W. Czarnowski, K. Wrzesniowska, J. Krechniak, Sci Total Environ, 191 (1996) 177.

[3] J.S. Fieldmann, P, Field Test Kits for Arsenic Evaluation in Terms of Sensitivity, Reliability, Applicability and cost Wiley, Oxford, 2008.

[4] H.J.M. Bowen, Environmental chemistry of the elements, Academic Press, London, 1979.

[5] K.W. Bruland, Earth Planet Sc Lett, 47 (1980) 176.

[6] W. Stumm, J.J. Morgan, Aquatic chemistry : chemical equilibria and rates in natural waters, Wiley, New York ; Chichester, 1996.

[7] L.E. Brand, W.G. Sunda, R.R.L. Guillard, Limnol Oceanogr, 28 (1983) 1182.

[8] J.M. Neff, Environ Toxicol Chem, 16 (1997) 917.

[9] A.M. Ure, C.M. Davidson, Chemical speciation in the environment, Blackwell Science, Oxford, 2002.

[10] J. Buffle, Complexation reactions in aquatic systems : an analytical approach, Ellis Horwood, 1988.

[11] P.W. Atkins, Shriver & Atkins' inorganic chemistry, Oxford University Press, Oxford, 2010.

[12] M. Waeles, J. Vandenhecke, J.Y. Cabon, C. Garnier, R.D. Riso, Estuar Coast Shelf S, 90 (2010) 221.

[13] K.K. Brandt, P.E. Holm, O. Nybroe, Environ Sci Technol, 42 (2008) 3102.

[14] I.A.M. Worms, K.J. Wilkinson, Anal Chim Acta, 616 (2008) 95.

[15] G.A. Jackson, J.J. Morgan, Limnol Oceanogr, 23 (1978) 268.

[16] D.A. Hansell, C.A. Carlson, Biogeochemistry of marine dissolved organic matter, Academic, Amsterdam ; London, 2002.

[17] E.L. Rue, K.W. Bruland, Limnol Oceanogr, 42 (1997) 901.

[18] F.M.M. Morel, N.M. Price, Science, 300 (2003) 944.

[19] B.L. Lewis, G.W. Luther, H. Lane, T.M. Church, Electroanal, 7 (1995) 166.

[20] J. Buffle, Complexation reactions in aquatic systems : an analytical approach, Ellis Horwood, Chichester, 1988.

[21] A. Nelson, R.F.C. Mantoura, J Electroanal Chem, 164 (1984) 237.

[22] L.M. Laglera, C.M.G. van den Berg, Mar Chem, 82 (2003) 71.

[23] K.N. Buck, K.W. Bruland, Mar Chem, 96 (2005) 185.

[24] D.M. Anderson, F.M.M. Morel, Limnol Oceanogr, 23 (1978) 283.

[25] K.N. Buck, J.R.M. Ross, A.R. Flegal, K.W. Bruland, Environ Res, 105 (2007) 5.

[26] W.G. Sunda, S.A. Huntsman, Limnol Oceanogr, 40 (1995) 132.

[27] L.E. Brand, W.G. Sunda, R.R.L. Guillard, J Exp Mar Biol Ecol, 96 (1986) 225.

[28] G. Peers, S.A. Quesnel, N.M. Price, Limnol Oceanogr, 50 (2005) 1149.

[29] E.L. Mann, N. Ahlgren, J.W. Moffett, S.W. Chisholm, Limnol Oceanogr, 47 (2002) 976.

[30] K.W. Bruland, Limnol Oceanogr, 34 (1989) 269.

[31] B.L. Vallee, D.S. Auld, Biochemistry-Us, 32 (1993) 6493.

[32] F.M.M. Morel, J.R. Reinfelder, S.B. Roberts, C.P. Chamberlain, J.G. Lee, D. Yee, Nature, 369 (1994) 740.

[33] Y. Shaked, Y. Xu, K. Leblanc, F.M.M. Morel, Limnol Oceanogr, 51 (2006) 299.

[34] W.G. Sunda, S.A. Huntsman, Limnol Oceanogr, 43 (1998) 1055.

[35] D.S. Chen, P.Y. Qian, W.X. Wang, Environ Toxicol Chem, 27 (2008) 1794.

[36] W.G. Sunda, S.A. Huntsman, Limnol Oceanogr, 45 (2000) 1501.

[37] M.A. Saito, T.J. Goepfert, Limnol Oceanogr, 53 (2008) 266.

[38] W.G. Sunda, S.A. Huntsman, Limnol Oceanogr, 41 (1996) 373.

[39] W.G. Sunda, S.A. Huntsman, Limnol Oceanogr, 28 (1983) 924.
[40] K.W. Bruland, J.R. Donat, D.A. Hutchins, Limnol Oceanogr, 36 (1991) 1555.
[41] M.J. Horsburgh, S.J. Wharton, M. Karavolos, S.J. Foster, Trends Microbiol, 10 (2002) 496.
[42] J. Mendez, C. Guieu, J. Adkins, Mar Chem, 120 (2010) 34.
[43] W.G. Sunda, S.A. Huntsman, G.R. Harvey, Nature, 301 (1983) 234.
[44] C.H. Vanderweijden, D. Hoede, J.J. Middelburg, H.A. Vandersloot, J. Wijkstra, Chem Geol, 70 (1988) 19.
[45] M. Mkandawire, Y.V. Lyubun, P.V. Kosterin, E.G. Dudel, Environ Toxicol, 19 (2004) 26.
[46] M.O. Andreae, Limnol Oceanogr, 24 (1979) 440.
[47] W.R. Cullen, H. Li, S.A. Pergantis, G.K. Eigendorf, L.G. Harrison, Chemosphere, 28 (1994) 1009.
[48] P. Salaun, B. Planer-Friedrich, C.M.G. van den Berg, Anal Chim Acta, 585 (2007) 312.
[49] A.M.M. Debettencourt, M.O. Andreae, Appl Organomet Chem, 5 (1991) 111.
[50] P.L. Smedley, D.G. Kinniburgh, Appl Geochem, 17 (2002) 517.
[51] J.F. Schamberg, Arch Dermatol, 143 (2007) 16.
[52] A.H. Smith, M.L. Biggs, L. Moore, R. Haque, C. Steinmaus, J. Chung, A. Hernandez, P. Lopipero, Arsenic Exposure and Health Effects (1999) 191.
[53] WHO, 1993.
[54] P. Ravenscroft, H. Brammer, K.S. Richards, Arsenic pollution : a global synthesis, Blackwell, Oxford, 2009.
[55] R. Nickson, J. McArthur, W. Burgess, K.M. Ahmed, P. Ravenscroft, M. Rahman, Nature, 395 (1998) 338.
[56] R.T. Nickson, J.M. McArthur, P. Ravenscroft, W.G. Burgess, K.M. Ahmed, Appl Geochem, 15 (2000) 403.
[57] J.M. McArthur, D.M. Banerjee, K.A. Hudson-Edwards, R. Mishra, R. Purohit, P. Ravenscroft, A. Cronin, R.J. Howarth, A. Chatterjee, T. Talukder, D. Lowry, S. Houghton, D.K. Chadha, Appl Geochem, 19 (2004) 1255.
[58] A.H. Smith, E.O. Lingas, M. Rahman, B World Health Organ, 78 (2000) 1093.
[59] D. Kinniburgh, P. Smedley, J. Davies, S.M.I. Huq, Water, Sanitation and Hygiene: Challenges of the Millennium (2001) 230.
[60] J.M. McArthur, P. Ravenscroft, D.M. Banerjee, J. Milsom, K.A. Hudson-Edwards, S. Sengupta, C. Bristow, A. Sarkar, S. Tonkin, R. Purohit, Water Resour Res, 44 (2008).
[61] P. Ravenscroft, J.M. McArthur, B.A. Hoque, Arsenic Exposure and Health Effects Iv (2001) 53.
[62] D.G.E. Kinniburgh, Arsenic contamination of groundwater in Bangladesh : vol 2: final report, British Geological Survey, 2001.
[63] W.G. Burgess, M.A. Hoque, H.A. Michael, C.I. Voss, G.N. Breit, K.M. Ahmed, Nat Geosci, 3 (2010) 83.
[64] D.G. Kinniburgh, W. Kosmus, Talanta, 58 (2002) 165.
[65] S.M. Cohen, L.L. Arnold, M. Eldan, A.S. Lewis, B.D. Beck, Crit Rev Toxicol, 36 (2006) 99.
[66] H.M. Guo, D. Stuben, Z. Berner, Q.C. Yu, Appl Geochem, 24 (2009) 657.
[67] E. Lombi, K.G. Scheckel, J. Pallon, A.M. Carey, Y.G. Zhu, A.A. Meharg, New Phytol, 184 (2009) 193.
[68] R. Stone, Science, 321 (2008) 184.
[69] J. Feldmann, P. Salaun, E. Lombi, Environ Chem, 6 (2009) 275.
[70] F.C. Adams, J Anal Atom Spectrom, 19 (2004) 1090.
[71] C. Vandecasteele, C.B. Block, Modern methods for trace element determination, Wiley, Chichester, 1993.
[72] C.M. Barshick, D.C. Duckworth, D.H. Smith, Inorganic mass spectrometry : fundamentals and applications, Marcel Dekker, New York, 2000.
[73] M. Popp, S. Hann, G. Koellensperger, Anal Chim Acta, 668 (2010) 114.

[74] M.A. Vieira, P. Grinberg, C.R.R. Bobeda, M.N.M. Reyes, R.C. Campos, Spectrochim Acta B, 64 (2009) 459.
[75] T. Nakazato, H. Tao, T. Taniguchi, K. Isshiki, Talanta, 58 (2002) 121.
[76] H. Louie, M. Wu, P. Di, P. Snitch, G. Chapple, J Anal Atom Spectrom, 17 (2002) 587.
[77] J. Buffle, M.L. Tercier-Waeber, Trac-Trend Anal Chem, 24 (2005) 172.
[78] J. Buffle, G. Horvai, In-situ monitoring of aquatic systems : chemical analysis and speciation, Wiley, Chichester, 2000.
[79] A. Tessier, D.R. Turner, Metal speciation and bioavailability in aquatic systems, John Wiley, Chichester, 1995.
[80] M. Pesavento, G. Alberti, R. Biesuz, Anal Chim Acta, 631 (2009) 129.
[81] P.M. Bersier, J. Howell, C. Bruntlett, Analyst, 119 (1994) 219.
[82] H.P. van Leeuwen, R.M. Town, J. Buffle, R.F.M.J. Cleven, W. Davison, J. Puy, W.H. van Riemsdijk, L. Sigg, Environ Sci Technol, 39 (2005) 8545.
[83] G.E. Batley, T.M. Florence, J Electroanal Chem, 55 (1974) 23.
[84] P.J. Brendel, G.W. Luther, Environ Sci Technol, 29 (1995) 751.
[85] M.L. Tercier, N. Parthasarathy, J. Buffle, Electroanal, 7 (1995) 55.
[86] D. Omanovic, M. Branica, J Electroanal Chem, 543 (2003) 83.
[87] M.L. Tercier, J. Buffle, Anal Chem, 68 (1996) 3670.
[88] W. Davison, H. Zhang, Nature, 367 (1994) 546.
[89] P. Salaun, F. Bujard, L. Berdondini, M. Koudelka-Hep, J. Buffle, Electroanal, 16 (2004) 811.
[90] E. Bakker, Anal Chim Acta, 350 (1997) 329.
[91] W. Davison, G.W. Grime, J.A.W. Morgan, K. Clarke, Nature, 352 (1991) 323.
[92] E.J.M. Temminghoff, A.C.C. Plette, R. Van Eck, W.H. Van Riemsdijk, Anal Chim Acta, 417 (2000) 149.
[93] C.M.G. van den Berg, Anal Chim Acta, 250 (1991) 265.
[94] J. Heyrovsky, J. Ku\030Ata, Principles of polarography, Czechoslovak Academy of Sciences ; New York ; London : Academic Press, Prague, 1966.
[95] C.M.A. Brett, A.M.O. Brett, Electrochemistry : principles, methods, and applications, Oxford University Press, Oxford, 1993.
[96] A.J. Bard, L.R. Faulkner, Electrochemical methods : fundamentals and applications, John Wiley, New York ; Chichester, 2001.
[97] Y.H. Gao, K. Oshita, K.H. Lee, M. Oshima, S. Motomizu, Analyst, 127 (2002) 1713.
[98] E.P. Achterberg, C.M.G. VanDenBerg, Mar Pollut Bull, 32 (1996) 471.
[99] P. Salaun, K. Gibbon-Walsh, C.M.G. van den Berg, Anal Chem, 83 (2011) 3848.
[100] K.Z. Brainina, N.A. Malakhova, N.Y. Stojko, Fresen J Anal Chem, 368 (2000) 307.
[101] M. Branica, D.M. Novak, S. Bubic, Croat Chem Acta, 49 (1977) 539.
[102] P.L. Croot, J.W. Moffett, G.W. Luther, Mar Chem, 67 (1999) 219.
[103] O. Mikkelsen, K.H. Schroder, Electroanal, 15 (2003) 679.
[104] O. Mikkelsen, K. Strasunskiene, S.M. Skogvold, K.H. Schroder, Curr Anal Chem, 4 (2008) 202.
[105] C.M.A. Brett, A.M.O. Brett, F.M. Matysik, S. Matysik, S. Kumbhat, Talanta, 43 (1996) 2015.
[106] A. Economou, Trac-Trend Anal Chem, 24 (2005) 334.
[107] E.A. Hutton, S.B. Hocevar, L. Mauko, B. Ogorevc, Anal Chim Acta, 580 (2006) 244.
[108] J. Wang, Electroanal, 17 (2005) 1341.
[109] R.G. Compton, C.E. Banks, J. Kruusma, R.R. Moore, P. Tomcik, J. Peters, J. Davis, S. Komorsky-Lovric, Talanta, 65 (2005) 423.
[110] Y. Nagaosa, J. Long, Anal Sci, 23 (2007) 1343.
[111] R.G. Compton, C.M. Welch, C.E. Banks, S. Komorsky-Lovric, Croat Chem Acta, 79 (2006) 27.
[112] Y. Nagaosa, J.J. Long, Int J Environ an Ch, 88 (2008) 51.
[113] Y. Nagaosa, P. Zong, J.J. Long, Int J Environ an Ch, 91 (2011) 421.
[114] C. Agra-Gutierrez, J.L. Hardcastle, J.C. Ball, R.G. Compton, Analyst, 124 (1999) 1053.
[115] M. Trojanowicz, Trac-Trend Anal Chem, 25 (2006) 480.

[116] L. Agui, P. Yanez-Sedeno, J.M. Pingarron, Anal Chim Acta, 622 (2008) 11.
[117] I. Svancara, A. Walcarius, K. Kalcher, K. Vytras, Cent Eur J Chem, 7 (2009) 598.
[118] S.M. Silva, A.M. Bond, Anal Chim Acta, 500 (2003) 307.
[119] R.G. Compton, J.S. Foord, F. Marken, Electroanal, 15 (2003) 1349.
[120] S.E.W. Jones, R.G. Compton, Curr Anal Chem, 4 (2008) 170.
[121] G.W. Tindall, S.H. Cadle, Bruckenstein.S, J Am Chem Soc, 91 (1969) 2119.
[122] G. Herzog, D.W.M. Arrigan, Trac-Trend Anal Chem, 24 (2005) 208.
[123] S.E.W. Jones, R.G. Compton, Curr Anal Chem, 4 (2008) 177.
[124] K.C. Honeychurch, J.P. Hart, Trac-Trend Anal Chem, 22 (2003) 456.
[125] P. Salaun, C.M.G. van den Berg, Anal Chem, 78 (2006) 5052.
[126] C.E. Reimers, Chem Rev, 107 (2007) 590.
[127] X.D. Xie, D. Stueben, Z. Berner, Anal Lett, 38 (2005) 2281.
[128] A.M. Bond, Analyst, 119 (1994) R1.
[129] J. Wang, Analytical electrochemistry, Wiley-VCH, New York ; Chichester, 2000.
[130] M.E. Abdelsalam, G. Denuault, S. Daniele, Anal Chim Acta, 452 (2002) 65.
[131] M. Wojciechowski, J. Balcerzak, Anal Chim Acta, 249 (1991) 433.
[132] G. Billon, C.M.G. van den Berg, Electroanal, 16 (2004) 1583.
[133] L. Nyholm, G. Wikmark, Anal. Chim. Acta, 257 (1992) 7.
[134] J.V. Macpherson, Electroanal, 12 (2000) 1001.
[135] J.V. Macpherson, N. Simjee, P.R. Unwin, Electrochim Acta, 47 (2001) 29.
[136] S.T. Crosmun, J.A. Dean, R. Stokely, Anal Chim Acta, 75 (1975) 421.
[137] G.U. Flechsig, O. Korbut, P. Grundler, Electroanal, 13 (2001) 786.
[138] A. Zirino, Lieberma.S, J Electrochem Soc, 120 (1973) C254.
[139] D. Omanovic, Z. Peharec, T. Magjer, M. Lovric, M. Branica, Electroanal, 6 (1994) 1029.
[140] C.E. Banks, R.G. Compton, Chem Anal-Warsaw, 48 (2003) 159.
[141] O. Mikkelsen, K.H. Schroder, Electroanal, 13 (2001) 687.
[142] I.J. Cutress, F. Marken, R.G. Compton, Electroanal, 21 (2009) 113.
[143] P. Grundler, G.U. Flechsig, Electrochim Acta, 43 (1998) 3451.
[144] C.S. Chapman, C.M.G. van den Berg, Electroanal, 19 (2007) 1347.
[145] Z.S. Bi, C.S. Chapman, P. Salaun, C.M.G. van den Berg, Electroanal, 22 (2010) 2897

2

Chapter 2
ARSENIC SPECIATION IN NATURAL WATERS BY CATHODIC STRIPPING VOLTAMMETRY

2. ARSENIC SPECIATION IN NATURAL WATERS BY CATHODIC STRIPPING VOLTAMMETRY

2.1. Introduction

Arsenic occurs in seawater as inorganic arsenate (As^{V}), arsenite (As^{III}), methyl arsonate and dimethylarsinate [1]. In groundwater from geochemically reducing conditions the dominant species is As^{III} [2]. The mobility of arsenic in soils or sediments is controlled by interaction with natural organic matter (NOM) [3], sulphides [4] and mineral oxides [5]. The arsenic species behave differently in terms of mobility, bioavailability, toxicity, and therefore arsenic speciation is required to understand its biogeochemical cycling and potential toxicity of waters. Arsenic and some of its species can be determined by inductively coupled mass spectrometry (ICP-MS), and electro-spray MS (ES-MS) coupled to chromatographic separation (HPLC, GC) [6]. These methods are suitable for speciation only if the species are not altered by the sample preparation and chromatographic separation as well as sample storage. Because of difficulties of stabilising the speciation in natural waters [7], it is important to have a speciation method which can be used in the field, ideally in situ in the tested water. For this reason, we have explored the possibility to determine the arsenic speciation in groundwaters using anodic (ASV) and cathodic (CSV) stripping voltammetry.

Existing CSV methods require the addition of copper [8], selenium [8], a pH 7 phosphate buffer [9], or an organic ligand [10], and, typically, the As^{III} is concentrated on a mercury electrode during deposition step, and reduced to As^{0} during the scan. In ASV, arsenite is reduced to As^{0} during the deposition step, on a solid electrode, and re-oxidised during the ASV scan. Gold electrodes have mostly been used in ASV of arsenic combined with acidic conditions [11].

A variety of gold electrodes have been used for this purpose, including a polycrystalline gold disk electrode [12], gold film on platinum [13], or glassy carbon [14], gold microelectrode arrays [15], micro-sized gold particles [16] and gold nanoparticles deposited on boron-doped diamond [17], or on glassy carbon [18]. A drawback of these methods is related to the loss of the original speciation

due to the sample acidification. In addition, the use of strong acid leads to corrosive conditions and interference from hydrogen generation prevents the determination of As^{V} [15].

Although arsenite is electrochemically reducible over the entire pH range [19], only a few methods make use of this property to determine arsenite at neutral or alkaline pH [9, 12, 20-22]. These methods are not suitable for in situ detection, because of insufficient sensitivity for low, natural levels. Recently a method was developed to determine As^{III} at neutral pH by ASV using a gold microwire electrode [23]. This method requires the presence of chloride and in preliminary experiments using groundwaters we found that the ASV response for arsenic suffered from non-linearity due to an un-resolved double peak which could only be eliminated by addition of either chloride, bromide or carbonate. Furthermore, all ASV methods on gold are at neutral pH affected by dissolved oxygen (DO) which is problematic for on-site or in situ measurement.

This work presents a CSV method specifically for the determination of As^{III} in freshwaters including groundwater. This method is novel in that no sample pre-treatment or reagent addition is required, enabling the determination of arsenite, in situ in the unaltered water at the original pH and in the presence of air. Combined inorganic arsenic (As^{III} + As^{V}) is determined subsequently by ASV after acidification of a sample aliquot to pH 1, thus enabling speciation in a single sample aliquot [23].

2.2. Experimental

2.2.1 Reagents and samples

All solutions were prepared with 18 MΩ deionised Milli-Q water. A 10^{-2} M As^{III} stock solution was prepared from As_2O_3 (purity 99.5 %, AnalaR BDH Chemicals Ltd, England), acidified with HCl to pH 2 and wrapped in aluminium foil to prevent oxidation of As^{III} by light. Standard solutions with concentrations of non-acidified 10^{-4}, 10^{-5} and 10^{-6} M As^{III} were prepared daily. 0.5 M H_2SO_4 used for conditioning of the electrode was from BDH (AnalaR grade). Elemental solutions (Cu, Pb, Hg, Sb^{III}, Mn, Zn, Cd, Ni, Fe, Bi^{III} and Se^{IV} used for interference experiments were diluted from AAS standard

solutions from Fluka or VWR; humic acid and sodium dodecylsulphate (SDS) were from Aldrich, Triton-X-100 from BDH (England) and fulvic acid was "Suwannee river fulvic acid" from the International Humic Substances Society.

Borehole water samples (unfiltered) were collected in acid washed polypropylene bottles by Severn Trent Water. Well samples were collected and sampled on-site in West Bengal. River and lake water were collected from Snowdonia (Wales, UK) and Ben Nevis (Scotland, UK), respectively. Mineral water (Evian) was obtained from a local supermarket.

2.2.2 Instrumentation

Voltammetric measurements utilised a battery-powered (dry, 10 Ah, 6 V) Palmsens potentiostat (Palmsens, Netherlands) associated with a modified version of the commercially available Ivium software (Palmsens). The working electrode (WE) was a 25 µm diameter gold wire (99.99 %, hard, Goodfellow) and the counter electrode (CE) a 200 µm iridium wire (3 mm long, Goodfellow), were fabricated as described previously [23, 24].

A solid-state pseudo reference electrode (RE) was homemade as described [25] from a 1.5 mm diameter, 2.5 cm, Ag wire (99.99 %, Rasmussen AS, Norway). The gold microwire WE and vibrator (1.5 V) were fitted into a single pipette tip (5 mL, shortened, polypropylene), more compact than that developed before [26]. The three electrodes were fixed immediately adjacent to each other using quick-setting epoxy (Araldite) leaving ca. 10 mm of the counter and reference electrodes exposed, and connected to a four core cable of 1.5 or 6 m. The apparatus was battery-powered for analyses in the field and the laboratory.

Some of the cydic voltammetry experiments were performed using a µ-Autolab(III) potentiostat (Ecochemie, Netherlands) associated with GPES software. In this case, the RE was double-junction, Ag/AgCl/3 M KCl. A microwire WE was fitted in the centre of the cell, the CE was a 2 cm iridium wire (0.2 mm diameter), and the solution was stirred using the standard rotating PTFE rod.

2.2.3 *Electrode conditioning*

The microwire WE was cleaned in 0.5 M H_2SO_4 by hydrogen generation at −1.7 V (15 s). The −1.7 V cleaning step was done when the electrode was new or when fouling was suspected. Subsequently the electrode was conditioned in the same solution by cyclic voltammetry (5 scans) from 0 to 1.5 V (100 mV s^{-1}).

2.2.4 *Voltammetric procedure to determine arsenite*

Each scan was preceded by a conditioning step to remove any deposited As from the electrode. Each measurement was in triplicate from which the average and standard deviation were derived.

The method was developed in 10 mM H_3BO_3 buffer (pH 9) in 0.01 M KCl and tested in undiluted groundwater. Water samples were analysed without deaeration and without addition of buffer or electrolyte, unless indicated. Typical voltammetric conditions were: E_{cond} = 0.55 V (10 s), E_{dep} = 0 V (60 s), t_{eq} = 3 s, stripping from 0 to −1.5 V at 1 V s^{-1}, step = 10 mV. The electrode was vibrated, or the solution stirred, during the conditioning and deposition steps. The background scan was the same as the analytical scan but with the deposition time reduced to 1 s. The deposition time was prolonged or shortened to increase or decrease the sensitivity. The sensitivity was calibrated by addition of As^{III} to the sample aliquot in the cell. Groundwater samples containing high levels (>10 µM) of iron were analysed with a modified procedure in which 1 mM EDTA was added to retain the iron in solution [7].

2.2.5 *Voltammetric procedure for total inorganic arsenic detection*

The total inorganic arsenic concentration (As^{V} + As^{III}) was determined as before [23]. The 20 mL sample aliquot was acidified to pH 1 by addition of 200 µL of 10 M HCl and the combined As^{V} was detected by square-wave ASV (50 Hz frequency, 25 mV amplitude, 8 mV step) using E_{dep} =−1.4 V, without de-oxygenation.

2.3. Results and discussion

2.3.1 Cyclic voltammetry and the adsorption mechanism

A peak was obtained for As^{III} / As^{0} by a CSV scan at −0.75 V in pH 9 buffered 0.01 M KCl after deposition at 0 V. Cyclic voltammetry (CV) was used to elucidate the reaction mechanism. Two cyclic voltammograms of 50 nM As^{III} are shown in Figure 1. The potential was held at 0 V for 60 s prior to running these two CV scans from 0 to −1 V to +0.5 V and back to 0 V. One reduction peak A was present at −0.75 V, and two oxidation peaks, B at −0.3 V and C at +0.2 V, were apparent in the first scan becoming much smaller by the second scan. The inset shows successive CV scans between 0 and −1V after 60 s deposition at 0V where peaks A and B gradually decrease with each subsequent scan due to desorptive loss of As from the electrode between 0 and −0.7 V. The presence of reduction peak A is consistent with adsorption of As^{III} on the gold surface at 0 V during the deposition step. When the potential was scanned in a negative direction As^{III} was reduced to As^{0} (peak A, equation (1)), which remained on the electrode. When the potential was scanned in a positive direction, the As^{0} was oxidised back to As^{III} (peak B, equation (2)) which remained adsorbed until it was oxidised to As^{V} (peak C, equation (3)). The absence of peak A (As^{III} reduction) in the second CV scan was because all As^{III} on the electrode had been oxidised to As^{V} which is electro-inactive at this pH and potential range [23]. Any As^{V} in the solution is therefore not detected by the CSV method. At potentials >peak C, the current increased again (D) due to the formation of gold-oxide at the surface of the gold electrode. The reduction peak, E, at ~0 V, corresponds to the reduction of this newly formed oxide.

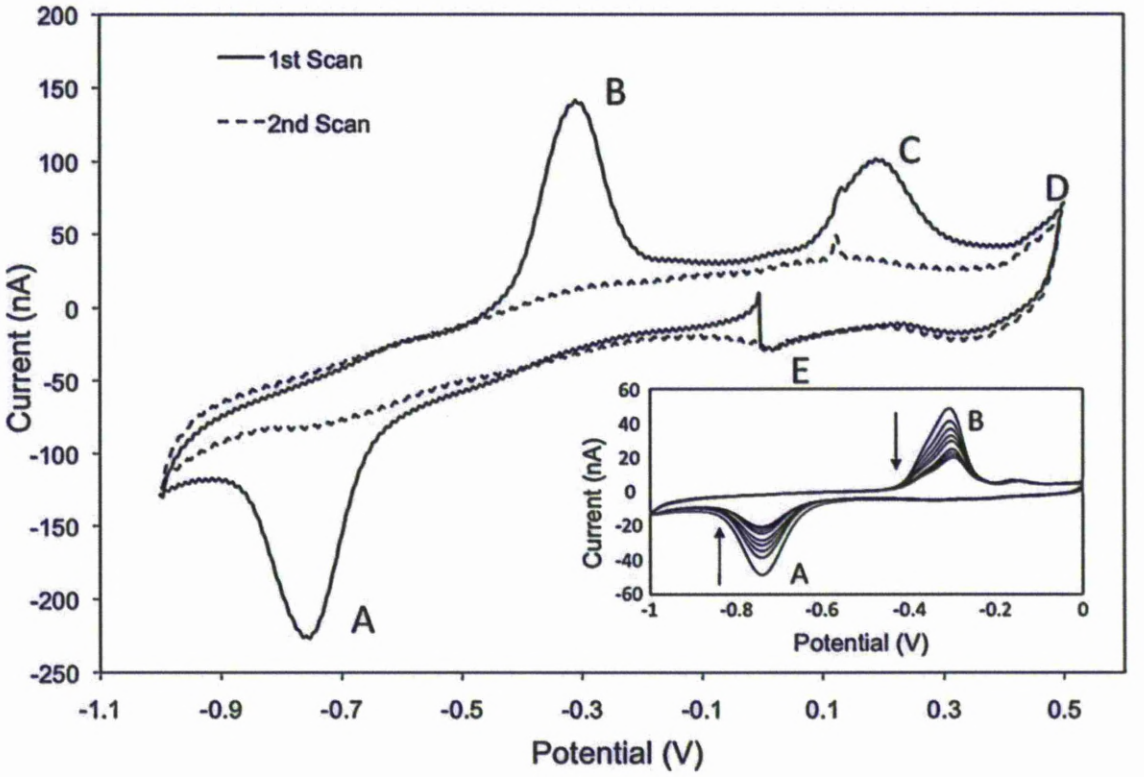

Figure 1. Cyclic voltammetry (CV) of 100 nM As^{III} in 0.01 M KCl, buffered at pH 9 using 0.01 M H_3BO_3. The first scan was initiated at 0V and preceded by 60 s adsorption (vibrated); the second scan immediately followed the first. The inset shows CV scans between 0 and −1.0 V; the first scan was preceded by a 60 s adsorption step; the peak heights are gradually decreasing due to the lack of an adsorption step between scans combined with desorption at potentials <–0.5 V (see Figure 2).

CV scans between −1 and 0V (inset Figure 1) show that As^{III} adsorbs at around 0 V. The large hysteresis between peaks A and B shows that the As^{III} / As^0 redox couple is electrochemically poorly reversible. Peaks A, B and C were already known to occur for high-arsenic levels in acid [27] and in phosphate buffer solutions (pH 5) [20] without As^{III} adsorption and at pH 7 [9] with As^{III} adsorption.

The chemical equations for the reaction mechanism are as follows:

Peak A : $As(OH)_3^0 + 3e^- \rightarrow As^0_{ads} + 3OH^-$ (1)

Peak B : $As^0_{ads} + 3OH^- \rightarrow As(OH)_{3ads}{}^0 + 3e^-$ (2)

Peak C : $As(OH)_{3ads}{}^0 + H_2O \rightarrow HAsO_4^{2-} + 4H^+ + 2e^-$ (3)

Any of the peaks, A, B and C, can be used for quantification of As^{III}. Peaks B and C can be used for ASV detection of arsenic, whilst peak A can be used for CSV detection. Peak C was not used because it tends to overlap with the Cu peak and was smaller than that for A or B. Peak B is used in ASV analysis but is strongly affected by the presence of DO. Preliminary experiments showed that the ASV method requires the addition of mM levels of chloride, bromide, carbonate or acid to avoid the formation of an un-resolved double peak and non-linear response in groundwater. Furthermore peak B was found to overlap with that for Sb^{III}. Peak A was found not to suffer from any of these interferences and was optimised for a CSV method for the detection of As^{III}.

2.3.2 Optimisation of the analytical parameters of the CSV method

The sensitivity for the detection of As^{III} was optimised in preliminary experiments in 0.01 M pH 9 borate buffer + 10 mM KCl. In each case the CSV scan was initiated from 0V. Comparative measurements using the square-wave (SW) and linear-sweep (LS) modes showed that there were no significant differences at low speed (200 mV s^{-1}), in agreement with the poor electrochemical reversibility of the As^{III} reduction. At greater scan-speed, where oxygen does not interfere (1–2 V s^{-1}), the SW signal was noisy whereas the LS peak was smooth. LS was therefore selected as the optimum stripping procedure.

Variation of the deposition potential showed (Figure 2A) that a signal for As^{III} was obtained after deposition at potentials between +0.3 and –0.5 V, with greatest sensitivity after deposition at ~0 V. Unexpectedly, no signal was obtained after deposition at potentials between –0.5 and –1.1 V, suggesting that Coulombic repulsion due to a negative charge on the electrode in this potential range resists arsenite adsorption. This repulsion is consistent with a negative charge on gold at potentials <–0.5 V due to strong adsorption of chloride [28]. Variation of the CV scan rate showed a linear relationship between the intensity of peak A and $(\text{scan rate})^{0.5}$ showing that the peak height was diffusion controlled. This is counter-intuitive as the arsenic had been pre-concentrated on the electrode so diffusion should not have played a role during the scan. The diffusion effect is caused by

the diffusion away from the electrode during the scan at potentials between −0.5 and the peak potential at −0.75 V, and this effect is greater for slower scan rates causing the peak height to drop. The diffusion away from the electrode at intermediate potentials is the cause for the decrease of peaks A and B upon successive CV scans (inset of Figure 1).

Peak A re-appeared at deposition potentials between −1.1 and −1.6 V, and had greatest peak height after deposition at −1.5 V. The formation of peak A after deposition at potentials <−1.1 V is due to the deposition of the As as As^0 after reduction of As^{III} at the electrode surface. A deposition potential of 0 V was selected as optimal for arsenic analysis, and not −1.5 V which gives better sensitivity in pure water, as it discriminates against the deposition of metals with potential interfering effects (Fe, Mn and Zn). Furthermore, repeated measurements in the presence of DO showed that the peak height was stable in this condition whereas it gradually decreased after deposition at −1.5 V due to oxidation of As^{III} to As^V [29].

2.3.3 pH effect

The pH for optimal CSV response for As^{III} detection was determined in a solution containing 2 mM KCl and 10 mM $NaSO_4$, in which the pH was buffered across a wide range using 10 mM $KHPO_4$, 30 mM $NaHCO_3$ and 10 mM H_3BO_3. The pH was varied by adding dilute H_2SO_4 from a starting pH of 12. Cyclic scans were used to obtain the response of the As^{III} / As^0 peak from the forward (negative) going scans and the response of the As^0/ As^{III} and As^{III} / As^V peaks from the reverse scans. Deposition was at 0 V. The CSV arsenite signal was obtained between pH 7 and 11 (Figure 2B) with an optimum sensitivity at pH ~9 – 9.5, decreasing at lower and higher pH values. The other peaks mirrored this behaviour indicating that the As^{III} deposition was the determining step for the peak height. The peak areas for the As^{III} / As^0 and As^0/ As^{III} peaks were almost the same, as expected because they are both for three electron reactions. The area of the As^{III} / As^V peak was about half of the others, instead of an expected 33 % less (two-electron reaction) due to desorption of some of the As^{III} during the scan before its oxidation to As^V.

The pKa values of $As(OH)_3^0$ are 9.2, 12.13 and 13.4 [30], which means that $As(OH)_3^0$ is present over the entire pH range where a response is obtained, and $As(OH)_4^-$ at higher pH values, suggesting that these are the species that adsorb on the electrode surface. The peak potential for the As^{III} / As^0 peak shifted to more negative potentials with increasing pH at a rate of 60 mV pH^{-1} close to the theoretical value of 59 mV predicted for reaction (1). The shift of the other peaks was similar at 67 mV pH^{-1} for As^0/ As^{III} and 58 mV pH^{-1} for As^{III} / As^V.

The main finding of this experiment was that As^{III} can be detected at neutral pH values between pH 7 and 9.5 which indudes the usual neutral pH range of natural water samples, which is convenient for monitoring purposes. For this reason natural waters can be analysed without any reagent addition. The sensitivity is greatest at pH values between 9 and 9.5, conveniently buffered using borate pH buffer.

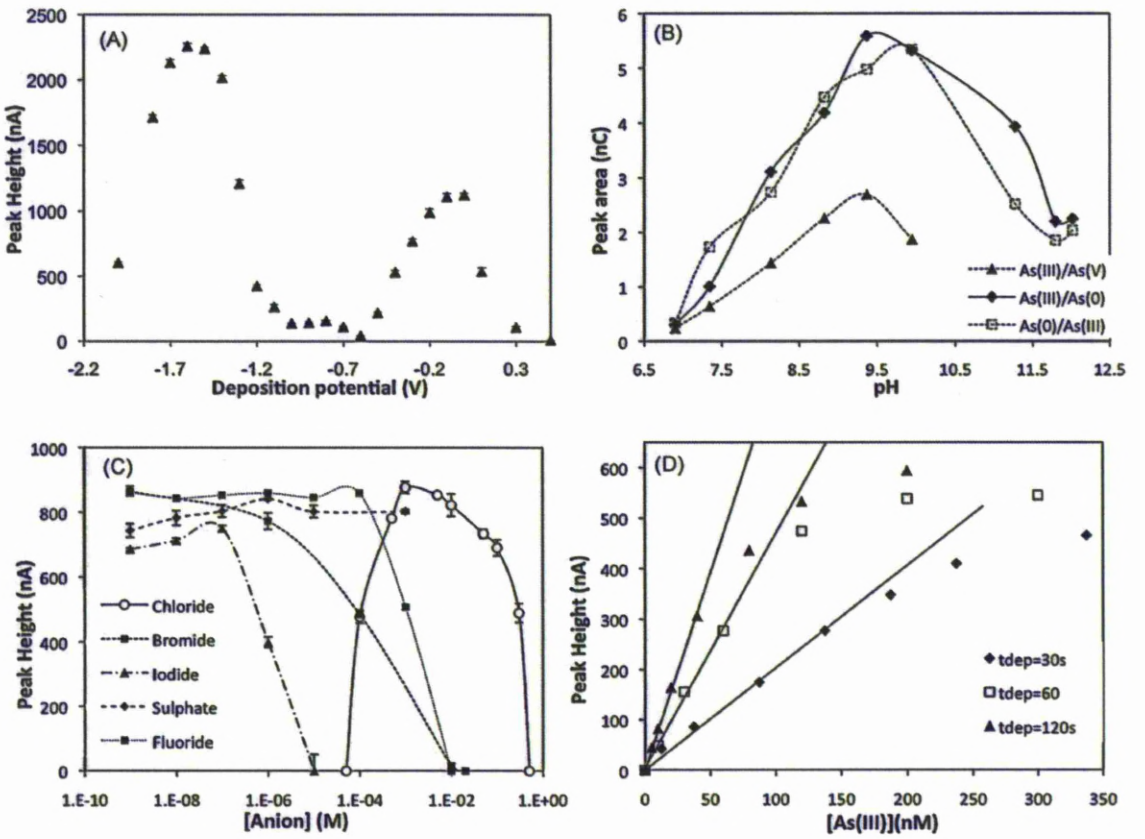

Figure 2. Optimisation of the analytical parameters for CSV of 100 nM As^{III} in 10 mM KCl, 10 mM H_3BO_3, pH 9; the deposition time was 60 s. **A)** Variation of the deposition potential; **B)** variation of the pH; **C)** interference testing of major anions; **D)** variation of the deposition time.

2.3.4 Chloride effect

Chloride adsorbs strongly on gold which affects the charge on the electrode [31] and may affect the interaction of gold with arsenic. This was assessed by monitoring the CSV response for As^{III} in borate buffer whilst varying the chloride concentration. The solution was deoxygenated to eliminate the reduction wave for DO which had an effect at low chloride. In the presence of DO and at low ionic strength (<0.001 M), the sensitivity for arsenic initially increased with the chloride concentration up to about 0.003 M Cl^- where the response became the same as that in deaerated solution. The CSV signal diminished gradually at higher Cl^- concentrations, largely disappearing at $[Cl^-] > 0.2$ M (Figure 2C). This decrease is either due to a competitive adsorption of As^{III} and Cl^- on the gold electrode, or chloride complexation (e.g. $As(OH)_2Cl$). The effect is that the CSV method is not suitable for arsenic measurement in saline waters, such as seawater with salinity greater than ~10. Assuming that the decreased sensitivity is caused by As^{III} complexation with chloride, causing the formation of mixed Cl–OH As^{III} species, the decrease in the signal confirms that the CSV signal is specific for the reduction of $As(OH)_3^0$ species adsorbed on the electrode. Any change in the speciation away from this species, due to pH change or competitive complexation with anions like chloride, would be a cause for the sensitivity to drop. The CSV method is therefore a sensitive tool for the speciation of inorganic As^{III}.

The peak potential for As^{III} was found to shift in a negative direction at a rate of 30 mV per decade of $[Cl^-]$ over the concentration range of 0.1–100 mM Cl^- suggesting the formation of a 3:2 $Cl:As^{III}$ species as three electrons are involved in the reduction. It is likely that mixed species of the type $As(OH)_2Cl^0$ and $As(OH)Cl_2^0$ are formed increasingly with higher Cl^- concentration, which could explain this shift. However, kinetic effects may play a role in the rate of formation of these species too.

2.3.5 Mechanism of the adsorption step

As^{III} is reduced at potentials <–0.8 V (Figure 1) so at the more positive deposition potential (0 V) used here, the arsenic is deposited as As^{III}. The pH effect suggests that optimal deposition takes place when $As(OH)_3^0$ or $As(OH)^{4-}$ is predominant. The surface of the gold electrode is kept in reduced condition (Au^0) during the arsenic measurement at potentials < 0.5 V. There are therefore no Au-hydroxide groups on the surface which could have substituted for one of the hydroxyl groups of the $As(OH)_3^0$ to give for instance an Au-O-$As(OH)_2$ inner-sphere complex. The potential of zero charge at the surface of gold is at ~–300 mV in 1 mM NaOH [31], i.e. the electrode is positively charged at the deposition potential of 0 V and negative at potentials < –0.3 V. The positive charge enhances the adsorption of the $As(OH)_3$ at 0Vin the pH range 6–9.5. At pH > 9.5 (Figure 2B), OH^- adsorption on the gold [31] could contribute to the decrease of the As^{III} / As^0 signal. The good response for As^{III} at low chloride levels is consistent with $As(OH)_3^0$ adsorption and it is unlikely that any $As^{III}_x(OH)_yCl_z$ species plays an important role.

The increased response after deposition at potentials < –1.1 V (Figure 1) is due to a different mechanism in which the As^{III} in the diffusion layer at the electrode surface is reduced and accumulated as As^0. The improvement in the deposition rate with increasingly negative potential was ascribed to a further thinning of the diffusion layer due to hydrogen generation. The As^0 is re-oxidised and adsorbed as As^{III} when the electrode potential is switched to 0 V prior to the CSV scan.

2.3.6 Interference by dissolved oxygen (DO)

The reduction current for DO (–0.4 to –0.7 V) overlaps and therefore interferes with the CSV peak for arsenic (at –0.7 V). An increase of the scan rate from low (10 mV s^{-1}) to high (2 V s^{-1}) caused the peak for DO to widen and flatten, due to the poor electrochemical reversibility of the oxygen reduction. A scan rate of 1 V s^{-1} was found to be optimal giving good sensitivity for arsenic and good discrimination against DO. The wide peak for DO was largely removed by background subtraction,

thus producing a peak for arsenic on a flat baseline. The mechanism of doing a background corrected measurement of As^{III} in the presence of DO is shown in Figure 3, showing the analytical scan (60 s adsorption), the background scan (1 s adsorption) and the background-corrected scan in the presence and absence of DO. The DO wave occurs at −0.4 V on the analytical scan. Interestingly, the background-corrected scan shows DO as an anodic peak at −0.4 V because the reduction of DO is largely masked due to partial coating of the electrode with As^{III}.

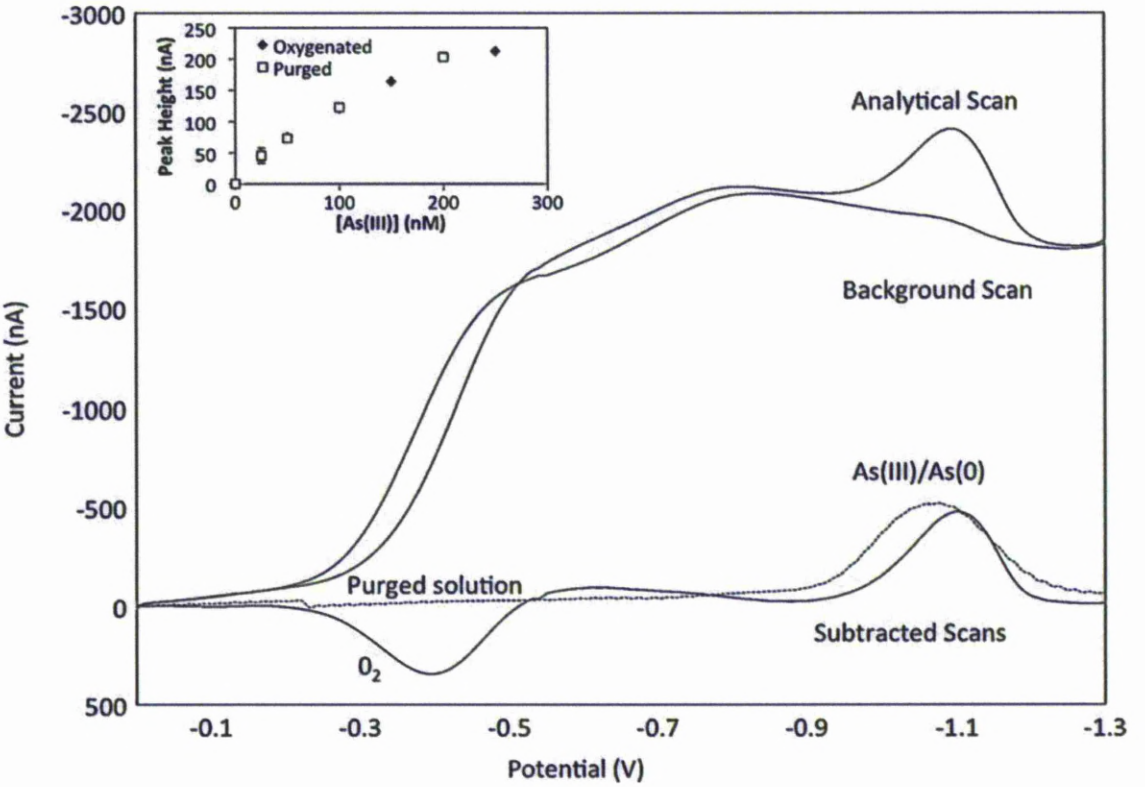

Figure 3. Background correction of the CSV scans for As in waters. The diagram shows the analytical scan (60 s deposition), the background scan (1 s deposition) and the background-corrected scan. The As^{III} peak is free of interference of DO for which a peak occurs at −0.4, 0.7 V more positive than for the As^{III} peak. A background-corrected scan is also shown for the same water after purging to remove DO. The response (peak height) is shown as a function of the As^{III} concentration for purged and unpurged solution in the inset.

2.3.7 Linear range and limit of detection

At a deposition time of 60 s, the CSV peak height was found to increase linearly with the concentration up to 150 nM As^{III} (Figure 2D). At higher concentrations the increase in the peak

height became less and the response flattened to a plateau characteristic of monolayer deposition of As^0 which is non-conductive and thus prevents further deposition of As^{III}. The linear range was extended by decreasing the deposition time, and the sensitivity increased by increasing the deposition time. For instance the response was linear to 300 µM As^{III} using an adsorption time of 0 s, 0.5 µM using 10 s adsorption and 7 nM using 300 s adsorption. The monolayer coverage of the electrode approached in all cases ~$4 \pm 0.5 \times 10^{-10}$ mol cm^{-2}, similar to that found previously [16].

The limit of detection (LoD) was calculated from 3× the standard deviation of eight successive determinations of a low level (3 nM) of As^{III}, using a 60 s deposition time. The standard deviation was 5 %, giving an LoD of 0.5 nM As^{III}. This could be lowered by a factor of 5 in clean, low arsenic waters, by extending the deposition time to 300 s.

2.3.8 Interferences

Various anions and cations were added to evaluate possible interference with the detection of arsenic. Measurements were in deaerated 2 mM KCl set to pH 9 using 0.01 M H_3BO_3 and containing 50 nM As^{III}. No significant effect was noticed up to 0.1 µM iodide, 1 µM bromide, 100 µM fluoride and 1 mM sulphate, but the arsenic signal decreased at higher anion concentrations (Figure 2C) presumably as a result of As^{III} complexation, causing the formation of mixed OH-anion As^{III} species such as $(As(OH)_2F)^0$, $(As(OH)_2Br)^0$ and $(As(OH)_2HSO_4)^0$, analogous to the formation of the mixed OH–Cl species. A major interference was found to be caused by sulphide which was found to cause a 50 % drop in the signal at 200 nM HS^-, either due to HS^- adsorption on the electrode, As^{III} complexation, or both. This could be a problem with analysis of sulphidic groundwaters. Additions of 100 µM Al, 15 µM Mn and 15 µM Fe did not interfere with the peak intensity, but caused the peak potential to shift in a negative direction. No significant interferences were observed from 1 µM Zn, 0.5 µM Bi or 0.2 µM Sb^{III}. Addition of 100 µM As^V did not alter the As^{III} peak, demonstrating that the deposition step is As^{III} specific. Addition of Sb^{III} did not interfere with the As^{III} signal in contrast to its known effect in the ASV procedure [23].

Addition of 10 µM Cu increased the CSV signal for As by 20 % and of 0.2 µM Pb caused the signal to drop by 50 %. Although the change in the peak intensity was small, addition of these metals resulted in a negative shift of the As^{III} peak potential by 10–20 mV $decade^{-1}$. The organo-arsenate compounds, monomethyl arsonate (MMA) and dimethyl arsinate (DMA) did not produce a peak in the CSV mode and were not found to interfere, up to at least 10 µM.

Organic material can interfere due to surfactant or complexation effects. Stepwise addition of humic acid (HA) up to 100 ppm caused a 50 % decrease in the peak for As^{III}. The absence of a peak potential shift suggests that any complex formed was poorly reversible. Addition of 50 ppm FA caused a 50 % decrease in the As^{III} signal. Surfactant effects were tested by addition of the non-ionic surfactant Triton-X-100 and the anionic surfactant SDS; no effect was caused by 10 ppm Triton, much higher than the 0.1 – 1 ppm Triton equivalents of surfactants usually encountered in natural systems [32] and giving better surfactant discrimination than the ASV method [23].

2.3.9 Application to As^{III} determination in natural waters

The CSV method was tested by determining As^{III} in a range of natural waters: raw borehole samples from Severn Trent Water, filtered groundwater samples from West Bengal (India), mineral water (Evian), river water from Snowdonia (Wales, UK), lake water from Ben Nevis (Scotland, UK) and laboratory tap water. The As^{III} concentration was below the limit of detection (~1 nM) in mineral, lake and river water. A CSV peak was obtained in these waters after a 20 nM As^{III} addition, indicating that these water matrices did not interfere with the electrochemical analysis. No signal was obtained for 120 nM As^{III} added to tap water, due to the presence of hypochlorite (ClO^-) which oxidises the As^{III} to As^{V} [23]. The detection limit for As^{III} in the lake and river water was double that in the synthetic borate buffer solution presumably due to interference by natural organics.

Up to 180 nM (14 ppb) inorganic As^{III} was found in the untreated borehole water samples from Severn Trent Water (UK), and up to 705 nM (53 ppb) in samples from West Bengal (Table 1). CSV scans (background-corrected scans) for As^{III} in pure electrolyte can be compared to those in raw

groundwater in Figure 4. It can be seen that the peak potential for As^{III} shows a negative shift in the groundwater compared to that in pure water, of which 150 mV was due to the use of the solid RE and the remainder was ascribed to the cumulative effect of various metal and anions present in the water. Scans are shown for a range of As^{III} additions leading into non-linearity of response, caused by saturation of the electrode surface.

Table 1. Arsenic speciation in groundwaters from various sources. Site W1–H are untreated borehole samples from Severn Trent Water; West Bengal samples were collected in an area with variable high arsenic in wells [33].

Site	As (III)	As(III)	As_{inorg}	$As_{inorg} + As_{org}$	Total As	
	CSV	**ASV**	**ASV**	**UV at pH 7, ASV**	**UV at pH 1, ASV**	**ICP-MS**
Severn Trent						
W1	127 ± 10	137 ± 12	152 ± 7			280
W2	92 ± 14	98 ± 10	151 ± 17			267
AH Blended Raw	130 ± 10	149 ± 17	214 ± 23			227
AH Borehole 1	176 ± 11	186 ± 9	195 ± 16			254
B	<0.9	<1	250 ± 25			254
S	5.2 ± 1	11 ± 1	12 ± 2	154 ± 8	242 ± 12	267
CC	<0.9	<1	39 ± 5	131 ± 11	194 ± 12	200
H	20 ± 1	14 ± 1	98 ± 2	155 ± 10	268 ± 14	294
West Bengal						
AP 5	705 ± 31				721 ± 42	844
AP 1	307 ± 10				350 ± 17	424

The field analysis included addition of 1mMEDTA to prevent iron-hydroxides from precipitating out during the measurement. Concentrations are in nMAs L–1. CSV analyses are at neutral pH, ASV after acidification to pH 1. The CSV method detects reactive As(III); the ASV method detects As(III) or all inorganic As depending on the deposition potential. Asinorg +Asorg is by ASV after UV-digestion at neutral pH; total As is either by ICP-MS, or by ASV after UV-digestion at pH 1; Severn Trent ICP-MS data were from Severn Trent; the West Bengal ICP-MS measurements were carried out by Miran Kalle Uroic (Aberdeen University).

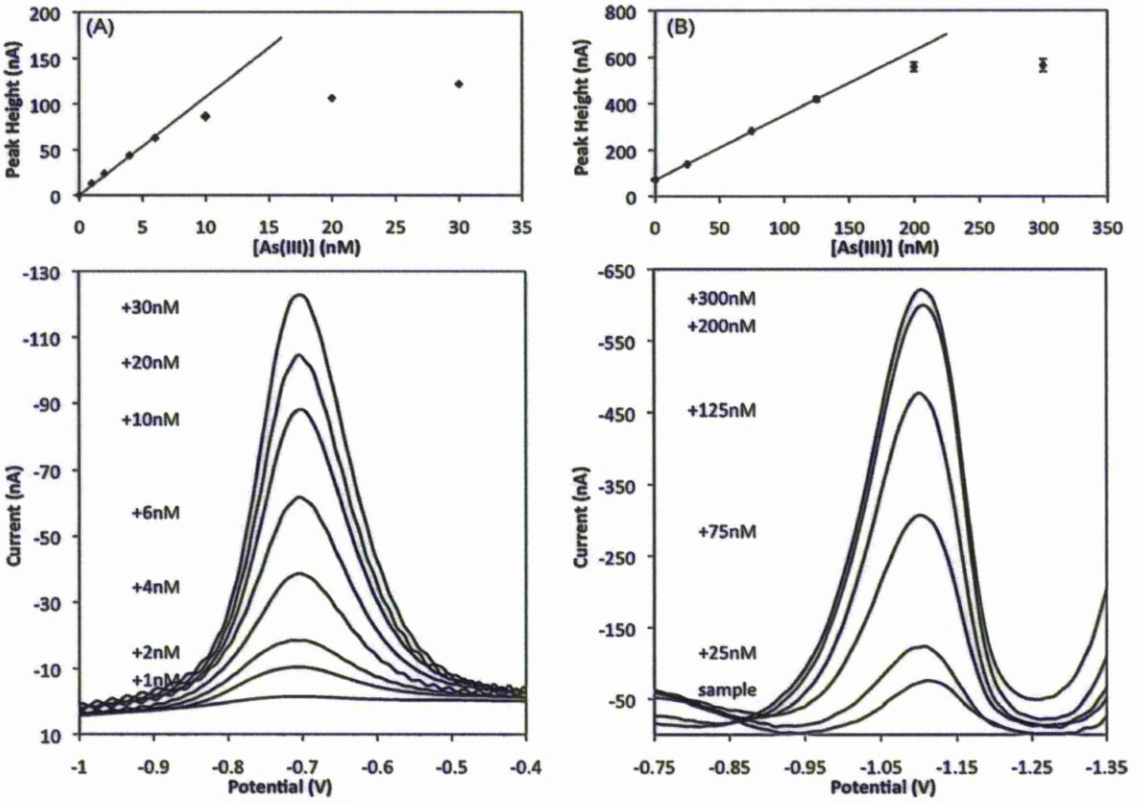

Figure 4. CSV scans for As^{III} in 10 mM KCl/ 0.01 M borate buffer, pH 9 **A)** and raw groundwater **B)**; deposition time 60 s. **A)** As^{III} standard additions. **B)** Scan 1 is for a background level of 20 nM As^{III} in the actual sample; the subsequent scans are for As^{III} additions of 20–300 nM.

2.3.10 Arsenic speciation

The arsenic speciation was determined by determination of reactive As^{III} at the original sample pH (7 – 8) using the CSV method, and compared to the determination of As^{III} and combined As_{inorg} (As^{III} + As^{V}) by ASV at pH 1, before and after UV-digestion at neutral pH. The total concentration of arsenic in some of the samples was determined by ICP-MS and by ASV after UV-digestion at pH 1. The results can be compared in Table 1. The concentration of As^{III} found by the new CSV method was very similar (within 10 %) to that found by the ASV method; however the ASV detected As^{III} was systematically greater by about 10 %. The ASV method measures at pH 1 so it is possible that the lower pH caused some release of As^{III} associated with colloidal or particulate matter.

The As^{III} was the predominant component of the inorganic As in most West Bengal samples if determined immediately upon sampling. In this case, the As^{III} was within 87 – 100 % of the total arsenic, indicating inorganic As^{III} was the dominant species in the samples tested. The As^{III} was found to be unstable upon storage, decreasing with time due to oxidation to As^{V} and adsorption on particulate matter (mostly Fe-hydroxides) [34]. Measurements as a function of time showed that this decrease was slow in the Severn Trent borehole samples (<5 % day^{-1}) compared to the Bengal samples with decreases of up to 90 % day^{-1} due to high levels of iron.

UV-digestion at neutral pH caused an increase in the concentration of inorganic As due to the release of organically bound As, and more organic-bound As was released after UV-digestion at pH 1 (total As). The difference in the results after UV-digestion at neutral pH and pH 1 may be caused by association of inorganic As with particulate Fe-hydroxides at neutral pH which might be released at pH 1. The total As found after UV-digestion at pH 1 was similar to that found by ICP-MS.

2.4. Conclusions

The CSV method for As^{III} in water works in unaltered conditions, i.e. at neutral pH values, in presence of DO and without the need for any reagents. It has a large analytical range, from low to high-arsenic waters. Rather than having to use sample dilution for high-arsenic containing groundwaters, it was found possible to use a very short deposition time. Interferences were found to have only minor effect, major anions and metals causing the peak potential to shift, whereas very high iron levels in originally reducing conditions can cause problems upon sample storage due to coprecipitation of As^{V}. A potential interference for some waters may be due to sulphide, but this was not encountered as a problem in the samples tested here. Because the CSV method measures As^{III} at natural pH and without the need for reagent addition or O_2 removal, it is suitable for monitoring purposes using automated apparatus. Repeated measurements of 130 nM As^{III} in 100 mL of groundwater showed that the CSV signal was stable for 10 h (20 measurements), suggesting that the CSV method can be used for long term monitoring of As^{III} in well water or streams. Preliminary measurements of

samples showed that the speciation of As is obtained by measurement of As^{III} by CSV at neutral pH, and inorganic As^{III} + As^{V} at pH 1 and total As by ASV after UV-digestion. Due to interference by high levels of chloride this method cannot be used in seawater with a salinity >10.

References

[1] M.O. Andreae, Limnol Oceanogr, 24 (1979) 440.
[2] P. Bose, A. Sharma, Water Res, 36 (2002) 4916.
[3] A.D. Redman, D.L. Macalady, D. Ahmann, Environ Sci Technol, 36 (2002) 2889.
[4] W.Y. Zhu, L.Y. Young, N. Yee, M. Serfes, E.D. Rhine, J.R. Reinfelder, Geochim Cosmochim Ac, 72 (2008) 5243.
[5] R.J. Bowell, Appl Geochem, 9 (1994) 279.
[6] H.R. Hansen, A. Raab, J. Feldmann, J Anal Atom Spectrom, 18 (2003) 474.
[7] P.A. Gallagher, C.A. Schwegel, X.Y. Wei, J.T. Creed, J Environ Monitor, 3 (2001) 371.
[8] M.R. Bin othman, J.O. Hill, R.J. Magee, J Electroanal Chem, 168 (1984) 219.
[9] Y. Du, W. Zhao, J.J. Xu, H.Y. Chen, Talanta, 79 (2009) 243.
[10] J. Zima, C.M.G. Van Den Berg, Anal Chim Acta, 289 (1994) 291.
[11] F.G. Bodewig, P. Valenta, H.W. Numberg, Fresen Z Anal Chem, 311 (1982) 187.
[12] J.H. Aldstadt, A.F. Martin, Analyst, 121 (1996) 1387.
[13] H.L. Huang, P.K. Dasgupta, Anal Chim Acta, 380 (1999) 27.
[14] J. Vandenhecke, M. Waeles, P. Le Corre, R.D. Riso, Anal Bioanal Chem, 388 (2007) 929.
[15] R. Feeney, S.P. Kounaves, Anal Chem, 72 (2000) 2222.
[16] A.O. Simm, C.E. Banks, R.G. Compton, Electroanal, 17 (2005) 335.
[17] Y.S. Song, G. Muthuraman, Y.Z. Chen, C.C. Lin, J.M. Zen, Electroanal, 18 (2006) 1763.
[18] X. Dai, O. Nekrassova, M.E. Hyde, R.G. Compton, Anal Chem, 76 (2004) 5924.
[19] G. Forsberg, J.W. Olaughlin, R.G. Megargle, S.R. Koirtyohann, Anal Chem, 47 (1975) 1586.
[20] F. Marken, L. Rassaei, M. Sillanpaeae, R.W. French, R.G. Compton, Electroanal, 20 (2008) 1286.
[21] D. Yamada, T.A. Ivandini, M. Komatsu, A. Fujishima, Y. Einaga, J Electroanal Chem, 615 (2008) 145.
[22] Y.X. Liu, W.Z. Wei, Electrochem Commun, 10 (2008) 872.
[23] P. Salaun, B. Planer-Friedrich, C.M.G. van den Berg, Anal Chim Acta, 585 (2007) 312.
[24] P. Salaun, C.M.G. van den Berg, Anal Chem, 78 (2006) 5052.
[25] M.A. Nolan, S.H. Tan, S.P. Kounaves, Anal Chem, 69 (1997) 1244.
[26] C.S. Chapman, C.M.G. van den Berg, Electroanal, 19 (2007) 1347.
[27] F. Brusciotti, P. Duby, Electrochim Acta, 52 (2007) 6644.
[28] Z.C.S. J. Lipkowski, A.C. Chen, B. Pettinger, C. Bilger,, Proceedings of the 7th International Fischer Symposium on Scales in Electrochemical Systems—from Angstroms to Meters, Karlsruhe, Germany, 1997, p. 2875.
[29] W.Z. Wei, Y.X. Liu, Electrochem Commun, 10 (2008) 872.
[30] M. Sadiq, T.H. Zaidi, A.A. Mian, Water Air Soil Poll, 20 (1983) 369.
[31] D.D. Bode, T.N. Andersen, H. Eyring, J Phys Chem-Us, 71 (1967) 792.
[32] B. Cosovic, V. Vojvodic, Mar Chem, 22 (1987) 363.
[33] J.M. McArthur, P. Ravenscroft, D.M. Banerjee, J. Milsom, K.A. Hudson-Edwards, S. Sengupta, C. Bristow, A. Sarkar, S. Tonkin, R. Purohit, Water Resour Res, 44 (2008).
[34] R. Nickson, J. McArthur, W. Burgess, K.M. Ahmed, P. Ravenscroft, M. Rahman, Nature, 395 (1998) 33.

3

Chapter 3

VOLTAMMETRIC DETERMINATION OF ARSENIC IN HIGH IRON AND MANGANESE GROUNDWATERS

3. VOLTAMMETRIC DETERMINATION OF ARSENIC IN HIGH IRON AND MANGANESE GROUNDWATERS

3.1. Introduction

Inorganic arsenic (As) pollution of drinking water is a global hazard [1] with new areas of contamination regularly reported [2]. West Bengal (India) and Bangladesh where millions of people consume water from shallow tube wells is the most reported on account of the population affected [3]. This contamination has been described by the World Health Organisation (WHO) as 'the largest poisoning of a population in history' [4]. Long term exposure to arsenic in drinking water has been identified as a cause of skin lesions [5] as well as large numbers of bladder, lung, kidney and skin cancers [6]. Increased awareness of chronic exposure has meant the national Indian drinking water limit of 50 μg L^{-1} (0.7 μM) of As, has now been deemed unsafe by WHO, with a provisional guideline value of 10 μg L^{-1} (0.13 μM) As. The As problem has recently been reviewed [7].

In groundwaters inorganic forms of arsenic, arsenite (As^{III}) and arsenate (As^{V}), dominate, whilst organic arsenic compounds, methylarsonic acid (MMA) and dimethyl arsinic acid (DMA), form a negligible percentage of the total arsenic [8]. It is essential to determine the speciation of arsenic in groundwater for its effects on geochemical mobility in groundwater and the uptake of arsenic by plants.

Stable arsenic species are commonly determined in the laboratory by hyphenated techniques coupling liquid chromatography (LC) to inductively coupled plasma mass spectrometry (ICP-MS) or atomic absorption/fluorescence spectroscopy (AAS/AFS) [9]. Sampling, storage and transport are required prior to the analysis in the laboratory, and each step may affect the original arsenic speciation [10]. For this reason field measurement of As species has major advantages related to immediate assessment of water toxicity, the possibility of direct mitigation action and prevention of changes in speciation during sample storage.

Instrumentation for voltammetric analysis is portable andtherefore suitable for on-site speciation, which makes it possible to evaluate water quality without sample transport. Voltammetric procedures to determine As^{III} in water have existed for a long time [11] and use either a mercury drop or a gold electrode, and are based on cathodic (CSV) [12, 13], or anodic stripping voltammetry (ASV) [14-16]. ASV using a mercury drop electrode has been used before for on-site As^{III} determination [17]. However, these methods require a chemical reduction step involving sample heating to determine total dissolved As, which is inconvenient in the field and has concomitant instability of the generated As^{III}. A recently developed method using a gold, microwire, electrode is very sensitive and can be used to determine As^{III} at natural pH in CSV mode [18], and combined (As^{III} + As^{V}) by ASV after mild acidification to pH 1 [19]. The CSV method has advantages for As^{III} measurement in the field as it is insensitive to interference by dissolved oxygen or copper [18], and should not require any reagents.

In regions of West Bengal there are near neutral-pH, reducing groundwaters, where As is released via reductive dissolution from oxides, especially iron oxyhydroxides (FeOOH) [20]. These waters have a specific chemical signature, with high levels of reduced species such as As^{III}, ferrous iron (Fe^{II}) and dissolved organic carbon (DOC) as well as high bicarbonate in solution [21]. Low As (<130 nM) waters in this region are associated with high levels of Mn [22]. The As in these waters appears to be predominantly As^{III} [14], with only a very minor proportion of organic As (<5 %) [23]. These waters were selected to validate the new CSV method [18] in a study of arsenic speciation.

Preliminary attempts at measuring the concentration of As^{III} in samples of these waters revealed a major interference making it impossible to obtain a signal for arsenic. Experiments in this work reveal that the interference was directly related to high micromolar levels of Fe and Mn, which were found to lower the response for As^{III}, and finally block it altogether. This work shows that the interference is eliminated by addition of ethylenediaminetetraacetic acid (EDTA) resulting in an improved CSV procedure suitable for arsenic in any waters. The experiments demonstrating the cause of the interference and its subsequent elimination using EDTA are described here. The new

method is applied in the field to groundwaters in West Bengal (India), and the results compared to reference analyses using conventional laboratory techniques.

EDTA and sample acidification with HCl have been used before to preserve the As speciation for extended sample storage with conflicting results [24, 25]. In the course of this work, the effectiveness of these two preservation methods is tested by comparison of analyses of samples in the field to those of preserved samples.

3.2. Experimental

3.2.1 Study area

Groundwaters were collected from the contiguous villages of Ardevok and Moyna in southern West Bengal at 22°44.43N, 88°29.450E (Indian/Bangladesh datum) in 24-Parganas (North) district, on the northern periurban fringe of the town of Barasat. The geology and groundwater composition, speciation apart, is described in [22]. This area was selected because of the level of detail on local geology, hydrogeology, and groundwater composition afforded by these prior studies. In the region, two connected aquifers exist. To the northeast is a palaeo-interfluvial aquifer of brown sand capped by a regional palaeosol: its groundwater is low in arsenic (<10 nM As) and high in manganese (>25 µM Mn), as the aquifer is poised at the stage of Mn-reduction. In the remainder of the study area is a palaeo-channel aquifer of grey sand that hosts water that is high in iron (20–140 µM Fe) and high in arsenic (>0.5–7 µM As): this part of the aquifer has experienced a considerable amount of Fe-reduction. In both water types, concentrations of bicarbonate are typically 8–16 mM as a result of microbial metabolism of organic matter.

3.2.2 Reagents

Solutions were made using 18 MΩ cm Milli-Q water (MQ). A 10^{-2} M As^{III} stock solution was prepared from As_2O_3 (purity 99.5 %, AnalaR, BDH Chemicals Ltd., England), acidified with HCl to pH 2 and

wrapped in aluminium foil to prevent photochemical oxidation. Standard solutions with concentrations 10^{-3}, 10^{-4}, 10^{-5} and 10^{-6} M As^{III} were prepared freshly every month at pH 2. H_2SO_4 (0.5 M) used for conditioning of the electrode was from BDH (AnalaR grade). Solutions of Fe^{II} and Mn^{II} (1 mM each) were prepared daily in deoxygenated MQ from $Fe^{II}Cl_2 \cdot 4H_2O$ and $Mn^{II}Cl_2 \cdot 4H_2O$ (BDH chemicals Ltd., England) acidified to 0.01 M HCl. The HCl was purified by sub-boiling distillation of commercially available AR grade HCl (Fisher Scientific) on a silica condenser. A 0.5 M stock solution of EDTA was prepared from the EDTA, disodium salt (purity 99.5 %, AnalaR, BDH Chemicals Ltd., England) and adjusted to pH 9 using NaOH.

A multielement standard for ICP-MS calibration was made up from single element ICP-MS standards (High Purity Standards, Charleston, SC) and diluted using water (18 MΩ cm) from an ELGA (Marlow, UK) system, and acidified using nitric acid (65 %, Fluka, Suprapure). Dimethylarsinate (DMA(V), $(CH_3)_2AsO_2Na$), 98 %, Strem Chemicals UK) was used for the quantification of all arsenic species due to the species-independent arsenic response of the ICP-MS.

3.2.3 Sample collection and pre-treatment

Ground water samples were collected in acid washed, Nalgene, low-density, polyethylene bottles from 23 hand-pumped domestic wells, or from clusters of wells forming two piezometers nests across the As gradient, covering an area of 750 m × 450 m, shown in a map [22]. Sampling from piezometer nests allowed the distribution of As and its speciation to be determined as a function of depth.

All samples were taken back to the laboratory for later analysis to check for stability and for comparison against other analytical methods. The following elements were determined in all samples: As^{III}, arsenate (As^{V}), total As, Mn, Fe, and copper (Cu). Samples from artesian wells were left unfiltered and were acidified to pH 1 with HCl to a final concentration of 0.1 M for later determination of total As, Fe and Mn. Piezometer samples (0.5 L) were extracted using a surface-mounted vacuum pump that sampled from 1 m above the top of the well screen in each of the

boreholes in the piezometer nests. In each case the water was pumped until clear and was then filtered through 0.45 µm acetate membrane filters; 10 mM EDTA was added (final pH 9) to these samples and they were stored at room temperature. To investigate changes in speciation upon storage 23 samples were stored with HCl and 12 with EDTA.

3.2.4 Instrumentation

Voltammetric measurements in the field utilised a battery powered (dry, 10 Ah, 6 V) Palmsens potentiostat (Palmsens, Netherlands) controlled by Ivium software (Palmsens). The software had been modified to enable automation of the measurements. The working electrode (WE) was a 25 µm diameter, gold microwire (2 mm long, 99.99 %, hard, Goodfellow), and the counter electrode (CE) was a 200 µm iridium wire (3 mm long, Goodfellow) [19, 26]. The Ag/AgCl reference electrode (RE) was a solid state pseudo-reference electrode, and was made from a 1.5 mm diameter, 2.5 cm, Ag wire (99.99 %, Rasmussen AS, Norway) [27]. To enable on-site detection, a vibrator was attached to the combined electrode [18, 28], which had a cable length of 6 m. In the laboratory the vibrating electrode was fitted in a Metrohm VA696 stand, controlled by a µAutolab(III) potentiostat (Ecochemie, Netherlands) and GPES software. In this case the reference electrode was double junction, Ag/AgCl(s), 3 M KCl.

1.1.1.7 Total As (As_T)

Inductively coupled plasma mass spectrometry (ICP-MS) (Agilent 7500c, Agilent Technologies, Tokyo, Japan) was used in normal mode for elemental determinations. The elements Mn (m/z 55), Fe (m/z 56 and 57), Cu (m/z 63), As (m/z 75), Sb (m/z 121), and as internal standard In (m/z 115), were recorded. All standards and samples were acidified with HNO3 to 1 % HNO_3. Calibration was with an external multi element calibration standard. The internal standard showed a decrease in signal intensity, so correction was necessary. Correction was made by dividing all counts per seconds (cps) of each standard and sample by the cps of the internal standard. The limit of detection (LOD) for

each element was: Mn 20 nM, Fe 35 nM, Cu 8 nM, As 5 nM and Sb 0.5 nM (3σ of blank). The determined As was defined as the total As (As_T) concentration.

1.1.1.8 Arsenic speciation by HPLC–ICP-MS

An Agilent 1100 HPLC system coupled to an Agilent 7500c ICP-MS was used to determine inorganic As^{III} (As^{III}_{HPLC}) and inorganic As^{V} (As^{V}_{HPLC}). The HPLC flow was set to 1 mL min^{-1} with an isocratic buffer (10 mM phosphate at pH 6.2). 50 µL of standard and sample were injected onto a PRP-X 100 anion exchange column (250 × 4.1 mm I.D., 10 µm, Hamilton, Reno, NV) tempered at 20°C. Chloride interference and selenium were measured at m/z 77 and 82, and indium was used as an internal standard and measured at m/z 115. Internal standard showed no decrease in signa intensity, therefore no correction was necessary. The LOD for arsenic was 25 nM (3σ of blank).

3.2.5 Voltammetric procedures for arsenic speciation: Electrode conditioning

The microwire WE was cleaned in 0.5 M H_2SO_4 by hydrogen generation at −1.7 V (15 s), when the electrode was new, or when fouling was suspected. Subsequently optimum behaviour of the electrode was tested in the same solution by cyclic voltammetry (3 scans) from 0 to 1.5 V (100 mV s^{-1}). In these scans the height and symmetry of the Au/Au_2O_3 reduction peak gives an indication of how the electrode is working, for example a shoulder on the negative side of the reduction peak can correspond to poor signal and a loss in peak height a loss of part of the electrode surface.

3.2.6 Reactive arsenite determination by CSV

Reactive As^{III} was determined immediately upon sampling by CSV [18]. The reactive As^{III} (As^{III}_R) is defined by the species $As(OH)_3^0$, which is detected by the CSV method and which is the predominant species in freshwaters of neutral pH. The $As(OH)_3^0$ represents detected inorganic As^{III} due to rapid interconversion of hydroxide species, whilst any organic As^{III} species would behave electrochemically inert towards CSV and are not detected. The water samples were analysed on-site immediately after sampling without deaeration and without addition of buffer or electrolyte, unless indicated. EDTA

(10 mM) was added to prevent interference by high levels of iron and manganese present in most samples. Voltammetric conditions were: E_{cond} = 0.55 V (10 s), E_{dep} = 0 V (60 s), t_{eq} =3 s, stripping from 0 to −1.5 V at 1 V s^{-1}, step height 10 mV. The sensitivity was calibrated by addition of As^{III} to the sample aliquot (50 mL) in the cell (a polyethylene beaker).

Comparative measurements of arsenite (As^{III}_{ASV}) were made by ASV [19] in the laboratory in samples which had been stored ~1 month with 0.1 M HCl, or with 10 mM EDTA (in this case 0.1 M HCl was added prior to analysis): E_{cond} = 0.55 V (5 s), E_{dep} = −0.4 V (60 s), t_{eq} =3 s, scan from −0.5 to 0.5 V, using the square-wave modulation (50 Hz, step size 8 mV, pulse height 50 mV). Calibration was by addition of As^{III} standard to the sample in the voltammetric cell sufficient to at least double the initial peak current. The thus detected As^{III} would include organic complexes (if they occur) if they dissociate upon acidification. Organic As-compounds (MMA and DMA) are not included in this fraction.

3.2.7 Combined inorganic arsenic

The combined concentration of inorganic arsenic, As_{inorg} (As^{V} + As^{III}), was determined by ASV of acidified samples (0.1 M HCl) in the laboratory and in the field using the same measuring conditions as for As^{III} except with a more negative deposition potential of −1.2 V (60 s). Samples with high levels of arsenic (>1 µM) were diluted with 0.1 M HCl. Any MMA and DMA would be included in this fraction at a reduced sensitivity (50 % lower for MMA and 70 % lower for DMA) [19], but not stable, covalent, organic species.

3.2.8 Use of EDTA to eliminate interference of Fe and Mn with As speciation by CSV

The effect of EDTA on interference by Fe and Mn on CSV of As^{III} was tested in model solutions containing 10 mM borate pH buffer (pH 8.9), 2 mM KCl and 20 nM As^{III}. Fe was added as Fe^{II} from 1 µM to 2 mM at varying concentrations of EDTA whilst measuring the CSV response for As^{III} using a deposition time of 30 s. The solution was nitrogen-purged to ensure that the added Fe^{II} remained in the reduced state. Similar experiments were carried out with Mn^{II}.

3.2.9 Species stability experiment in the field

The concentration of As^{III}_R and As_{inorg} were monitored as a function of time after collection of a large unfiltered water sample (20 L) from a deep well (station 5) which was left exposed to the sun from 8 AM. The original concentration of As_{inorg} was 320 nM (25 μg L^{-1}) which was 99 % As^{III}_R. Sub-samples were taken at ~hourly intervals, and subjected to immediate analysis of As^{III}_R (CSV, pH 8.8, with 10 mM EDTA) and As_{inorg} (ASV, 0.1 M HCl).

3.3. Results and discussion

Preliminary measurements of reactive arsenic (As^{III}_R) in groundwaters, some of which very high (>500 μM) in Fe and Mn, were found to be impossible due to interference with the CSV signal. Good sensitivity was obtained in model groundwaters with only low levels of Fe or Mn, but additions of Fe and Mn caused the CSV response for As to diminish to zero. Figure 1 shows that the response for As is fully depressed at Fe and Mn >30 μM.

Even higher levels of either Fe or Mn are typical for these groundwaters and were the cause of the lack of a CSV signal for As. The high Fe in the groundwaters occurred as Fe^{II} as it originated from reductive dissolution from As bearing Fe-hydroxides, in response to ingress of organic matter [22]. We hypothesise that, during the voltammetric measurement, the Fe^{II} becomes oxidised to Fe^{III}-hydroxide at the surface of the electrode, thus blocking the surface. For instance, the conditioning potential of 0.55 V is amply sufficient to oxidise Fe^{II} and Mn^{II} to their more oxidised, insoluble, state, causing them to precipitate on the electrode surface. If this mechanism is true, then addition of a strong chelating agent should be sufficient to eliminate this problem. Preliminary experiments using EDTA were successful and optimisation of this method is reported here.

Addition of EDTA, whilst repeating the gradual additions of Fe, caused the decrease in the CSV response to move to higher Fe concentrations as any oxidised Fe became complexed and remained dissolved (Figure 1A). At 10 mM EDTA the CSV response was unaffected until 500 μM Fe, whilst for

20 mM EDTA the response was unaffected until 1.5 mM Fe (Figure 1A). The effect of adding EDTA on the interference by Mn was similar to that of Fe (Figure 1B). Up to 0.6 mM Mn was tolerated for 10 mM EDTA and up to 1.5 mM for 20 mM EDTA. The concentrations of Fe and Mn where the interference occurs are high, but these high concentrations are typical for ground waters affected by organic matter causing anoxia [22]. Addition of 10 mM EDTA was selected for CSV of As^{III} in the high-iron groundwaters from West Bengal, as this was found to be sufficient to eliminate the iron interference and to stabilise the CSV response for most samples.

The stable CSV response suggested that, in addition to resolving the interference, the effect of EDTA on retaining oxidised Fe and Mn species in solution could stabilise the As speciation of the water samples for extended sample storage. Further measurements in the field were used to confirm the predominant species of As in freshly collected groundwaters, and samples were stored in the presence of either EDTA or acid to verify successful stabilisation of the As speciation.

The quantitative elimination of the CSV signal for As with increasing levels of Fe and Mn, and its amelioration by addition of EDTA, are evidence that Fe and Mn are the cause for the interference in these groundwaters. It is likely that their oxides precipitate on the surface of the electrode during the conditioning step at 0.5 V. Apparently, in the absence of EDTA, the oxides remained on the electrode, physically blocking access of arsenite ions during the deposition step. The CSV response was stabilised by EDTA because this kept the oxidation products in solution. The stable CSV response for $As(OH)_3^0$ at 10 mM EDTA suggests that the dissolved arsenite speciation was also stabilised, because the oxidised Fe did not form a solid, adsorptive, hydroxide. The arsenite stabilisation was verified with measurements in samples after prolonged storage, which is shown below.

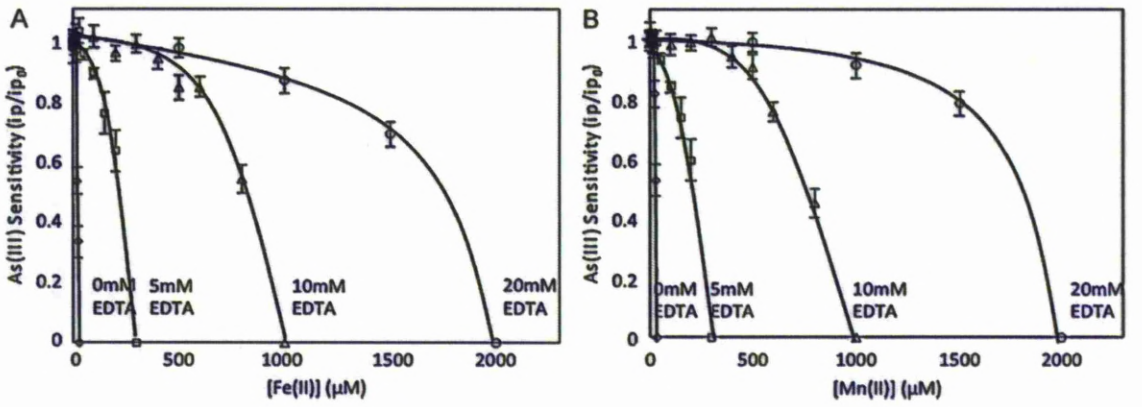

Figure 1. Effect of varying the concentration of EDTA on interference of Fe and Mn with the determination of As^{III} in freshwaters. **A)** CSV sensitivity for As^{III} as a function of the Fe concentration. **B)** CSV sensitivity for As^{III} as a function of the Mn concentration. The interference of very high Fe and Mn in groundwaters is eliminated at 10–20 mM EDTA.

3.3.1 Arsenic distribution in groundwaters of the field site in West Bengal

The speciation of As was determined before and after sample storage to verify whether 1) the speciation, and 2) the total concentration of arsenic, can be preserved for long-term storage, and to determine the rate of change in the speciation in unpreserved samples. The water composition with respect to metals (Fe, Mn and Cu) was determined by ICP-MS in acidified aliquots and is shown along the As speciation in Table 1. Levels of Fe were found to range from 4 to 141 µM (0.2–8 mg L^{-1}), of Mn from 0.8 to 45 µM (0.03–2.4 mg L^{-1}), and of Cu from 4 nM to 1.3 µM (0.2–80 µg L^{-1}).The concentration and distribution of Mn, Fe and total As are similar to those found previously on the same site [22]. The previous work showed that high As was associated with high Fe and low As with high Mn.

Two depth profiles were constituted from piezometric wells drilled to different depths closely together, at a low As- and a high As-site (DP and AP, for locations see map [22]). The total As in the depth profiles was found to vary between 10 and 98 nM (0.8 and 7 µg L^{-1}) at station DP (a low-As site) and between 0.15 and 7 µM (11 and 512 µg L^{-1}) at station AP (a high-As site). Total As was highest (98 nM) at greatest depth in the deepest sample of DP (56 m), whilst it was highest (7 µM) at intermediate depth (21 m) of site AP (Figure 2).

Table 1. Speciation of arsenic and general composition of the groundwater; <values were below the indicated limit of detection; – indicates a % for both values below the limit of detection.

				Voltammetry					HPLC				ICP-MS			
Date Collected	Site	Depth (m)	pH	$As(III)_{CSV}$ (nM) On-site	$As(III)_{ASV}$ (nM) lab	$As(III)+(V)_{ASV}$ (nM) lab	% As(III) on-site	% As(III) lab	As(III) (nM)	As(V) (nM)	sum total (nM)	% As(III)	As (nM)	Fe57 (μM)	Cu (nM)	Mn (μM)
07/03/2009	4	45.7	7.0	1491±80	1350±95	1480±75	101	92	1267	210	1476	86	1534	82	456	8
	41	32.3	7.0	13±3	12±1	19±2	71	64	< 25	< 25	< 25	-	16	7	6	45
	13	44.5	6.9	1710±16	860±60	2390±170	71	36	234	2208	2440	10	2043	6	5	19
	17	43.9	7.3	12±3	< 1	16±2	75	-	< 25	< 25	< 25	-	12	6	10	34
	39	49.4	7.2	40±5	40±3	40±3	100	100	44	< 25	44	100	16	11	13	14
08/03/2009	15	48.8	6.9	15±1	< 1	15±2	-	-	< 25	< 25	< 25	-	17	7	13	45
	16	33.5	6.9	1998±26	1260±90	2290±160	88	55	785	1511	2295	34	2288	35	11	45
	18	44.2	7.0	11±1	< 1	12±2	91	-	< 25	< 25	< 25	-	11.2	4	8	28
	43	43.3	7.1	11±1	8±2	13±1	84	60	< 25	< 25	< 25	-	12.3	4.4	16	34
	3	18.3	7.1	12700±680	9310±625	13400±940	95	70	3265	11253	14503	23	17035	96	1272	0.7
09/03/2009	10	42.7	7.0	12±1	7±1	12±1	100	56	< 25	< 25	< 25	-	14	22	11	28
	32	29.3	7.0	1880±190	1660±116	1880±132	100	89	1508	233	1739	87	2072	116	171	0.9
	38	41.1	7.1	5540±300	5530±390	6110±430	91	91	5500	640	6133	90	7182	141	523	1.5
	30	39.6	7.1	817±42	650±45	930±65	88	70	432	553	984	44	881	5	6	12
	27	41.1	7.0	500±14	490±35	610±43	82	81	522	76	597	87	544	10	4	10
11/03/2009	21	33.5	7.0	4350±65	4170±290	5530±388	79	75	4042	1531	5568	73	6851	112	261	0.6
	7	45.7	7.0	6840±35	6680±470	7690±539	89	87	6707	1074	7773	86	8073	53	303	0.3
	24	39.6	7.0	5780±150	5160±360	6040±423	96	86	5501	636	6131	90	6966	107	442	0.7
	20	33.5	7.0	5700±130	5320±370	6080.±425	94	87	5321	750	6065	88	6288	56	358	0.5
	1a	137.2	6.90	110±5	98±7	160±11	69	62	138	104	242	42	138	20	27	2
	5	115.8	7.15	350±31	390±30	395±28	89	100	415	< 25	421	100	415	33	11	3
	23	125	7.28	20±3	13±2	24±2	83	56	22	< 25	< 25	-	22	15	32	2
	300		7.30	43±5	34±3	37±3	100	92	38	< 25	38	100	38	8	53	1.5

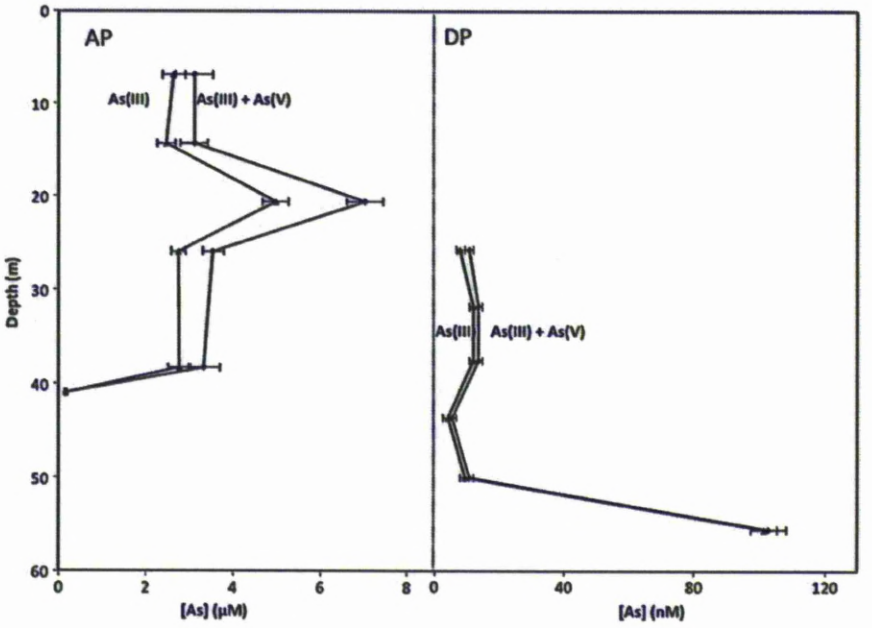

Figure 2. Speciation of As as a function of depth in adjacent piezometric wells drilled to different depths. Site **AP:** high-As, high-Fe waters; site **DP:** low-As, high-Mn waters.

3.3.2 Rapid changes in the speciation and concentration of As upon well-water exposure to air–oxygen and sunlight

The concentration of As^{III} and inorganic As (As_{inorg}) were monitored as a function of time after collection of a large unfiltered water sample (20 L) from deep well 5 which was left exposed to the sun from 8 AM. The original concentration of inorganic As was 320 nM (25 µg L^{-1}) which was 99 % As^{III}. Sub-samples were taken at ~hourly intervals, and subjected to immediate analysis. The As^{III} concentration was found to rapidly decrease, its concentration dropping by ca 70 % within an hour (Figure 3), and dropping to zero after 5 h. Inorganic As was found to decrease more slowly withtime (loss of 75 % in 10 h) indicating that As^{III} is first rapidly oxidised to As^{V} and As^{V} is subsequently removed from the solution by adsorption on newly formed Fe and Mn oxides. The concentration of dissolved Fe was not monitored during this experiment, but visual inspection showed that flocs of Fe(III)-hydroxides started to form from about 1 to 2 h, indicating that the process of Fe-oxidation

overlapped with that of As-oxidation, suggesting that Fe-oxidation may have catalysed the As-oxidation.

The rapid removal of As from groundwater, and its oxidation to As^{V} (Figure 3), illustrate the importance of either stabilising the sample immediately (EDTA, acid) and/or analysing the sample immediately after collection. The rapid As^{III} oxidation can be due to a combination of several parameters. Thermodynamically driven oxidation by atmospheric oxygen can take days [29] so it is likely that this is not the main driver. The oxidation could be stimulated by solar irradiation, previous work showing a 54 % oxidation of As^{III} within 45 min [30]. The rate of oxidation is known to be increased in the presence of Fe^{III} due to charge transfer to radicals from iron oxides [31]. Fe^{III} can then adsorb and co-precipitate the As^{V}, which is in agreement with our experimental field data. Bacterial activity may also be a contributory factor, as it has been reported to oxidise and remove As^{III} in the presence of Fe^{II} and Mn^{II} [32].

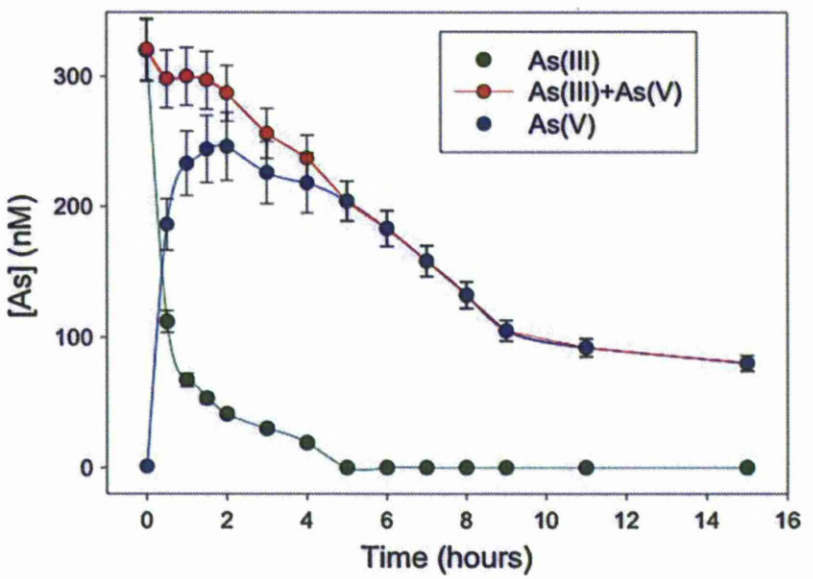

Figure 3. Changes in the arsenic speciation as a function of exposure time to air and sunlight, of a freshly collected, 10 L, well sample.

Subsequent to the As oxidation, precipitation of Fe-hydroxides removed the arsenate out of solution. A settlement and decantation method has previously been recommended as a simple method to reduce As pollution [33], and our data shows that this should be effective.

The subsequent study of arsenic speciation in the field was carried out immediately after sample collection and using EDTA to eliminate Fe and Mn interference and oxidative As removal. for the reduction of As to As^{III} is subject to further research, but it is currently thought to be a microbiological phenomenon [32].

Comparison of the $As^{III}{}_{R}$ (CSV) and combined inorganic As (As^{III} + As^{V}) data (ASV) shows that on average 14 % of the inorganic As was As^{V}. However in-spite of the systematic difference between $As^{III}{}_{R}$ and inorganic As, the $As^{III}{}_{R}$ in several samples amounted to 100 % of the combined As (Table 1). The short-term sample exposure experiment (Figure 3) shows that the speciation in unpreserved samples changes rapidly, suggesting that some of the As^{III} may have become oxidised to As^{V} between sample collection and stabilisation by addition of acid or EDTA, which may have contributed to the systematic presence of As^{V} in the stored samples.

The ASV data showed that As_{inorg} was 91 ± 1 % of total As (Figure 4B).The high proportion of inorganic As leaves only a small fraction (up to 9 ± 1 %) of the As in a non-labile, probably organic, species. Organic arsenic species were not detected by the HPLC–ICP-MS measurements, suggesting that the small difference between total (ICP-MS) and inorganic As was due to a systematic difference between the two different techniques, or to undetected complexation with humic substances in the groundwaters.

Samples from various depths in adjacent piezometric wells showed a larger spread in the As^{III} % than those from the other wells, with a range from 32 to 106 %, and an average of 77 %. A possible reason for the greater spread is that the piezometric wells are rarely used so the water may be subjected to air for longer or mixing during sampling.

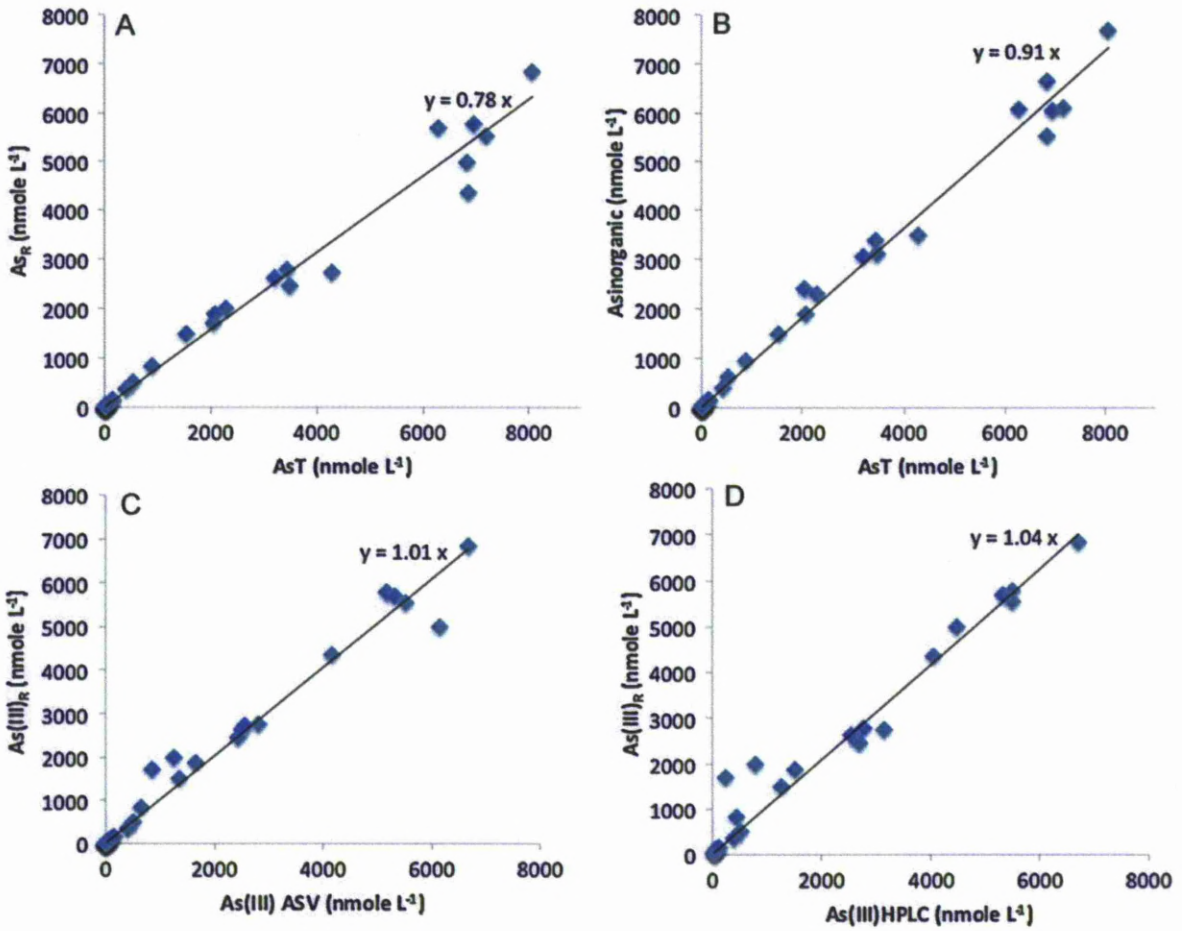

Figure 4. Effect of sample storage on arsenic concentration and speciation by comparison of measurement in the field to that in the laboratory. **A)** Reactive As^{III} (CSV in the field) vs. total As (ICP-MS); **B)** inorganic As (ASV, lab) vs. total As; **C)** Reactive As^{III} (field) vs. As^{III} (ASV in the laboratory) and **D)** reactive As^{III} (field) vs. As^{III} (HPLC in the laboratory).

3.3.3. Comparison of the speciation determined in the field to that in the laboratory

The inorganic As^{III} detected as As^{III}_R in the field was essentially the same as that found by the ASV method in the laboratory (As^{III}_R = 101 ± 2 % of As^{III}_{ASV}) (Figure 4C). It was also the same as that found using the reference HPLC–ICP-MS method (As^{III}_R = (1.04 ± 0.03) × As^{III}_{HPLC}, n = 22) (Figure 4D). These data show that the field measurement of inorganic As^{III} by CSV is in excellent agreement with data obtained by reference techniques in the laboratory.

The field data for inorganic As (As^{III}_R) were produced by CSV using battery powered apparatus. The close co-variation between the As^{III}_R with that of total arsenic (slope 0.78 ± 0.02), indicates that the

field-measured As^{III}_{R} can be used as predictor of the total As in the samples. This finding much facilitates the monitoring of arsenic in the field. The reason for the good agreement is, that the reduced As is the predominant form of As in these samples, and that the reduced As occurs as $As(OH)_3^0$, which is the species detected by the CSV method.

An alternative to CSV is ASV [19], which can also be carried out in the field using the same apparatus as used here. The ASV method was used here to monitor total As during the short-term storage experiment. ASV requires addition of HCl: it was not possible to transport the HCl by air to the field and we could acquire this locally only in the course of this study. CSV was selected for the measurement of As^{III} because this is measured at near natural pH and it was initially thought this would be the best way to retain the original speciation. It was initially hoped that the CSV method would be reagentless, but it was found to require EDTA to eliminate Fe interference. The use of EDTA in the field presented no problem as the EDTA is readily shipped or carried as hand luggage. In the event, the As^{III} found by CSV in the field was the same as that found by ASV in stored samples, because the HCl was found to stabilise the As^{III}.

The ASV method was found to suffer from interference from Cu and Fe(II): the peak for Cu (at 0 V) overlaps that for As (at −0.2 V) at high Cu concentration (>100 nM Cu) and several samples were found to have a greater concentration of Cu (Table 1). This Cu interference is a known problem for As^{III} detection by ASV using gold electrodes [19, 34, 35]. High levels of Fe (>50 µM) as Fe^{II} were also found to interfere with the ASV method, lowering the ASV sensitivity for As. Both interferences were resolved by sample dilution with 0.1 M HCl.

The sensitivity of the CSV method for As in groundwaters was less than in model solutions due to competitive adsorption of organic matter on the electrode. As a result the limit of detection was 3 nM As^{III}_{R} (90 s adsorption time, determined in a sample containing 10 nM As^{III}_{R}) compared to 0.5 nM As^{III}_{R} in model solutions [18].

Advantages of the CSV method are a longer linear range, no interference by Cu, and elimination of the Fe interference by the EDTA addition up to 1 mM Fe, so dilution was required for only a few samples. So, though both CSV and ASV can be used in the field for detection of As^{III} in groundwaters, the CSV method has advantages.

3.3.4 Sample storage of the As speciation

The close agreement between the As^{III} found in the field by CSV and that found by ASV in samples stored for a month (As^{III}_{R} = 101 ± 1 % of As^{III}_{ASV}) (Figure 4C) shows that the As^{III} was successfully stabilised by either 0.1 M HCl or 10 mM EDTA. This was confirmed by the HPLC–ICP-MS data, which agreed within 4 %. This work therefore confirms the previous finding that As^{III} is stabilised by addition of EDTA [24, 25].

The mechanism of the As^{III} stabilisation by EDTA is probably through the complexation and solubilisation of the Fe and Mn species, thus preventing the formation of reactive hydroxide species. The long term stabilisation without the addition of bactericidal agents, suggests that changes in the Fe redox speciation are the main agent catalysing the As^{III} oxidation in these groundwaters, although bacterial activity is thought to play a role in other waters [32]. Photochemical effects (if any) were largely excluded, as the samples were stored in polyethylene bottles.

3.3.5 Storage effects on total arsenic

Total inorganic arsenic measured within 1 month (either on-site or in the laboratory) (voltammetry at pH 1) can be compared to that (obtained by ICP-MS) after storage (stored acidified for 2 month) in figure 4A. The slope of the straight fit to the data is 0.91, indicating that inorganic As amounted to 91 % of total As, and was well preserved by acidification. This is expected as co precipitation of As with Fe or Mn does not occur in this condition. The good agreement between the voltammetric and ICP-MS data suggests that organoarsenic species constitute a negligible fraction of the total arsenic as these would have been detected as part of total As by the ICP-MS method but not by voltammetry

unless the samples are UV-digested. It should be noted that here two different techniques are compared, using independent calibrations; agreement within 9 % is therefore very good. A significant organic As component in these samples was not detected by the HPLC method, which confirms the previous finding that organoarsenic species are minor in reducing groundwaters of this type [36].

3.3.6 Storage effects on the speciation of arsenite [As^{III}]

The As^{III} was found to be stabilised equally well by addition of EDTA (pH 8.5) and by acidification to pH 1 with HCl (Figure 4B). The concentration of As^{III} found in freshly collected samples by voltammetry in the field was equal to that found by HPLC analysis of samples stored in the presence of 10 mM EDTA or in acidified water (pH 1). This data shows that the original As speciation in the samples was stabilised, allowing storage over several months. Three of the acidified samples showed significantly higher values that the expected 1:1 relationship which could indicate some oxidation of As^{III} during storage. The good correlation confirms previous work that the As speciation is preserved by the addition of EDTA [24, 25]. A major added advantage of the EDTA addition is the elimination of the interference of high Fe and Mn on the voltammetric detection of As^{III} in the field. A further practical advantage of using EDTA over acid is that EDTA is safe to handle in the field and not classified as a dangerous chemical, which is more convenient and cheaper for shipping purposes than HCl.

3.4. Conclusions

Close agreement with laboratory reference techniques shows here that the speciation of arsenic in groundwaters is readily measured in the field using CSV and battery powered apparatus. Interference by very high (mM) levels of Fe and Mn is successfully eliminated by addition of 10 mM EDTA, thus facilitating the on-site measurements. The addition of EDTA, and separately of 0.1 M HCl, was also effective in stabilising the redox speciation of As for several months, confirming previous

work and enabling sample storage for later comparative analysis. This effect of EDTA, without the need for bactericidal compounds, shows that changes in the redox speciation of Fe are the main agent catalysing the oxidation of As^{III} to As^{V} in well waters, bacteria playing no role, and photochemical effects remaining untested.

The validation of the method in the field shows that most of the As (78 ± 0.02 %) in the study area (West Bengal, India) occurs as inorganic As^{III}. Without preservation the As^{III} becomes rapidly oxidised to As^{V}; subsequent oxidation of Fe^{II} to Fe^{III} removes the As^{V} within a few hours by adsorption on precipitating Fe^{III}-hydroxides. The close co-variation between the As^{III}_{R} with that of total arsenic (slope 0.78 ± 0.02), indicates that the field-measured As^{III}_{R} can be used as predictor of the total As in the samples.

The good sensitivity of the field method, with a limit of detection 3 nM (0.2 μg L^{-1}) As, means that groundwaters can be tested to well below the recommended health limit of 10 μg L^{-1} As. The ability to determine As in groundwaters using inexpensive portable apparatus with excellent sensitivity and accuracy much facilitates the testing of suspect well waters in the field.

References

[1] P.L. Smedley, D.G. Kinniburgh, Appl Geochem, 17 (2002) 517.
[2] J. Buschmann, M. Berg, C. Stengel, L. Winkel, M.L. Sampson, P.T.K. Trang, P.H. Viet, Environ Int, 34 (2008) 756.
[3] D.K. Nordstrom, Science, 296 (2002) 2143.
[4] A. Smith, P. Lopipero, J. Chung, R. Haque, A. Hernandez, L. Moore, C. Steinmaus, Epidemiology, 11 (2000) S93.
[5] J.F. Schamberg, Arch Dermatol, 143 (2007) 16.
[6] A.H. Smith, C. Hopenhaynrich, M.N. Bates, H.M. Goeden, I. Hertzpicciotto, H.M. Duggan, R. Wood, M.J. Kosnett, M.T. Smith, Environ Health Persp, 97 (1992) 259.
[7] P. Ravenscroft, H. Brammer, K.S. Richards, Arsenic pollution : a global synthesis, Blackwell, Oxford, 2009.
[8] W.R. Cullen, K.J. Reimer, Chem Rev, 89 (1989) 713.
[9] C. B'Hymer, J.A. Caruso, J Chromatogr A, 1045 (2004) 1.
[10] P.A. Gallagher, C.A. Schwegel, X.Y. Wei, J.T. Creed, J Environ Monitor, 3 (2001) 371.
[11] G. Forsberg, J.W. Olaughlin, R.G. Megargle, S.R. Koirtyohann, Anal Chem, 47 (1975) 1586.
[12] J. Zima, C.M.G. van den Berg, Anal Chim Acta, 289 (1994) 291.
[13] H. Li, R.B. Smart, Anal Chim Acta, 325 (1996) 25.
[14] S.B. Rasul, A.K.M. Munir, Z.A. Hossain, A.H. Khan, M. Alauddin, A. Hussam, Talanta, 58 (2002) 33.
[15] A.O. Simm, C.E. Banks, S.J. Wilkins, N.G. Karousos, J. Davis, R.G. Compton, Anal Bioanal Chem, 381 (2005) 979.
[16] R. Feeney, S.P. Kounaves, Anal Chem, 72 (2000) 2222.
[17] A. van Geen, Y. Zheng, Z. Cheng, Z. Aziz, A. Horneman, R.K. Dhar, B. Mailloux, M. Stute, B. Weinman, S. Goodbred, A.A. Seddique, M.A. Hope, K.M. Ahmed, Chem Geol, 228 (2006) 85.
[18] K. Gibbon-Walsh, P. Salaun, C.M.G. van den Berg, Anal Chim Acta, 662 (2010) 1.
[19] P. Salaun, B. Planer-Friedrich, C.M.G. van den Berg, Anal Chim Acta, 585 (2007) 312.
[20] J.M. McArthur, P. Ravenscroft, S. Safiulla, M.F. Thirlwall, Water Resour Res, 37 (2001) 109.
[21] R.T. Nickson, J.M. McArthur, P. Ravenscroft, W.G. Burgess, K.M. Ahmed, Appl Geochem, 15 (2000) 403.
[22] J.M. McArthur, P. Ravenscroft, D.M. Banerjee, J. Milsom, K.A. Hudson-Edwards, S. Sengupta, C. Bristow, A. Sarkar, S. Tonkin, R. Purohit, Water Resour Res, 44 (2008).
[23] A. Shraim, N.C. Sekaran, C.D. Anuradha, S. Hirano, Appl Organomet Chem, 16 (2002) 202.
[24] P.A. Gallagher, C.A. Schwegel, A. Parks, B.M. Gamble, L. Wymer, J.T. Creed, Environ Sci Technol, 38 (2004) 2919.
[25] A.J. Bednar, J.R. Garbarino, J.F. Ranville, T.R. Wildeman, Environ Sci Technol, 36 (2002) 2213.
[26] P. Salaun, C.M.G. van den Berg, Anal Chem, 78 (2006) 5052.
[27] M.A. Nolan, S.H. Tan, S.P. Kounaves, Anal Chem, 69 (1997) 1244.
[28] C.S. Chapman, C.M.G. van den Berg, Electroanal, 19 (2007) 1347.
[29] D.W. Oscarson, P.M. Huang, C. Defosse, A. Herbillon, Nature, 291 (1981) 50.
[30] M. Bissen, F.H. Frimmel, M.M. Vieillard-Baron, A.J. Schindelin, Chemosphere, 44 (2001) 751.
[31] S.J. Hug, O. Leupin, Environ Sci Technol, 37 (2003) 2734.
[32] R.S. Oremland, J.F. Stolz, Trends Microbiol, 13 (2005) 45.
[33] R. Nickson, J. McArthur, W. Burgess, K.M. Ahmed, P. Ravenscroft, M. Rahman, Nature, 395 (1998) 338.
[34] A. Giacomino, O. Abollino, M. Lazzara, M. Malandrino, E. Mentasti, Talanta, 83 (2011) 1428.
[35] Y. Du, H.Y. Chen, W. Zhao, J.J. Xu, Talanta, 79 (2009) 243.
[36] R.J. Bowell, Appl Geochem, 9 (1994) 27

4

Chapter 4
DETERMINATION OF ARSENATE IN PH 8 SEAWATER USING A MANGANESE COATED GOLD MICROWIRE ELECTRODE

4. DETERMINATION OF ARSENATE IN PH 8 SEAWATER USING A MANGANESE COATED GOLD MICROWIRE ELECTRODE

4.1 Introduction

Arsenic (As) in the marine environment exists in two oxidation states (+5 and +3), where the As^{V} can occur either free, inorganic, or as organic compounds [1], which complicates its biogeochemical cycling in natural waters including seawater [2]. As forms oxyanions based on a tetrahedral coordination with oxygen [3]. In oxygenated seawater, As primarily exists as the $HAsO_4^{2-}$ anion, which chemically closely resembles the corresponding species formed by phosphorus, HPO_4^{2-} [3]. In the euphotic zone, As occurs not only in the form of arsenate but also as the species arsenite and dimethylarsenic [4]. Toxicity of As^{V} is believed to be due to its chemical similarity with phosphate anions. Both As^{V} and phosphate have tetrahedral symmetry, in which the central cation, As^{5+} or P^{5+}, is at the centre of a tetrahedron, surrounded by four oxygen atoms [2]. Both oxyanions have similar size and their hydrolysis behaviour is very similar with pK_A values of 2.2, 6.97 and 11.53 and of 2.12, 7.21 and 12.67 for As^{V} and P^{V} respectively [3]. Consequently, inorganic As^{V} is thought to be the species taken up by marine algae via the phosphate uptake route [5]. For this reason there is special interest in being able to determine the concentration of inorganic As^{V}.

The average total inorganic arsenic concentration in seawater is around 19 nM in the south Atlantic [6] and 24 nM in the North Pacific [1]. Arsenate is the major fraction of the dissolved As in ocean water [3, 4, 7] and coastal surface seawater [8, 9] amounting to 80-100 %. The major As species in North Atlantic surface water are: 15.7 ± 1.3 nM As^{V}; 0.45 ± 0.21 nM As^{III} and 0.14 ± 0.12 nM dimethylarsenic (DMA) [10]. A fraction of the total arsenic could also be a refractory organic arsenic species in estuarine waters [11] originating from organism mediated transformation [12].

To measure inorganic As in seawater, hydride generation is used to separate arsenic from its matrix lowering the detection limit. As is then detected by atomic emission spectroscopy [13], graphite furnace atomic absorption [2] or atomic fluorescence spectroscopy [14]. Although such

spectroscopic methods have good sensitivity and speciation capabilities they are not readily used for in-situ or on-site analysis. An altemative is to use voltammetry that is eminently portable, potentially enabling detection in the field.

Voltammetric methods for As detection have been recently reviewed [15]. For a long time As^{V} has been considered to be electro-inactive [16] and so As^{V} is detected as As^{III} by anodic stripping voltammetry (ASV) [17, 18] or cathodic stripping voltammetry (CSV) [19, 20] after chemical reduction of As^{V} to As^{III} . Direct analysis of As^{V} is possible using a gold, or gold-coated, electrode in acidic conditions: 1 M HCl [21], or 0.1 M HCl [22]. Less acidic conditions are achieved using microelectrodes: using a microwire electrode As^{V} can be measured in pH 1 water with good sensitivity by ASV and with a reduced sensitivity up to pH 4 [17], or even lower sensitivity at pH 5 using a gold modified boron doped diamond electrode [23]. The electrochemical evidence so far therefore is that As^{V} is electro-inactive at neutral pH but that it can can be determined by ASV after plating as elemental As in acidic conditions. Lowering the pH is a drawback for speciation as it could release any As^{V} associated with colloidal or particulate hydroxides (such as on Fe-hydroxides or Mn-oxides that are poorly soluble at neutral pH but dissolve in acid), thus artificially increasing the concentration of reactive, ionic As^{V}.

Recent work in our laboratory showed that As^{V} interferes with the ASV signal of Mn^{II} in neutral pH seawater [24]. Further work presented here shows that this interference is caused by an unusual redox couple between As^{V} and elemental Mn leading to a method for the voltammetric detection of inorganic As^{V} in neutral pH seawater using a Mn-coated electrode.

4.2 Experimental

4.2.1 Reagents

Water used to prepare reagents and preliminary working solutions was 18 M Ω cm deionised water (MQ water) (Millipore Elix 3 attached to Milli-Q gradient). 10^{-2} M As^{III} and 10^{-2} M As^{V} stock solutions

were prepared from As_2O_3 (purity 99.5 %, AnalaR BDH Chemicals Ltd., England) and $Na_2HAsO_4 \cdot 7H_2O$ (purity 98.5 %, AnalaR BDH Chemicals Ltd., England), respectively. The As_2O_3 was initially dissolved in 10^{-4} M NaOH. These stock solutions were acidified with HCl to pH 2. Standard solutions with concentrations of 10^{-5} M were prepared freshly from the stock solution at the beginning of a set of experiments and also stored at pH 2 using 0.01 M HCl. HCl was purified by sub-boiling distillation on a quartz condenser. 0.5 M H_2SO_4 used for electrode conditioning was from BDH (AnalaR grade). Metal solutions (Cu, Pb, Sb^{III}, Zn, Cd, Ni, Fe and Bi^{III}) used for interference experiments were diluted with MQ water from AAS standard solutions from Fluka or VWR and stored at pH 2 (0.01 M HCl); sodium dodecylsulphate SDS was from Aldrich, Triton X-100 from BDH (England), humic acid and fulvic acid was "Suwannee river fulvic acid" from the International Humic Substances Society. A 0.5 M stock solution of ethylenediaminetetraacetic acid (EDTA) was prepared from the disodium salt (purity 99.5 %, AnalaR, BDH Chemicals Ltd, England) and diluted in MQ water. Ammonia solution (purity 35 %, MOS, UK) was purified by sub-boiling distillation on a quartz condenser. A 1 M aqueous solution of 4-(2-hydroxyethyl)-1-piperazineethanesulfonic acid (purity 99 %, Acros organics, UK) (HEPES) pH buffer had its pH adjusted to pH 7.85 with addition of 0.5 M NaOH (Fisher scientific, UK). A 1 M stock solution of sodium hypochlorite was made from sodium hypochlorite salt (Acros Organics, England).

4.2.2 Certified reference material

To confirm the methods validity, inorganic arsenic (As_{inorg}) was measured in reference seawater (NASS-5 from the National Research Council Canada). The pH was neutralised using NH_3 and then buffered using 10 mM HEPES, resulting in a final pH of 7.85.

4.2.3 Sample collection and pre-treatment

Seawater used for optimisation experiments was collected from the Irish Sea, filtered (0.2 µm filtration cartridge) and stored in an acid rinsed 50 L polyethylene container (July 2010). Individual

seawater samples were collected at a depth of 7 m during surveys of the Irish Sea with the research vessel Prince Madog (March, July and September 2010) using a rosette-mounted, Niskin bottle, modified to obtain samples uncontaminated with metals (Teflon coated spring on the outside, no rubber inside). These samples were filtered (0.2 µm Sartobran, UK filtration cartridge) and transferred to 500 mL acid washed, Nalgene, low-density, polyethylene bottles, stored frozen on board the ship.

4.2.4 Instrumentation

Voltammetric instrumentation was a 663 VA electrode stand from Metrohm, Switzerland, interfaced to a µAutolab(III) (Eco Chemie, Netherlands) computer controlled potentiostat. Data was processed with GPES 4.9 software. A 50 mL three-electrode cell was used containing the working electrode (WE), a counter electrode (CE) consisting of a 200 µm iridium wire (from Goodfellow, UK), heat-sealed in a propylene pipette tip, 3 mm protruding. The cell was PTFE for analyses and a separate, glass cell was used for electrode preparation in 0.5 M H_2SO_4. The reference electrode was double-junction, glass, Ag/AgCl/KCl (3 M)/KCl (3 M). The WE was a bare gold microwire electrode, prepared similarly to before [25-27]: a 10 µM diameter gold microwire (99.99 %, hard, Goodfellow) was heat-sealed in a 100 µL polypropylene pipette tip (uncoloured) with about 0.5 mm protruding. This tip was then fitted onto a 1 mL polypropylene pipette tip, which had a vibrator incorporated and an insulated connecting single core electrical cable protruding ~1 cm at the bottom, which made contact with the WE. This design differed from before [28] where the vibrator was fixed on the side of the WE, whilst in the new design the WE was friction-fitted on the vibrating tip, thus facilitating insertion in the voltammetric cell and replacement of the WE.

Natural organic matter in seawater was removed, when required, by UV digestion of seawater samples (30 mL) using a high-pressure 125 W UV lamp. The quartz sample tubes were conditioned using neutral pH seawater prior to use to minimise adsorption, and irradiation was for 45 min.

4.2.5 Electrode conditioning

The WE was cleaned by hydrogen generation in 0.5 M H_2SO_4 at –3 V (15 s) with agitation when the electrode was new or when fouling was suspected. The symmetry and height of the reduction peak for the gold oxide monolayer obtained using cyclic voltammetry (5 scans) from 0 to 1.5 V (100 mV s^{-1}) were used to verify the electrode [29].

4.2.6 Voltammetric procedures to determine arsenate

The potential scans of As^{V} were by anodic stripping voltammetry (ASV) in the square wave mode (frequency = 50 Hz, amplitude = 25 mV and step = 8 mV). An aliquot of water was placed in the voltammetric cell and the solution was de-aerated by purging for 5 min. Prior to each scan the electrode was cleaned using a conditioning potential at +0.55 V (5 s); the deposition potential was –1.35 V (60 s), the quiescence time was 3 s, and the ASV scan was from -1.2 V to +0.5 V. The electrode was vibrated (1.5 V) during the cleaning step and the deposition step. A background scan was carried out using the same parameters as the analytical scan but with the deposition time reduced to 1 s, and was subtracted from the analytical scan to obtain the background-corrected scan. The derivative of the As^{0}/As^{III} peak at –0.25 V was used for quantification. The sensitivity was calibrated by repeating the measurement after addition of As^{V} standard.

4.3 Results and discussion

ASV scans after deposition at -1.35 V in UV-digested seawater of pH 8 gave peaks at -0.95 V, -0.55 V, -0.25 V and +0.2 V (figure 1). The Mn concentration in this seawater had been raised to 100 nM Mn^{II}, whilst other elements occurred at natural trace levels, including As^{V} at 20 nM and Cu and Zn at ~10 nM. The peak at -0.55 V was due to Zn, and at +0.2 V due to Cu, whilst addition of Mn^{II} caused the peaks at -0.95 V and -0.25 V to increase. Previous work has shown that the peak at -0.95 V is due to Mn[24], whilst the peak at -0.25 V responds to oxidation of As (As^{0}/As^{III}), that is normally obtained

after deposition of As by reduction of dissolved As^{III} [17]. In this case the concentration of ambient As^{III} was negligible (<1 nM) and the As had apparently been plated from dissolved As^{V} under the influence of dissolved Mn^{II}. The As^{V} peak was only obtained in the presence of Mn. Experiments were carried out to elucidate the mechanism of this reaction.

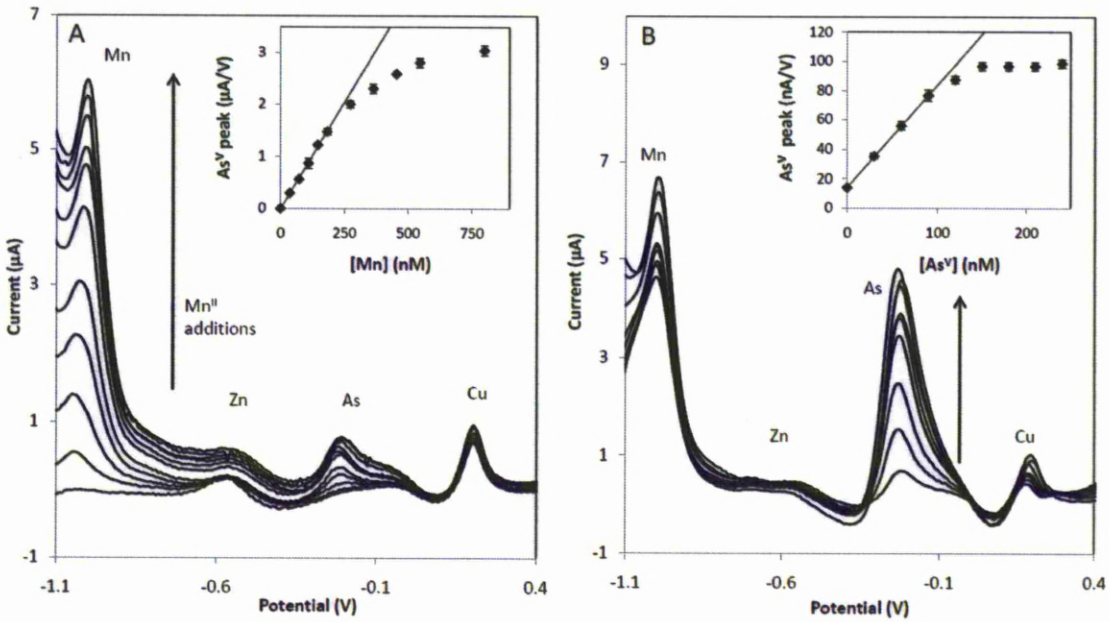

Figure 1. ASV scans for Mn and As in UV digested seawater (Liverpool Bay, Irish sea). The scans show the effect of additions of Mn^{II} (A) and of As^{V} (B). **A)** E_{dep} =-1.3 V; inset shows the increase of the As^{V} peak derivative with Mn^{II} addition; **B)** t_{dep}= 60 s and E_{dep}= -0.9 V with 1 µM Mn^{II}; the inset shows the response for As^{V}.

4.3.1 Measurement of As^{V} by ASV in the presence of Mn

The voltammetric response for As^{V} was studied in UV-digested seawater containing 20 nM As^{V} and 100 nM Mn, buffered at pH 7.8 with 10 mM HEPES. Separate additions of As^{III} and As^{V} confirmed that that they produced the same peak at -0.25 V that was the As^{0}/As^{III} oxidation peak. This means that As^{V} is either reduced directly to As^{III} at the deposition potential used, or that an unknown chemical reduction intervenes causing the As^{V} to be reduced to As^{III} at the electrode surface after which it is detected as As^{III}. Mn additions were found to affect the As peak (figure 1A), causing the height of the As peak to be increased with the addition of both Mn^{II} and As^{V} (figure 1B). With Mn^{II}

additions the As peak increased linearly until 200 nM Mn, after which the response began to plateau (figure 1A). The signal for Mn at -0.95 V was also found to reach a plateau due to saturation of the electrode with Mn^0. The co-variation in the response for As^V and the deposition of Mn^0 on the electrode indicates that elemental Mn is somehow involved in the As deposition.

To maximise the response for As and to make it independent of variations in the ambient concentration of Mn^{II} it was convenient to add an excess of 1 µM Mn^{II} to samples in the voltammetric cell: this level is far into the plateau response for As^V (figure 1A) and is much greater than expected for seawater, except perhaps in anoxic sedimentary porewaters.

In the presence of 1 µM Mn^{II} the As peak was found to increase linearly with additions of As^V (figure 1B, inset) up to 100 nM As^V for a deposition time of 60 s after which the response gradually levelled off. The Mn peak at -0.95 V showed a small decrease as a result of the As^V additions. The quantitative response for As^V in the presence of a fixed concentration of Mn shows that ASV in the presence of Mn can be used to measure As^V in water and this was further optimised.

4.3.2 Variation of electrochemical parameters

The deposition potential was varied in seawater buffered with 10 mM HEPES with 25 nM As^V and 1 µM Mn. A signal for As^V was obtained only for deposition potentials below -1 V, which is also the potential window where Mn was deposited. The response for As^V increased with more negative deposition potential until -1.3 V after which it decreased (figure 2A). This effect was analogous to that on the response for Mn (figure 2A) illustrating the close relationship between the response for As^V and the amount of elemental Mn on the electrode. The effect of the deposition potential on the response for As^V in seawater containing 200 nM As^V and 1 µM Mn^{II} is illustrated in figure 2A (inset), showing one scan after deposition at -1.3 V and one after deposition at -0.9 V. After deposition at -1.3 V, both the Mn peak at -0.95 V and the As peak at -0.25 V are apparent, but after deposition at -

0.9 V both peaks are absent because the Mn had not been deposited. The sensitivity for As^V was greatest after deposition at -1.3 V, which was the potential selected for further experiments.

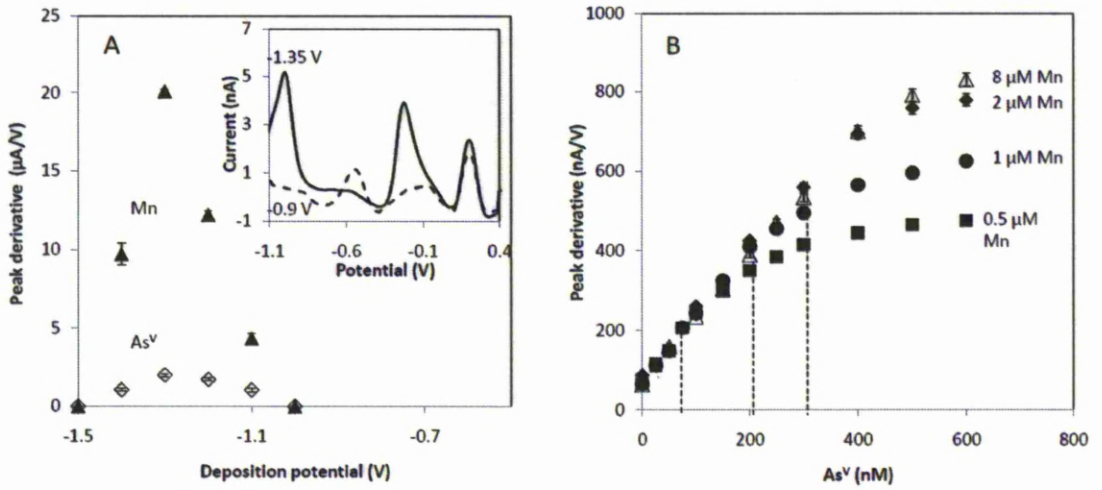

Figure 2. Optimisation of the analytical parameters for ASV of As^V in UV-digested seawater buffered to pH 7.9 using 10 mM HEPES buffer in the presence of 2 µM Mn^{II}. **A)** Variation of the deposition potential on the response for 25 nM As^V. Inset: scans for 200 nM As^V; full line E_{dep} =-1.3 V, dashed line E_{dep} = -0.9 V. **B)** Effect of varying the concentration of Mn on the linear range and sensitivity for As^V.

4.3.3 Linear range of As^V response

In seawater containing 1 µM Mn^{II}, the As^V signal increased linearly with increasing additions of As^V until 100 nM, after which the increase began to reach a plateau. This plateau is caused by a saturation of the surface of the electrode with a monolayer of non-conductive As^0. The same plateau was reached by extending the deposition time at a constant concentration (25 nM) of As^V. From no signal at 0 s the As^V signal increased initially linearly with deposition time to 120 s and subsequently reached the plateau suggesting near-saturation conditions after deposition between 240 s and 480 s.

Because of the requirement for Mn, the linear range can be expected to depend on the amount of Mn plated on the electrode. Variation of the concentration of Mn in separate determinations of the linear range showed that with increasing concentration of Mn, the linear range for As^V was increased from 75 nM As at 0.5 µM Mn, to 300 nM As in the presence of 2 µM Mn (figure 2B). A further

addition of Mn^{II} up to 8 µM gave no further increase in the As^{V} linear range suggesting that the electrode surface was saturated with Mn.

4.3.4 Reaction mechanism of the reduction of As^{V} by Mn

As direct electrochemical reduction of As^{V} is not possible at neutral pH values, the effect of Mn must lie in its reduction of As^{V} to As^{III} and so allowing As deposition at pH 8. Elemental Mn is freshly produced on the electrode surface during deposition of adsorbed Mn^{II} in underpotential conditions at potentials between -1.2 and -1.4 V [24], and this Mn is in principle available for a redox reaction with As^{V} when in close proximity (in the first molecular, or Helmholtz, layer). This is the unusual reaction hypothesized here to explain the As^{V} reduction to As^{III} at the electrode surface.

Equations (1) – (3) summarise the probable reactions at the working electrode during the deposition step at -1.3 V:

$$Mn^{II} + 2e^- \leftrightarrow Mn^{0} \qquad (1)\ \text{(electrochemical)}$$

$$As^{V} + Mn^{0} \rightarrow As^{III} + Mn^{II} \qquad (2)\ \text{(chemical)}$$

$$As^{III} + 3e^- \leftrightarrow As^{0} \qquad (3)\ \text{(electrochemical)}$$

Equation (1) describes deposition of elemental Mn at the surface of the electrode at -1.3 V. The Mn is present in excess causing the electrode to be nearly saturated with elemental Mn and to behave as a Mn coated electrode at this stage. In spite of the near saturation of the electrode with Mn, the surface is not coated with a monomolecular layer of Mn as only about 14 % of the surface area is Mn-coated at saturation due to competitive anion adsorption [24].

Equation (2) describes the chemical reduction of As^{V} to As^{III} that is coupled to oxidation of Mn^{0} to Mn^{II} in the first molecular (Helmholtz) layer of the electrode. This causes a loss of elemental Mn from the surface as it is oxidised to Mn^{II}, which is reflected in a lowering of the Mn peak at enhanced

levels of As^{V} (see below). The As^{III} produced by the chemical reduction of As^{V} at the electrode surface is then reduced further to As^{0} electrochemically and deposited on the electrode (equation 3).

During the ASV scan the Mn is oxidised at -0.95 V, and subsequently the As at -0.25 V. The As^{0}/As^{III} peak is produced on the bare gold electrode as all the Mn has already been oxidised. This means that the As^{0} is deposited on the gold rather than on the elemental Mn, as otherwise the As would be lost when the Mn is oxidised at -0.95 V. For this reason the peak potential is the same as that found previously for As^{III} in neutral pH seawater on the gold electrode [17].

The combination of the chemical redox couple (equation 2) with the plating step adds a kinetic delay to the plating of As. For this reason, the ASV sensitivity for As^{III} added to seawater under the same conditions is greater than that for As^{V} by a factor of ~2.5 (this is conditional on the concentration of Mn and deposition potential used). In view of this lower sensitivity for As^{V}, the reduction mechanism of As^{V} by Mn was ~40 ± 4 % (n=3) (at a solution concentration of 2 µM Mn) efficient compared to the deposition of added As^{III}.

4.3.5 Effect of As^{V} on the Mn peak

Additions of As^{V} caused the signal for Mn to decrease in line with expectation for the reaction mechanism proposed in equation. 2. The effect of the As^{V} additions on the response for 500 nM Mn^{II} was measured in anodic stripping chronopotentiometry mode (ASC) as this mode gives a linear response with increasing concentration of Mn [24]. The signal for Mn was found to decrease linearly with additions of As^{V} up to 100 nM As^{V}, and non-linearly thereafter when the decrease in the Mn response and the increase in the As response both levelled off (figure 3A). As the peaks for Mn and As are a measure of the amounts of Mn and As residing on the electrode at the end of the deposition step, the decrease in the Mn peak, and the increase of the As peak, with increasing dissolved As^{V} can be used to obtain the ratio at which Mn is oxidised by the reduction of As^{V} to As^{III}. This should be a molar ratio 1 for As to Mn, as the reduction of As^{V} to As^{III} and the oxidation of Mn to Mn^{II} both require 2 electrons (equation 2).

The molar ratio was obtained by conversion of the reduction currents (from the ASC peak areas in Coulombs) to moles by division with nF (where F=Faraday constant, and n=number of electrons, which is 3 for As/As^{III} and 2 for Mn/Mn^{II}). A plot of the molar amounts on the electrode in figure 3B revealed a ratio of As^{V} reduced and deposited as As^{0} over Mn^{0} reoxidised of approximate unity (0.96 ± 0.06), providing evidence for the proposed mechanism of equation 2. The relationship was initially linear but became non-linear at higher concentrations of As (>100 nM As^{V}) due to non-linearity in the response of As^{V} (figure 3A).

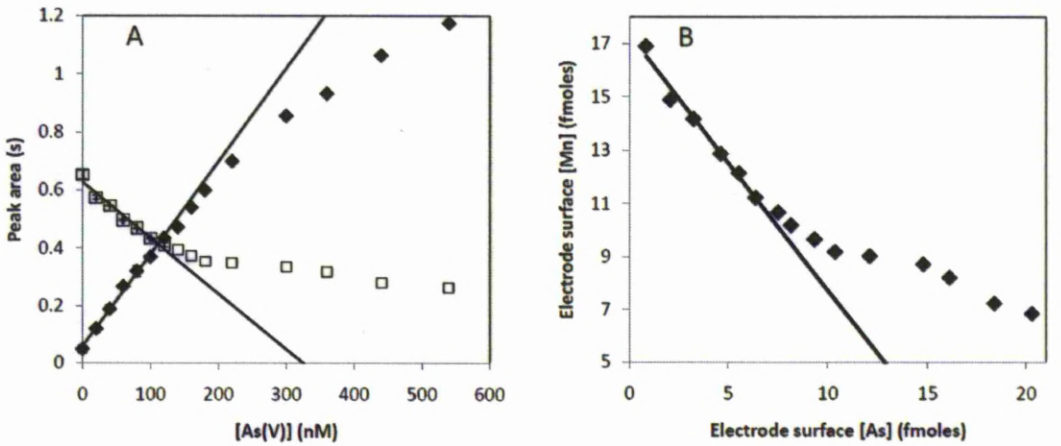

Figure 3. Determination of the molar ratio at which elemental Mn is oxidised to Mn^{II} by As^{V}. **A)** The ASC peak areas for Mn and As as a function of the concentration of dissolved As^{V} after deposition at -1.3 V from pH 8 seawater containing 2 µM Mn. **B)** Plot of the molar quantity of Mn on the electrode surface as a function of that of As; both were calculated from the peak areas in A) as described in the text. The straight was fitted by linear least squares regression to data up to 120 nM dissolved As^{V} and has a slope of -0.96 ± 0.06.

4.3.6 Effects of other metals on the ASV response for As^{V}

Various other metals were added to seawater whilst measuring the ASV response for As^{V}, in order to evaluate whether the mechanism is unique to Mn. 1 µM concentrations of Ti^{III}, V^{V}, Cr^{VI}, Cd^{II}, Fe^{III}, Co^{II}, Ni^{II}, Mo^{VI}, Zn^{II}, Ga^{III} and Sn^{II} were added to seawater containing 10 mM HEPES (pH 7.85) and 100 nM As^{V}. The deposition potential was varied between -0.6 V and -1.4 V in 0.2 V steps to verify the effect for each metal. The As peak was not increased by the addition of any of these metals,

indicating that the effect of elemental Mn on the reduction of As^{V} to As^{III} at natural pH is unique to this metal.

4.3.7 Comparison of ASC and square-wave ASV

As^{V} can be measured equally well using either anodic stripping chronoamperometry (ASC) with an oxidising current of 5 nA or square wave anodic stripping voltammetry (SWASV). SWASV was used during this work unless stated otherwise.

4.3.8 Surface coverage of As^{V} on the gold electrode

The surface area of the electrode was determined in 0.5M H_2SO_4 as before [29], giving a total area of 2.68×10^{-4} cm^2 (from a monolayer gold oxide reduction current of 1.21×10^{-7} C and a monolayer capacity of 450 μC cm^{-2}). The approximate electrode length was estimated at 0.7 mm using a roughness factor of 1.2 [29].

The area occupied by the plated As was calculated from its oxidation current in coulombs, from the surface area of ASV scans in linear sweep mode (scan rate 10 mV/s). The maximum amount of As^{V} that can be deposited on the electrode was obtained by fitting of the data to the following version of the Langmuir equation [30]:

$$C_m/i_r = C_m/i_m + 1/(Bi_m) \quad (4)$$

where C_m is the dissolved As^{V} concentration, i_m is the maximum current (at which monolayer coverage should be attained) and B is a constant related to the free energy of adsorption. Then i_m was converted to moles by using $\Gamma_m = i_m/nF$ where n is the number of electrons and F is the faraday constant (96,000 C mol^{-1}). This is then multiplied by Avogadro's constant (6.02×10^{23}) to give the number of molecules at the surface of the electrode. The number of molecules was multiplied by the size (flat surface area) of each atom, using πr^2 and an atomic radius of 115 pm [31]. This was then

divided by the surface area of the electrode to obtain the electrode coverage with arsenic as a fraction of the total area.

The electrode coverage by As was determined at Mn^{II} concentrations between 0.5 and 2 µM. The maximum surface coverage for As^{V} was 4 % with 0.5 µM Mn, 5 % with 1 µM Mn and 6 % with 2 µM Mn. These rather low saturation densities suggest that the non-linearity of response was not caused by electrode saturation with As, but rather potential saturation of the active sites on the gold.

4.3.9 Effect of variation in the salinity

The effect of variation in the salinity on the sensitivity for As^{V} was determined in seawater at various dilutions with MQ water. In each case the pH was buffered to pH 7.85 with 10 mM HEPES and the deposition potential was -1.3 V. Each aliquot contained 1 µM Mn^{II} and standard additions of As^{V} were made up to 100 nM. The sensitivity (S) for As^{V} was found not to be affected by changes in salinity between 1 and 34 ($S = 0.41 \pm 0.009$ µA V^{-1} nM, $n = 7$).

4.3.10 Effect of variation of the pH

The pH was varied to investigate its effect on the response for As^{V} in seawater, which was buffered over a small pH range (pH 6-8.5) with 10 mM K_2HPO_4, 10 mM $NaHCO_3$ and 10 mM H_3BO_3. The pH was decreased with addition of HCl from a starting pH of 8.5. The SWASV response for As^{V} was determined using a deposition potential of -1.3 V and with 1 µM Mn. There was no effect on the As^{V} signal in the tested pH range. Lower pH values were not tested because the Mn would then be deposited within the hydrogen wave as it was thought that this could cause unknown amounts of Mn to become oxidised from the electrode surface.

Seawater has a natural pH ~8, however without pH buffer, the pH drifts up to around 8.6 during purging to remove dissolved oxygen where it increasingly stabilises by buffering of the carbonate system. The pH experiment showed that the response for As^{V} is not affected by minor pH variations

in this range so analyses of seawater were carried out without any pH buffer addition, which simplified the procedure. However, stored, acidified, samples require pH buffering for instance using HEPES after pH neutralisation, as then all carbonate will have evolved as CO_2.

4.3.11 As speciation

Using the new method the speciation of inorganic As can be achieved at neutral pH. As^{V} can be measured in the presence of Mn with a deposition potential of -1.3 V, whilst As^{III} is detected without Mn addition and using a deposition potential >-1 V where Mn is not deposited (figure 2A) to eliminate effects of Mn which can occur naturally in seawater though normally at a much lower concentration.

4.3.12 Limit of detection

The limit of detection (LOD) was calculated from 3x the standard deviation of 7 measurements using the optimised parameters (1 µM Mn, 10 mM HEPES buffer (pH 7.85), 30 s deposition time) in UV digested seawater containing 19.2 nM As^{V}. The standard deviatio n was 3.5 % giving a limit of detection of 2.3 nM As^{V}. The LOD was also measured at a much lower concentration of As^{V} in MQ water containing 2 mM KCl, 1 µM Mn and 10 mM HEPES with a final pH of 7.85. For 1 nM As^{V} and a 180 s deposition time the LOD was 0.2 nM. Extension of the plating time would lower these LODs further.

4.3.13 Arsenate signal stability

The response for As^{V} in 400 mL seawater was measured every hour for 20 h in a 500 mL Nalgene bottle. 1 µM Mn^{II} was added and the sample was purged with N_2 for 15 min whilst the solution was being stirred using a magnetic stirrer before the experiment, and was N_2-blanketed during the experiment. The water contained 25 nM As^{V}. The standard deviation of the As^{V} peak height over 20

h was 4 % (n=20). The stability of response indicates that the gold wire electrode can be used for extended on-site, or in-situ, analysis, with only intermittent calibration.

4.3.14 Interferences

Dissolved oxygen was found to interfere with the As^{V} signal in ASV due to the oxygen wave at -0.2 V. Sample solutions were therefore purged with N_2 before analysis. It was attempted to eliminate the oxygen interference by scanning with a high square-waver frequency (300 Hz): this caused the height of the As peak to increase, and the oxygen peak to become less pronounced. However, the high frequency caused the scans to be more noisy which was found to increase the limit of detection so we did not succeed in eliminating oxygen interference and all analyses were done after purging with an inert gas.

4.3.14.1 Interference of As^{III} on As^{V}

The ASV signal for As^{V} is obtained by chemical reduction to As^{III} by elemental Mn, followed by the electrochemical reduction of As^{III} to As. The signal for As^{V} is therefore the same as that for As^{III}. Detection of As^{V} therefore has to be corrected for any As^{III} initially present in the sample. The concentration of As^{III} in seawater is normally much less than that of As^{V} [4] but its concentration varies and its presence has to be checked for. The most simple way to make this correction is to subtract the peak height (or the entire scan using appropriate software) for As^{III} after deposition at -0.9 V (which shows As^{III} exclusively) from that of a scan after deposition at -1.3 V (which shows combined As^{III} + As^{V}). The corrected peakheight is due to As^{V} and the sensitivity calibrated by addition of As^{V} standard. This calibration cannot be used to quantify the sensitivity for the As^{III} detected in the first scan as its sensitivity is approximately 2.5x greater than that for As^{V}, probably because the reduction step of As^{V} to As^{III} introduces a kinetic delay in As^{V} deposition. This procedure therefore gives a value for the concentration of As^{V}, whilst that of As^{III} is determined in a separate sample aliquot using deposition at -0.9 V with calibration using As^{III}.

Alternatively, all dissolved As^{III} is readily oxidised to As^{V} using an oxidant and inorganic As^{III} and As^{V} are then determined together (= As_{inorg}) using deposition at -1.3 V with calibration using As^{V} standard. The oxidation of As^{III} to As^{V} is much easier than the reverse reaction that requires purging with SO_2 and heating [32]. For instance, As^{III} is oxidised within seconds to As^{V} by traces of Cl_2 produced at the counter electrode prior to the determination of As^{V} in 0.1 M HCl [17]. Analogous to that we tested hypochlorite (NaOCl) and found that addition of 20 µM NaOCl to the voltammetric cell was sufficient to oxidise all As^{III} to As^{V} within seconds in seawater of natural pH without interference with the analysis. H_2O_2 was not a suitable oxidant as it produced an interfering oxygen reduction wave. In the presence of NaOCl all of the As occurs as As^{V} and the detected As^{V} equals the concentration of the combined inorganic As (As_{inorg}). The concentration of As^{V} originally in the sample is then computed from a determination of As^{III} in a separate sample aliquot using deposition at -0.9 V. This procedure was used to determine the As speciation in seawater samples below.

4.3.14.2 Interference by other metals

Various metals were added to verify whether these could pose an interference with the determination of As^{V} in seawater. The metal additions were to levels much greater than naturally occurring in seawater. The test solution was UV-digested seawater containing 25 nM of As^{V} and 1 µM Mn^{II}. No significant interferences were caused by sequential addition of 100 µM Al, 500 nM Fe^{III}, 200 nM Ni, 500 nM Zn, 20 nM Pb and 100 nM Bi. Addition of 2 µM Cu decreased the As^{V} signal by 50 %; copper is a known interference for the detection of As^{III} by ASV at low pH, but in this neutral pH method up to 2 µM Cu (about 100x greater than typical for coastal waters) is tolerated albeit at a reduced sensitivity. 200 nM Cd caused a 30 % drop in the As^{V} signal. The signal for Sb^{III} was close to that of As and overlapped, however Sb^{III} occurs at low levels in seawater (typically <0.2 nM [3] which is 100x less than that of As^{V}) so Sb is unlikely to cause interference with the detection of As^{V}. Furthermore, Sb^{III} is oxidised to Sb^{V} by OCl^{-} (added to determine total As after oxidation of any As^{III} to As^{V}) and Sb^{V} is not reduced by elemental Mn, which means that Sb does not interfere with the determine of total As after its oxidation to As^{V}.

4.3.14.3 Interference of monomethylarsenic (MMA) and dimethylarsenic (DMA)

Addition of 1 µM MMA and DMA did not produce an ASV signal and did not cause an interference with the measurement of As^{V} using the new ASV method in the presence of MnII. On the other hand, comparative measurements by ASV in acidic conditions (0.1 M HCl) showed that MMA gave a peak indistinguishable from that for As^{III} and As^{V}, though at a 60 % lower sensitivity. The new neutral pH ASV method at neutral pH is therefore advantageous in that it determines the inorganic As^{V} specifically without interference by MMA or DMA. Tests showed that neither MMA nor DMA is converted to inorganic As^{V} by UV-digestion at pH 8. Inorganic As^{III} was found to be converted to As^{V} by the UV-digestion.

4.3.14.4 Interference of organic matter

Organic material can interfere with the voltammetric signal due to surfactant or complexation effects. Stepwise addition of humic acid (HA) caused the sensitivity for As^{V} in seawater to decrease by 30 % by 2 ppm HA, 50 % by 3 ppm HA, and 70 % by 8 ppm HA. Similarly, addition of 5 ppm fulvic acid (FA) caused a 50 % decrease in the As^{V} signal. Natural waters contain humic substances, water from the Irish Sea for instance containing up to 0.6 ppm [33], which is likely to affect the measurement. The effect could be due to surface-active effects or complexation with As^{V} (complexation with Mn^{II} is not a likely cause as it is present in vast excess). Standard additions of As^{V} made at several concentrations of HA showed no upward curvature so we did not obtain evidence for HA complexation of As^{V}.

Surfactant effects were tested by addition of the non-ionic surfactant Triton-X-100 and the anionic surfactant SDS. 1 ppm Triton caused the As^{V} signal to decrease by 50 % whilst no effect was observed with addition of up to 10 ppm SDS. Coastal waters can contain compounds with a surfactant effect similar to between 0.01 and 0.5 ppm of Triton [34]. Our experiments suggest that surface-active effects rather than As^{V} complexation have played the main role in the interference of HA and FA on the ASV sensitivity for As^{V}.

4.3.15 Certified reference material

Total As in certified reference seawater NASS-5 (National Research Council Canada) was determined by ASV in the presence of 1.5 µM Mn and 20 µM NaClO after UV digestion and adjustment of the pH to 7.85 using NH_3 and HEPES buffer. A concentration of 17.1 ± 0.3 nM As was obtained, which is in close agreement with the reference value of the NASS-5 (16.96 ± 0.12 nM As).

4.3.16 Application to seawater samples collected in Liverpool Bay

The new ASV method was used to determine arsenic speciation in seawater from the Irish Sea (Liverpool Bay). The salinity varied between 30.6 and 33.8. Twelve samples were collected during March, July and September 2010 (4 from each month) and stored in 500 mL Nalgene bottles at natural pH and frozen on-board within minutes of collection, or at pH 2 and not frozen. The frozen samples were analysed for As speciation after defrosting overnight, followed by careful swirling to ensure any partides became re-dissolved. The As speciation of the samples was determined by measuring As^{III} at natural pH, with a deposition potential of -0.9 V [17]. Inorganic As (As_{inorg}, that is combined inorganic As^{III} and As^{V}) was determined at natural pH in the presence of Mn and hypochlorite using the method described in this paper. Comparative measurements were by ASV at pH 2 (0.01 M HCl) [17]. The same two methods were used to determine total As (As_{tot}) as As^{V} after UV-digestion. Inorganic As^{III} was found to occur at levels of 1.6 -2.6 nM in the four samples from July (i.e. amounting to about 10 % of total As was As^{III}, the remainder was As^{V}), whereas As^{III} was <0.1 nM (<1 % of total As) in the samples from March and September 2010. Possibly As^{V} in the July samples was reduced to As^{III} under the influence of breakdown of organic matter originating from decaying algae blooms, which is to be investigated in further field studies.

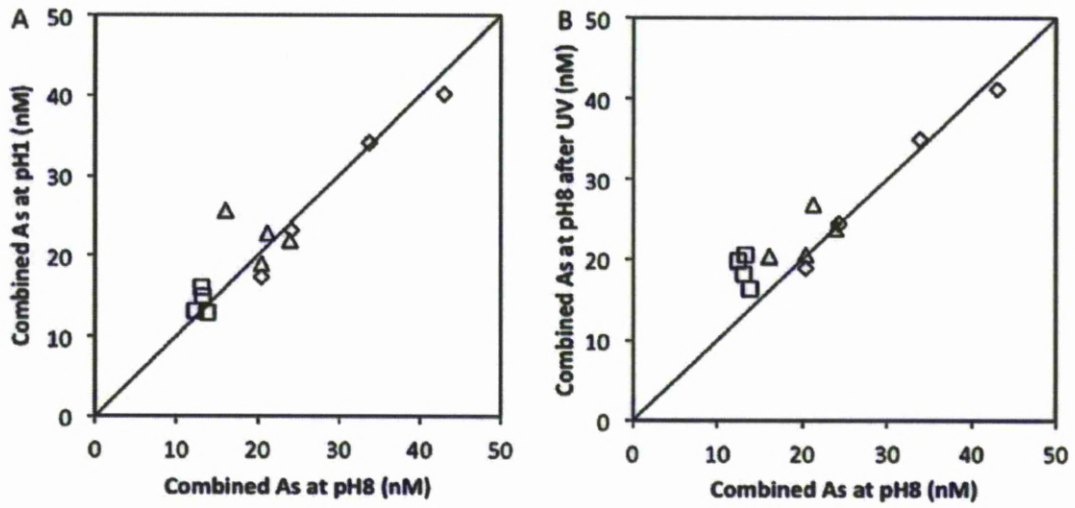

Figure 4. Comparative measurements of arsenic in seawater by ASV at pH 2 and by the new neutral pH method in the presence of 2 µM Mn^{II}. The solid line represents a 1:1 ratio. **A)** Comparative As^{V} in seawater samples from March (squares), September (triangles) and July (diamonds). **B)** Effect of UV-digestion at pH 8 on the concentration of As^{V} found by the pH 8 method. (Error bars were left out for clarity and are of a similar size to the data points).

Comparative measurement of As_{inorg} was as As^{V} by ASV at pH 2 [17] to enable comparison against the new neutral pH ASV method. A plot of the two data sets was found to fall on a straight with a slope of 0.99 ± 0.04 (figure 4A) indicating that the same concentration was found for As^{V} by the two methods. The similarity in the data validates the new method.

UV-digestion was used to evaluate effects of organic As species. UV-digestion at pH 8 caused the average concentration of $As_{inorg, pH8}$ to increase by 3 nM (the increase was most pronounced for low-arsenic samples) to an average of 24 ± 7 nM (n=12) (figure 4B). The July samples showed no increase by the UV-digestion (n=4); for September this increase was 3 nM (n=4) and March 6 nM (n=4). The UV-digestion results suggest the presence of organic arsenic (such as MMA or DMA) in these waters in March and September, but not in July. UV-digestion at pH 2 caused a larger increase in As_{inorg} to 27 ± 7 nM (n=12). For the September samples the increase over inorganic As was 5 nM (n=4), for March 10 nM (n=4) and for July 2 nM (n=4).

4.4 Conclusions

The experiments show that As^{V} is detected by ASV in seawater at its original pH. The requirement of Mn on the electrode surface suggests an unusual reaction mechanism in which elemental Mn is oxidised by As^{V}, which in its turn is reduced to As^{III}. The stoichiometric ratio is unity for the redox couple of Mn/As, which provides evidence for the hypothesised reaction mechanism. In our experiments Mn was always added to a concentration of 1-2 μM to have best sensitivity for As. Samples naturally containing high levels of Mn^{II} do not require this addition and then it is possible to measure As^{V} directly without the need of any reagent addition. Advantages of the new method are a lack of requirement of strong acids, and the possibility to study arsenic speciation in unmodified samples as measurements take place at the original sample pH, avoiding the possibility that the concentration of reactive As^{V} is altered as a result of releases from colloidal or suspended particulate matter.

References

[1] M.O. Andreae, Limnol Oceanogr, 24 (1979) 440.
[2] J. Vandenhecke, M. Waeles, J.Y. Cabon, C. Garnier, R.D. Riso, Estuar Coast Shelf S, 90 (2010) 221.
[3] J.J. Middelburg, D. Hoede, H.A. Vandersloot, C.H. Vanderweijden, J. Wijkstra, Geochim Cosmochim Ac, 52 (1988) 2871.
[4] M.O. Andreae, Deep-Sea Research, 25 (1978) 391.
[5] W. Maher, S. Foster, D. Thomson, Mar Chem, 108 (2008) 172.
[6] G.A. Cutter, L.S. Cutter, Mar Chem, 49 (1995) 295.
[7] M.J. Ellwood, W.A. Maher, Deep-Sea Res Pt I, 49 (2002) 1971.
[8] W.A. Maher, Water Res, 19 (1985) 933.
[9] P. Anninou, R.R. Cave, Estuar Coast Shelf S, 82 (2009) 515.
[10] G.A. Cutter, L.S. Cutter, Mar Chem, 61 (1998) 25.
[11] A.M.M. Debettencourt, M.O. Andreae, Appl Organomet Chem, 5 (1991) 111.
[12] W.R. Cullen, L.G. Harrison, H. Li, G. Hewitt, Appl Organomet Chem, 8 (1994) 313.
[13] K. Jitmanee, M. Oshima, S. Motomizu, Talanta, 66 (2005) 529.
[14] A.M. Featherstone, E.C.V. Butler, B.V. O'Grady, P. Michel, J Anal Atom Spectrom, 13 (1998) 1355.
[15] D.E. Mays, A. Hussam, Anal Chim Acta, 646 (2009) 6.
[16] L. Meites, J Am Chem Soc, 76 (1954) 5927.
[17] P. Salaun, B. Planer-Friedrich, C.M.G. van den Berg, Anal Chim Acta, 585 (2007) 312.
[18] Y.C. Sun, J. Mierzwa, M.H. Yang, Talanta, 44 (1997) 1379.
[19] C.M. Barra, M.M.C. dos Santos, Electroanal, 13 (2001) 1098.
[20] A. Profumo, D. Merli, M. Pesavento, Anal Chim Acta, 539 (2005) 245.
[21] H.L. Huang, D. Jagner, L. Renman, Anal Chim Acta, 207 (1988) 37.
[22] E.A. Viltchinskaia, L.L. Zeigman, D.M. Garcia, P.F. Santos, Electroanal, 9 (1997) 633.
[23] G. Cepria, S. Hamida, F. Laborda, J.R. Castillo, Anal Lett, 42 (2009) 1971.
[24] K. Gibbon-Walsh, P. Salaun, C.M.G. van den Berg, Environ Chem (2011) Submitted.
[25] K.S. Gibbon-Walsh, P. van den Berg C.M.G Talanta, accepted (2011).
[26] L. Nyholm, G. Wikmark, Anal Chim Acta, 257 (1992) 7.
[27] G. Billon, C.M.G. van den Berg, Electroanal, 16 (2004) 1583.
[28] C.S. Chapman, C.M.G. van den Berg, Electroanal, 19 (2007) 1347.
[29] P. Salaun, C.M.G. van den Berg, Anal Chem, 78 (2006) 5052.
[30] C.M.G. van den Berg, Anal Chim Acta, 164 (1984) 195.
[31] P.W. Atkins, Shriver & Atkins' inorganic chemistry, Oxford University Press, Oxford, 2010.
[32] J. Zima, C.M.G. Van Den Berg, Anal Chim Acta, 289 (1994) 291.
[33] L.M. Laglera, G. Battaglia, C.M.G. van den Berg, Anal Chim Acta, 599 (2007) 58.
[34] B. Cosovic, V. Zutic, V. Vojvodic, T. Plese, Mar Chem, 17 (1985) 127.

5

Chapter 5
DETERMINATION OF MANGANESE AND ZINC IN COASTAL WATERS BY ANODIC STRIPPING VOLTAMMETRY WITH A VIBRATING GOLD MICROWIRE ELECTRODE

5. DETERMINATION OF MANGANESE AND ZINC IN COASTAL WATERS BY ANODIC STRIPPING VOLTAMMETRY WITH A VIBRATING GOLD MICROWIRE ELECTRODE

5.1 Introduction

Both essential elements, manganese and zinc, play an important role in biogeochemical processes in natural aquatic systems, as their deficiency or antagonism with iron may affect oceanic plankton growth [1]. Mn speciation is controlled by its two redox states, Mn^{II} and Mn^{IV}, with a concentration in ocean waters (Pacific) typically between 0.5 and 2 nM [2]. Zn exists as Zn^{II} in natural waters and its speciation is controlled by organic complexation in estuarine [3], coastal [4] and ocean waters [5, 6]. Zn generally occurs at concentrations between 0.1 and 10 nM in ocean waters [7], with higher concentrations found in coastal waters [8].

Mn and Zn in seawater are measured in the laboratory using inductively coupled plasma mass spectrometry (ICP-MS) after separation and preconcentration, using for instance $Mg(OH)_2$ co-precipitation [9]. Mn can also be detected in-situ in the ocean using fibre-optic spectrophotometry [10].

There are many papers concerning the voltammetric detection of Zn and Mn, but only comparatively few have the sensitivity to detect trace levels in seawater. Voltammetric methods for Zn in seawater were initially based on anodic stripping voltammetry (ASV) using the mercury drop electrode (HMDE) [11], or a mercury film electrode for improved sensitivity [12, 13]. However, better sensitivity is obtained by cathodic stripping voltammetry (CSV) [14] (limit of detection (LoD) <0.1 nM). Both bismuth [15] and a gold-disk microelectrode [16] have more recently been proposed as good electrode materials to measure Zn in natural waters. For Mn the reduction potential is more negative than that for Zn and therefore nearer to the hydrogen wave, which restricts the electrodes that can be used. Mn can be determined by ASV using mercury-based electrodes [17]. Gold- and silver-disk electrodes (30 to 40 µm) have also been used, but with limited success [18]. Mn can also

be determined by CSV using a glassy carbon electrode [19], electrodes based on graphite [20] or boron-doped diamond (sonoelectroanalysis) [21] with a limit of detection of 9 nM. Existing methods for Mn have insufficient sensitivity for its determination at natural levels in seawater.

An advantage of electroanalytical methods is their portability, enabling detection and speciation in the field, on-site and sometimes in-situ, eventually eliminating the need for sample collection and storage. Here we develop a method based on a vibrating gold microwire electrode (VGME), which has advantages related to its robustness and sensitivity, facilitating analysis in the field. The hydrogen wave on the gold electrode is more positive than on mercury, which could be a disadvantage because of its proximity to the negative reduction potential for Mn. However, the peaks for Mn and Zn are located at more positive potentials than on mercury (away from the hydrogen wave) as a result of under-potential deposition (UPD), which means that both can be determined at neutral pH values. UPD is caused by interaction between the plated metal (here Zn and Mn) and the metal that makes up the electrode (here gold). Bruckenstein and co-workers initially played an important role in the development of UPD principles [22], which are now receiving increased interest with 122 papers published on this topic in 2010 (Web of Science search February 2011). UPD enables detection of specific metals in waters at trace levels using metal-based electrodes, and has recently been reviewed [23]. The gold microwire electrode selected here has advantages related to ease of preparation and insensitivity to hydrogen development [24]. The vibration of a 10 µm VGME lowers the thickness of the diffusion layer to ~1 µm, which greatly improves mass transport and lowers the detection limit.

Conditions are given here to determine both Zn and Mn at trace levels in coastal seawater using the VGME. The new method extends the applications of the gold microwire electrode, which currently is suitable for detection of copper, mercury [25, 26], arsenic [27] and antimony [24] in seawater, and arsenic speciation in freshwater [28].

5.2 Experimental

5.2.1 Reagents

Water used to prepare reagents and preliminary working solutions was 18 M Ω cm deionised water (Millipore Elix 3 with Milli-Q gradient deioniser and UV). Standard solutions of Mn^{II} and Zn^{II} were prepared by appropriate dilution of stock solutions (1000 mg L^{-1} in nitric acid, atomic absorption standard (AAS) solutions, purity 99.5 %, AnalaR BDH Chemicals Ltd, UK), acidified to pH 2 with HCl. Any unacidified stock solutions were prepared freshly for use. HCl was purified by sub-boiling distillation on a quartz condenser. H_2SO_4 (0.5 M) used for electrode conditioning was from BDH (AnalaR grade). Metal solutions (Cu, As, Pb, Hg, Sb^{III}, Mn, Zn, Cd, Ni, Fe, Bi^{III} and Se^{IV}) used for interference experiments were diluted from AAS standard solutions from Fluka or VWR; sodium dodecylsulfate (SDS) was from Aldrich, Triton X-100 from BDH (England), humic acid and fulvic acid was 'Suwannee river fulvic acid' from the International Humic Substances Society. A 0.5 M stock solution of ethylenediaminetetraacetic acid (EDTA) was prepared from the EDTA disodium salt (purity 99.5 %, AnalaR, BDH Chemicals Ltd, England). Ammonia solution (purity 35 %, Fischer Scientific, UK) was purified by sub-boiling distillation on a quartz condenser. HEPES buffer (purity 99 %, Acros organics, UK) contained 1-M 4-(2-hydroxyethyl)-1-piperazineethanesulfonic acid (HEPES, Fisher scientific, UK) and 0.5 M NaOH, and had its pH adjusted to 7.85 using NaOH.

5.2.2 Certified reference material (CRM)

To confirm the validity of the methods Mn and Zn were measured in CRM: NASS-5 from the National Research Council Canada. The CRM was acidified with nitric acid to pH 1.6, neutralised using NH_3 and then buffered using 10 mM HEPES, resulting in a final pH of 7.85.

5.2.3 Sample collection and pretreatment

Seawater used for optimisation experiments was collected from the Irish Sea, filtered (0.2 µm) and stored in an acid rinsed 50 L polyethylene container. Individual seawater samples were collected (7 m depth) during a survey of the Irish Sea with the research vessel Prince Madog (June and July 2009, and September 2010) using a rosette-mounted, Niskin bottle (General Oceanics, 5 L), modified to obtain samples uncontaminated with metals (Teflon coated spring on the outside, no rubber inside). These samples were filtered (0.2 µm filtration cartridge) and transferred to 500 mL acid-washed Nalgene low-density polyethylene bottles and stored frozen on board the ship.

5.2.4 Instrumentation

Voltammetric instrumentation was a 663 VA electrode stand from Metrohm, Switzerland, connected by an interface (IME, Autolab) to a µAutolab(III) (Metrohm, Switzerland) potentiostat. Data were processed with GPES 4.9 software. A 50 mL three-electrode cell was used containing the working electrode (WE) consisting of a gold microwire, a counter electrode (CE) consisting of a 200 µm iridium wire (from Goodfellow, UK), and a reference electrode (RE). The iridium wire of the CE was heat-sealed in a propylene pipette tip, with 3 mm protruding. The cell was PTFE for analyses and a separate glass cell was used for electrode preparation in 0.5 M H_2SO_4. The reference electrode was double-junction, glass, Ag/AgCl/KCl (3 M)/KCl (3 M). The gold microwire electrodes were prepared similarly to before [24, 26, 29], but the fitting was adapted to facilitate tip replacement and vibration (patent applied for). The gold microwire (99.99 %, hard, Goodfellow) was fitted within a 100 µL polypropylene pipette tip (uncoloured). This tip was then fitted onto a 1 mL polypropylene pipette tip, which had a vibrator incorporated and a connecting electrical cable protruding ~1 cm at the bottom, which made contact with the WE. The vibrator was driven by a 1.5 V power supply (home-built converter of 5 to 1.5 V), which was interfaced to, and powered by, the IME (Autolab, Metrohm, Switzerland), and controlled by the stirrer on/off trigger in the software (GPES, Autolab). The diameter of the microwire electrode was 10 µm and the length was ~0.5 mm.

Natural organic matter in seawater was destroyed, when required, by UV irradiation of seawater samples (30 mL) using a 125 W UV lamp. The quartz sample tubes were conditioned using neutral pH seawater before use to minimise adsorption, and irradiation was for 45 min. In other experiments samples were acidified (10 µL of 50 % HCl per 10 mL of seawater), UV-digested, and then neutralised using ammonia and HEPES buffer.

5.2.5 Electrode conditioning

The working electrode was cleaned in 0.5 M H_2SO_4 by hydrogen generation at –3 V (15 s) when the electrode was new, or when fouling was suspected. The electrode was verified using cyclic voltammetry (CV) (typically 5 cycles) from 0 to 1.5 V and back (100 mV s^{-1}) in the 0.5 M H_2SO_4. A good functioning electrode should show a oxidation peak for gold at 1.1 V, which forms a monolayer of Au_2O_3, and a symmetrical gold reduction peak in the returning scan at 0.9 V [25]. The cyclic voltammograms usually settle down and reach stability by the second scan.

5.2.6 Determinations of the surface area of the electrode

The real surface area of the electrode was determined as described previously [25], by measuring the area of the gold reduction peak after formation of an oxide monolayer (capacity of 450 µC cm^{-2} on polycrystalline gold [30]) in the returning (negative going) CV scan after reversing the positive-going CV scan at 1.5 V. This area is derived by calculating the charge (in coulombs) for the reduction of Au_2O_3 from the area of the reduction peak; assuming monolayer coverage this is the total area of the electrode [25]. The geometric area by chronoamperometry was determined by fitting of the diffusion limited current in 10 mM ferricyanide and 0.5 M KCl to a modified version of the Cottrell equation [25] developed for microwire electrodes.

5.2.7 Voltammetric procedure to determine Mn

Mn was determined by anodic stripping chronopotentiometry (ASC) as this was found to be insensitive to interference from the hydrogen ion reduction current, in contrast to ASV. An aliquot of seawater (pH ~8) was placed in the voltammetric cell, and the solution was deaerated by purging for 5 min. Prior to each scan the electrode was cleaned using a conditioning potential of +0.55 V (5 s) with the vibrator on, the deposition potential was –1.35 V (60 s) with the vibrator on, the quiescence time was 3 s and the ASC scan was 0.5 V. The oxidation current was 5 nA. The Mn peak was at –0.95 V and the peak area was used for quantification. The sensitivity (*S*) was calibrated by repeating the measurement after addition of Mn standard, and *S* was calculated from: *S* = (increased response for Mn)/(concentration of added Mn).

5.2.8 Voltammetric procedure to determine Zn

ASV scans of Zn were obtained in the same aliquot as used for Mn. Zn was determined after Mn because it is not affected by Mn additions. The conditioning potential was +0.55 V (5 s), the deposition potential –0.9 V (60 s), and a –1.2 V desorption potential was applied for 1 s, before the scan, to remove adsorbed organics and anions [25]. A 3 s quiescence time was used and scans were recorded from –0.9 to +0.5 V. A background scan, made after each analytical scan at a deposition time of 1 s, was subtracted from the analytical scan. ASV parameters: square-wave mode, step: 8 mV, amplitude: 50 mV, frequency: 50 Hz. The derivative of the Zn peak was used for quantification and the peak was located at –0.55 V.

5.3 Results and discussion

5.3.1 Optimisation of the analytical parameters for the measurement of Mn and Zn

Compared to measurements carried out on mercury electrodes, peak potentials for metals deposited on the gold microelectrode are shifted to more positive values as a result of under-

potential deposition (UPD) [31]. Using the gold microwire, the ASV peak for Zn was located at –0.55 V, and for Mn at –0.95 V, in pH 8 seawater (Figures 1A and C). Using the mercury electrode the Zn peak is located at –0.98 V [32] and Mn at –1.6 V [33], both in seawater. The Zn peak therefore shows a positive shift of 0.4 V, and the Mn peak of 0.6 V, on the gold electrode.

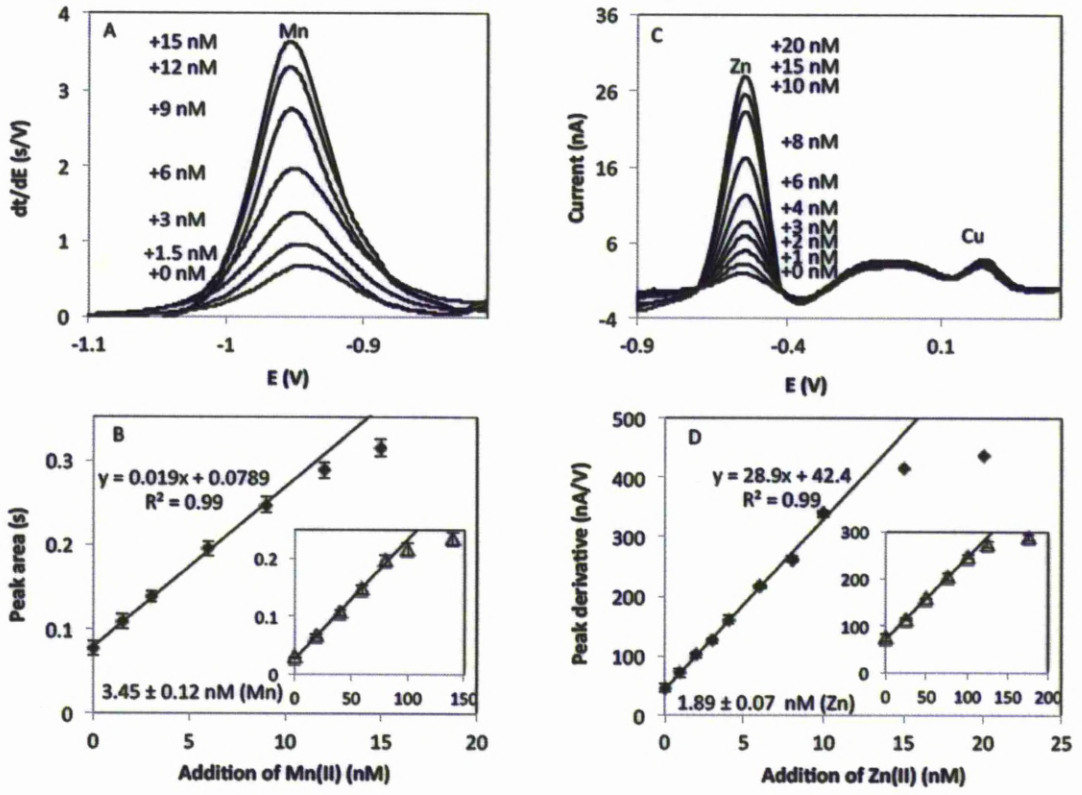

Figure 1. Scans for Mn (A) and Zn (B) in UV digested seawater (Liverpool Bay, Irish Sea). **A)** Scans for standard additions of Mn using anodic stripping chronoamperometry (ASC) 5 nA current). **B)** Linear calibration for Mn for t_{dep} 300 s, inset t_{dep} 60 s. **C)** Scans for standard additions of Zn using square wave mode. **D)** Linear calibration for Zn for t_{dep} 300 s, inset t_{dep} 60 s.

Although both Zn and Mn can be determined in seawater using square-wave ASV (SWASV), the peak for Mn is close to the base of the hydrogen wave. Addition of Mn caused the hydrogen wave to shift to more positive values in the analytical scan, encroaching on Mn and causing its peak to increase in a non-linear fashion and making it difficult to quantify the Mn using SWASV at low concentrations. In contrast, scans using ASC were found to be unaffected by the hydrogen ion reduction, displaying a flat baseline and linear calibration for Mn starting from low nanomolar levels (Figure 1B).

Zn could be measured using either ASC or SWASV, but a better signal/noise ratio was obtained using SWASV where the Zn peak was better shaped and smoother, which was particularly important for low Zn concentrations. Only one peak was produced for Zn using the VGME in seawater, without a shoulder, in contrast to measurements using a gold-disk electrode [16] where a shoulder was apparent on the anodic side of the peak.

Variation of the deposition potential (Figure 2A) showed that the peak for Zn was obtained after deposition at potentials between –0.7 and –1.5 V with optimum sensitivity between –0.9 and –1.2 V. A deposition potential of –0.9 V was selected for Zn as this maximised the response for Zn without causing any deposition of Mn. The peak potential for Zn was –0.58 V, so optimal deposition was at an over-potential of 0.3 V.

In comparison Mn was detected in seawater only after deposition within a very narrow (50 mV) potential range, between –1.3 and –1.35 V. This range could be extended to below –1.35 V in dilute pH buffer solutions, suggesting that the decrease in seawater was caused by anion effects rather than as a result of hydrogen generation. This effect on Mn differs from that of Cu which has a stable response until –1.5 V, steeply dropping to zero at –1.6 V, and for Zn which decreased more gradually (Figure 2A), decreasing by 40 % at –1.4 V, before disappearing after deposition at –1.6 V. The peak potential for Mn was –0.95 V, so the over-potential for Mn deposition was 0.3 V. A deposition potential of –1.35 V was selected for the Mn determination in seawater.

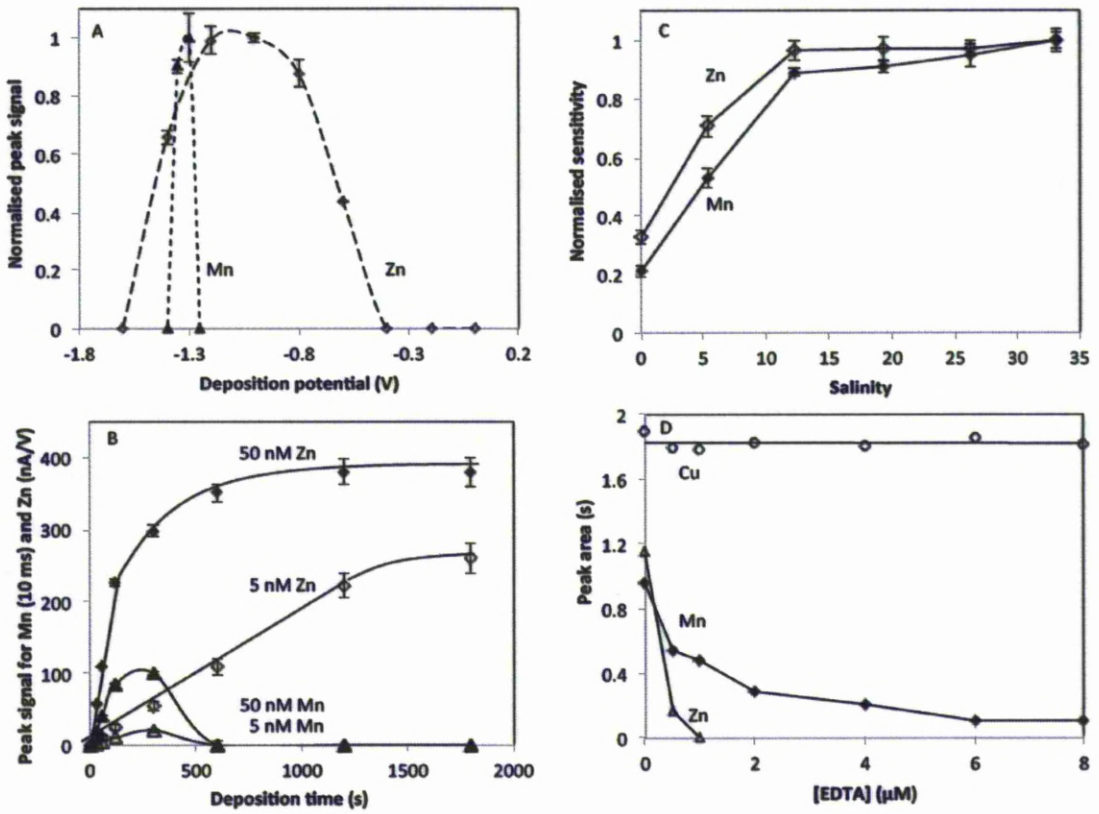

Figure 2. Optimisation of the analytical parameters for ASV of Zn and ASC of Mn in UV digested seawater containing 10-mM HEPES buffer (pH 7.8). **A)** Variation of the deposition potential; B**)** variation of the salinity; **C)** variation of deposition time; and **D)** effect of addition of EDTA.

5.3.2 Effect of variation of the salinity

The effect of variation in the salinity on the sensitivity for Zn and Mn was determined in seawater at various dilutions with deionised water. The pH was buffered to pH 7.85 with 10-mM HEPES and E_{dep} was –1.35 V for Mn and –0.9 V for Zn. The sensitivity for both Zn and Mn was found to be stable when the salinity was lowered from 34 to 15, but it was found to decrease at lower salinities, to 20 % of that for Mn at salinity near 0, and 35 % of that for Zn (Figure 2B). The decreased sensitivity is related to the importance of anions as a contributing factor to the UPD deposition of Mn and Zn on the gold electrode. A similar salinity effect exists for Cu and Pb on gold [16] suggesting that this is a feature of UPD.

5.3.3 *Effect of varying the pH on the response for Zn and Mn*

The response for Mn and Zn in seawater was investigated as a function of the pH, which was buffered over a wide pH range with 10-mM NaAc, 10 mM K_2HPO_4, 10 mM $NaHCO_3$ and 10 mM H_3BO_3. The pH was decreased by addition of HCl from a starting pH of 8.5. A deposition potential of –1.35 V was used for both Mn and Zn. A separate experiment was carried out using a deposition potential of –0.9 V to deposit Zn without Mn. The experiment was repeated to verify the unexpected difference in response for Zn and Mn. The Mn response decreased from pH 8.5 to 5.5 (Figure 3A), and became gradually masked by the hydrogen wave, which shifts to more positive potentials by 59 mV per pH unit according to the Nernst equation, in this case fully masking the Mn peak at pH values below 5.5. The Mn peak potential showed a small positive shift (5 mV per pH unit) with decreasing pH (Figure 3B) indicating that the UPD of Mn on the gold electrode is pH insensitive.

The effect of the pH on the response for Zn depended on whether Mn was deposited (E_{dep} –1.35 V) or not (E_{dep} –0.9 V). At both deposition potentials the Zn peak was obtained between pH 8.5 and 2.5, becoming increasingly masked by the hydrogen wave at pH < 3 and fully masked at pH < 2.5.

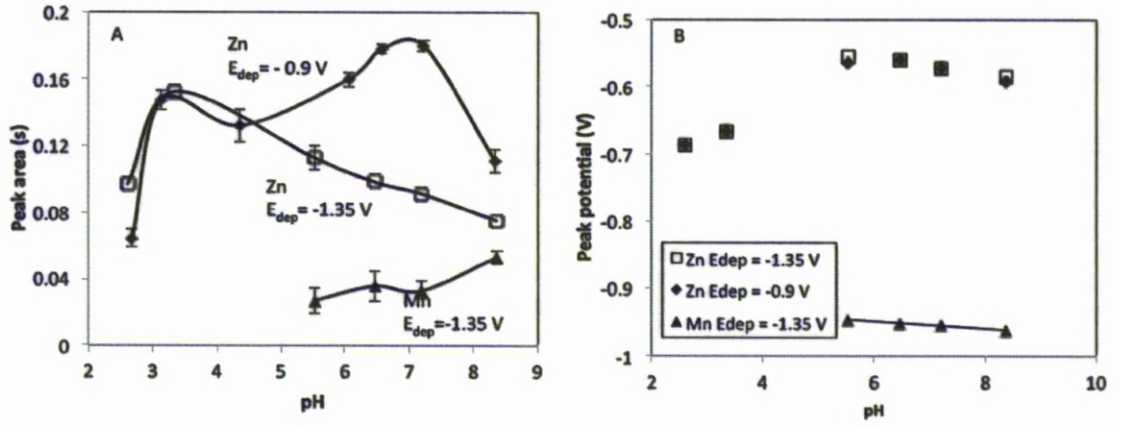

Figure 3. Effect of variation in the pH on the voltammetric response for 30 nM Mn and 25 nM Zn in seawater; all scans in the ASC mode at a current of 5 nA. The pH was buffered using a mixed buffer containing 10 mM NaOAc, 10 mM $KHPO_4$, 10 mM $NaHCO_3$ and 10 mM H_3BO_3. The pH was varied by additions of HCl; the error bars indicate the standard deviation of three consecutive scans. **A)** Effect of the pH on the peak area; **B)** effect of the pH on the peak potential, the meaning of the symbols the same as in (A).

Between pH 2.5 and 4.5 the sensitivity for Zn was the same at the two deposition potentials. Using E_{dep} = −0.9 V, the sensitivity for Zn generally increased with increasing pH between pH 4 and 9, reaching a maximum at 6.8 < pH < 7.5, whereas it decreased with increasing pH after deposition at −1.35 V. The Zn response at the maximum between pH 6.5 and 7.5 was a factor of two greater than that when Mn was co-deposited (E_{dep} −1.35 V). Interference experiments (see below) showed that this difference was a result of interference by Mn. The peak potential for Zn showed a small positive shift (10 mV per pH unit) with pH decreasing from 8.5 to 5.5 before shifting to negative values at lower pH values (150 mV over 3 pH units) (Figure 3B). The small positive shift at pH 8 to 6.5 was attributable to the increased peak size which tends to cause a shift in the direction of the scan on solid electrodes. The larger negative shift at lower pH values indicates that the Zn interaction with the electrode, which underlies the UPD process and which has a strong effect on the peak potential, became weaker. This pH effect on the Zn peak potential on gold also occurs on platinum [34], suggesting that ionic interactions plays a role in the UPD process.

The pH data show that the optimal pH range for measurement of Zn is between pH 3.5 and 8.5, and for Mn is between pH 6 and 8.5. The pH of samples that have been acidified should therefore be raised, for instance using acetate buffer to pH 4.5 to enable measurement of Zn, or using HEPES to pH 7.8 to allow detection of Zn and Mn. UV-digestion is recommended before the analysis to eliminate masking as a result of organic complexation, for total concentrations.

Unacidified seawater has a natural pH of ~8. Without pH buffer, the pH drifts up to ~8.6 during purging to remove dissolved oxygen at which point the majority of the CO_2 has been removed and the buffer capacity of the carbonate system is significantly greater than at pH 8.1. The response for Mn and Zn is not affected by minor pH variations in this range so analyses of seawater were carried out without any reagent addition, which simplified the procedure and eliminated any metal contamination attributable to the reagents.

5.3.4 *Signal stability*

The response for Mn and Zn in 400 mL of seawater was measured every hour for 30 h in a 500-mL Nalgene bottle. No reagents were added to the seawater, but it was purged with N_2 before the beginning of the experiment, and was N_2-blanketed during the experiment. The water contained 25 nM of Zn and 30 nM of Mn. The Mn peak height was stable over this time with a standard deviation of 3 % (n = 30) over 30 h. Over the same time, the signal for Zn decreased by 20 % (0.7 % h^{-1}) and had a relative standard deviation of 6 % (n = 30); this decrease was a result of adsorption on the bottle as the calibrated sensitivity of the electrode in seawater was unchanged after the stability experiment. The stability of the response indicates that the gold wire electrode can be used for extended on-site, or in-situ, analysis, with only intermittent calibration.

5.3.5 *Peak measurement from its height, area, or derivative*

Comparative measurements were made of the response for Zn as a function of concentration where the response was measured using the peak height and the derivative peak height. No systematic difference was found between the two measuring types, but the derivative method was found to be more reliable for automated peak finding procedures at low metal concentration (low signal/noise ratio). On the other hand, the peak area was always measured during the ASC scans for Mn, the derivative method giving no advantage as the baseline of the ASC scans was flat and unaffected by the hydrogen ion reduction current.

5.3.6 *Linear range and sensitivity*

Optimised conditions were used to establish the linear response range and limit of detection for Zn and Mn in seawater. Using a 300 s deposition time the Zn peak was found to increase linearly with the Zn concentration up to 10 nM Zn after which the increase levelled off (Figure 1D). The linear response range was extended to 100 nM at a shorter deposition time of 60 s (inset of Figure 1B)

indicating that the levelling off was caused by electrode saturation after which the UPD process was weakened.

The response for Mn was linear to 10 nM for 300 s deposition, levelling off at higher concentrations, and this linear range was increased to 80 nM using a 1 min deposition time. The increase in the linear range of Mn was greater than the factor of 5 expected, which could be attributed to a decrease in the relative interference of other metals at the shorter deposition time.

The deposition time was varied to investigate whether the sensitivity is enhanced with a longer deposition time. The response initially increased linearly with the deposition time, followed by a levelling off of the response for Zn, and an unexpected decrease in response for Mn (Figure 2C). For 5 nM Zn the increase was linear up to 1200 s before levelling off. The sensitivity for 5 nM Mn first increased linearly with time up to 200 s (Figure 2C), the increase then diminished at 300 s, decreasing to zero after 500 s deposition. At higher Zn and Mn concentrations (50 nM) the increase was linear for Zn up to 60 s, and for Mn the sensitivity began to level off at 150 s and dropped again after 300 s. The levelling off of the response for Zn can be ascribed to saturation of the electrode with approximately a monolayer of Zn after which the UPD process diminishes. However, the disappearance of the peak for Mn with increased deposition time suggests that something else interfered with the Mn determination at increased deposition time.

5.3.7 Maximum coverage of the electrode

The surface area of the electrode was determined as described in the Experimental section. The total area was 3.38×10^{-4} cm^2 (corresponding to an oxide reduction charge of 1.52×10^{-7} C), whereas the geometric area was determined as 2.20×10^{-4} cm^2. The geometric area was smaller than the total area because it excludes roughness, a dimension less than the thickness of the diffusion layer. In this case the roughness factor was 1.5 in accordance with previous results [25].

The response for Mn and Zn is non-linear at high metal concentrations because of progressive saturation of the gold surface. The amount of Zn plated was calculated from the charge of the ASV peak obtained in linear sweep mode (scan rate 10 mV s^{-1}). The amount of plated Mn was obtained similarly from the surface area of the ASC scans. The maximum amount of Zn (Mn) that could be deposited on the electrode was obtained by fitting of the data to the following version of the Langmuir equation [35]:

$$C_m/i_o = C_m/i_m + 1/(Bi_m) \quad (1)$$

where C_m is the dissolved metal concentration, i_m is the maximum current (at which monolayer coverage should be attained), i_o is the actual oxidation current (in Coulombs) for each measurement, and B is a constant related to the free energy of adsorption.

The space occupied by plated Zn (Mn) was then calculated by multiplication with the atomic size obtained from the atomic radius (135 pm for Zn and 140 pm for Mn) [36] (this assumes that Mn and Zn are fully reduced, in the metallic form, on the electrode). The maximum loading of Zn amounted to 0.331×10^{-4} cm^2 and of Mn to 0.476×10^{-4} cm^2. This meant that 14 % of the total electrode area was covered with Mn, and 10 % with Zn. In both cases the maximum coverage is high, not far from the total available, considering that the electrode could in part be covered with adsorbed anions or plated with other metals. The Mn was deposited at a more negative potential (–1.35 V) than Zn (–0.9 V), which may have caused a greater repulsion of the anions during the deposition step, which may be the reason for the higher coverage with Mn.

The high coverage with Zn and Mn indicates that the non-linearity at high metal concentrations was caused by near monolayer saturation of the electrode.

5.3.8 Limits of detection (LOD)

The LOD was determined from three times the standard deviation of seven measurements using the optimised parameters in UV digested seawater with low levels of Mn and Zn. The LOD was 0.3 nM Zn

and 1.4 nM Mn using a 300 s deposition time. These LODs are lower than previously reported on mercury-free electrodes. For Zn this can be lowered to 150 pm by extending the plating time to 10 min. Although very good, and sufficient to determine Zn in clean ocean water, it is less good than achievable (LOD of 30–40 pm Zn) on a mercury-plated, rotating-disk electrode (10 min in-situ Hg plated in the presence of thiocyanate) [13], but the microwire has advantages related to electrode simplicity (no polishing and no deposition of a film) and it does not require any reagents.

5.3.9 Certified reference seawater

These newly developed methods were successfully tested in certified reference seawater NASS-5 (National Research Council Canada) after the pH was readjusted to 7.85 using NH_3 and HEPES buffer. Using ASC a Mn concentration of 17.5 ± 0.8 nM was obtained, which is within the confidence interval of the reference value in the NASS-5 ([Mn] = 17.0 ± 1.04 nM). Using SWASV a concentration of 1.8 ± 0.2 nM Zn was obtained, which was also within the confidence interval of the reference Zn concentration ([Zn] = 1.6 ± 0.6 nM).

5.3.10 Effect of metal complexation on the response for Mn and Zn

EDTA was used as model ligand to investigate possible effects of organic complexation. Addition of EDTA to UV-SW containing 30 nM Mn and Zn caused their response to be lowered. Figure 2D shows the effect, along with the effect on Cu for comparison. The effect of EDTA was strongest on Zn, which was fully masked by 1 µM EDTA, whereas the Mn signal was lowered by 50 % at 1 µM EDTA and further at higher levels. Conditional stability constants for EDTA with these metals in seawater are: log K'_{CuEDTA} = 10.3, log K'_{ZnEDTA} = 8.0 and log K'_{MnEDTA} = 5.4 (these conditional stability constants were calculated from constants valid for ionic strength of 0.1 M and at 25 °C [37] corrected for side-reaction of EDTA with the major ions in seawater using an ion-pairing model to calculate the free concentrations of the major ions). The steeper decrease for Zn than for Mn is in agreement with the comparative complex stabilities. The response for Cu was unaffected by the EDTA additions in spite of the high stability of the Cu complexes because of the high over-potential for Cu (the Cu peak at

the gold electrode is at +0.2 V, so the over-potential is 1.5 V), causing reduction of the CuEDTA complex.

5.3.11 Interference by dissolved oxygen (DO)

Dissolved oxygen was found to interfere with voltammetry of Zn and Mn, causing a large background current and a broad peak centred at –0.7 V. Sample solutions were therefore purged with N_2 for 5 min before analysis. The pH tended to shift to ~8.6 because of partial degassing of CO_2, but this pH change was not found to affect the peak signals for Zn or Mn.

5.3.12 Interference by metals

The response of the Zn and Mn signal to various metals was tested in UV digested seawater containing 30 nM Zn and 30 nM Mn, at a deposition time of 60 s at –1.35 V. No significant interference was caused for either Mn or Zn with addition of 100 µM Al, 15 µM Fe, 1 µM Bi or 1 µM Sb^{III}. An addition of 50 µM Cu decreased the Mn signal by 50 % and the Zn peak by 75 %. Addition of 1 µM Pb reduced the Zn signal by 50 %, whereas the Mn signal was unaffected. All these metal additions were at least 1000 times greater than natural levels. Zn and Mn interfere with each other when they are deposited at –1.35 V. Addition of 300-nM Mn led to a 50 % decrease in the Zn signal and addition of 400 nM Zn gave a 50 % decrease in the Mn signal: this effect was caused by saturation of the electrode surface. The Mn interference on the Zn response was eliminated using a deposition potential of –0.9 V. The Zn interference on Mn could be reduced by addition of 1 µM EDTA.

5.3.13 Interference by As^{III} and As^{V}

Only one element caused interference at the near-natural level in seawater: addition of 100 nM arsenic (as As^{III} or As^{V}) led to a 50 % decrease of the response for Mn and Zn after deposition at –1.35 V. The effect of As^{III} can be understood because this is plated on the gold electrode and can be

determined by ASV using the gold microwire electrode [27]. Arsenic is a metalloid and its deposition ultimately leads to a non-conductive coating on the electrode, preventing the further deposition of other elements. Because the predominant species of As is As^{V}, there is normally very little As^{III} (~1 nM or less) so interference of As^{III} should not be an issue. The effect of As^{V} is unexpected because it is considered to be electro-inactive at neutral pH whereas As^{III} is deposited at potentials < –0.6 V [27]. Using deposition at –0.9 V (only Zn is deposited then) addition of 300 nM As^{III} gave a 50 % decrease in the Zn response, but not As^{V} which even at a concentration of 1 µM had no effect. The interfering effect of As^{V} on Mn (deposition at –1.35 V) was minor using a deposition time of 60 s, but its effect increased with increasing deposition time and was the cause for the decrease in the response for Mn when the deposition time was increased beyond 300 s, and caused a reduced sensitivity even at shorter deposition times (Figure 2B). The As^{V} interference therefore makes it impossible to lower the LOD for Mn to sub-nanomolar levels in seawater as the deposition time at –1.35 V cannot be extended beyond 300 s.

5.3.14 Interference by organic matter

Organic material can interfere because of surfactant or complexation effects. Humic substances form complexes with metals in seawater [38] and also have a surfactant effect which is ~1 % of that of Triton-X-100 [39]. Stepwise addition of humic acid (HA) up to 25 ppm caused a 50 % decrease in the peak for Zn, and addition of 35 ppm HA caused a 50 % decrease for Mn. Addition of 50 and 60 ppm fulvic acid (FA) caused a 50 % decrease in the response for Zn and Mn, respectively.

Surfactant effects were tested by addition of the non-ionic surfactant Triton-X-100 and the anionic surfactant SDS; 15 ppm Triton caused the Mn signal to decrease by 50 %, whereas a much stronger effect was seen for Zn with 0.5 ppm Triton decreasing the peak by 50 %. No effect was observed for Mn or Zn with addition of up to 10 ppm SDS. Although Mn would not be affected, the Zn signal may suffer from surfactant interference, because surfactant levels in coastal waters are typically in the range of 0.1–1 ppm Triton equivalents [39]. The high level of Triton required to suppress Mn

suggests that the effect caused by HA and FA was attributable to Mn complexation. The much stronger surfactant effect on Zn suggests that this effect cannot be ruled out as a partial explanation for the Zn signal suppression caused by HA and FA. Unlike Mn, however, HA and FA are known to form strong complexes with Zn in seawater, sufficient to begin to bind Zn from 1-ppm HA or FA [38].

5.3.15 Sample UV digestion at neutral pH or after acidification

With a view to eliminating the need for sample acidification, it was tested whether Mn and Zn adsorbed on the quartz tubes used for UV-digestion if this was carried out at natural pH. Three samples from Liverpool Bay (collected in September 2010) were analysed for Zn and Mn after UV digestion at natural pH and at pH 2.5 (addition of 10 µL of 50 % HCl per 10 mL). The quartz UV digestion tubes were conditioned for use at pH 2.5 or at neutral pH by rinsing either with dilute acid or with seawater sample (three times) before use. After UV digestion at pH 2.5 the pH was readjusted to 7.85 using NH_3 and 10 mM HEPES buffer. The average concentration of Mn after UV digestion at natural pH was 2 % (n = 3) lower than after UV digestion at pH 2.5 (Table 1), however the difference was within the standard deviation of the measurements. For Zn the concentration after UV digestion at natural pH was systematically 6 % (n = 3) lower than after UV digestion at pH 2.5, with each sample being slightly lower. This small loss suggests that adsorption losses of Zn occurred on the surface of the quartz tubes during UV digestion in spite of the conditioning. It is therefore advisable to acidify the samples before UV digestion.

Table 1. Effect of UV digestion at natural pH or pH 2.5 on labile Mn and Zn concentrations (nM) in seawater (Liverpool Bay, Irish Sea, September 2010)

Station	Salinity	Mn		Zn	
		pH 8	pH 2.5	pH 8	pH 2.5
1	32.11	94 ± 5	95 ± 4	27 ± 2	29 ± 1
7	32.54	71 ± 3	70 ± 3	25 ± 1	27 ± 1
35	32.01	102 ± 5	109 ± 6	37 ± 2	39 ± 2

5.3.16 Application to coastal seawater

The new ASV and ASC methods were used to determine Zn and Mn in seawater from the Irish Sea (Liverpool Bay). A series of water samples was collected from a single site (CTD Station number 31: Latitude: 53°37.002'N, Longitude: 3°55.398'W) at hourly intervals over a 15 h period (July 2009). The tidal period was ~11 h and the salinity varied between 33.6 and 33.9. The water depth was ~40 m and the tidal height variation was ~7 m. The samples were stored in 500 mL Nalgene bottles at natural pH and frozen on-board within minutes of collection. These samples were then analysed with no pretreatment (other than de-aeration) for Zn and Mn within a week of their collection, immediately after overnight defrosting followed by careful swirling to ensure any partides became re-dissolved.

The concentration of Zn varied in the range of 2 to 20 nM, and Mn between 2 to 15 nM: this variation was a result of tidal movement moving waters of slightly lower and higher salinity across the sample location (Figure 4). Trend lines through the data for Zn and Mn as a function of the salinity show that both varied in a non-linear fashion: their concentrations are increasing with decreasing salinity, but the increase is beginning to level off at a salinity of 33.7. Causes for this non-linearity may be sought in a local source for these metals: benthic re-suspension combined with release from sediments under reducing conditions could be a source of Mn^{II}, from reduction of MnO_2, and associated Zn. Similar processes have been shown previously for UK coastal waters [40].

The concentrations of Zn and Mn are within the range found previously in the Irish Sea [8]. Seasonal variation in dissolved Mn as a result of localised anoxia in surface sediments, is another example of the sedimentary release in coastal waters around the UK [8, 41, 42] and suggests that an estuarine benthic source can play a role in the non-linearity of the metal data.

A plot of the concentrations of Mn and Zn as a function of the sampling time shows that their concentrations co-vary with the tide (Figure 4B) where Zn and Mn have the highest concentration at the low salinity point (low tide). This variation is likely a result of the admixture of Mn and Zn rich bottom waters at the time when the tidal direction reverses.

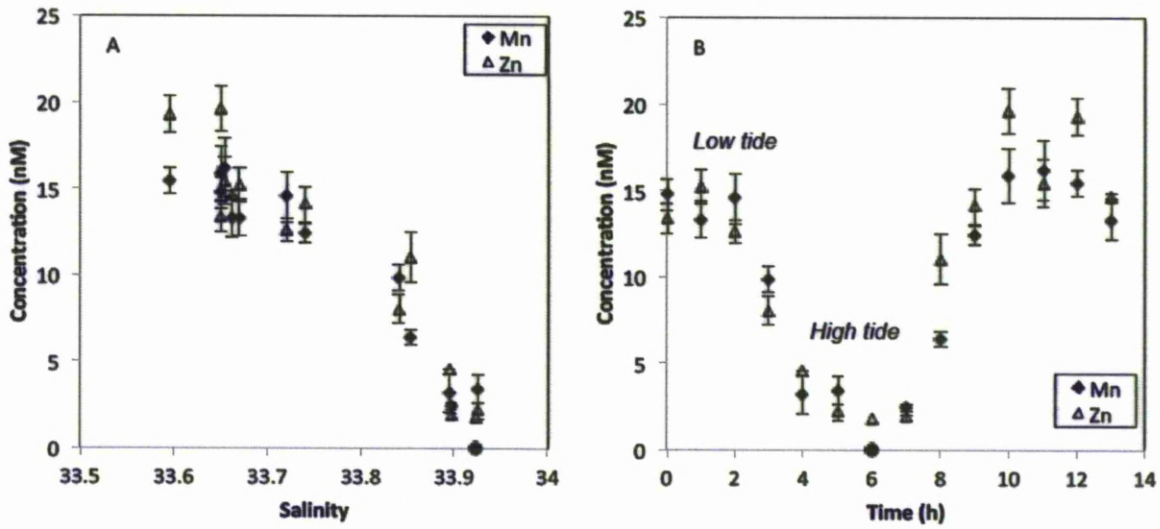

Figure 4. Monitoring of Mn and Zn over a tidal cycle in surface seawater over 15 h at a station in Liverpool Bay (Station 31, Irish Sea). The error bars are the standard deviation obtained from the standard additions. **A)** Variation of Mn and Zn with salinity; **B)** Mn and Zn as a function of time. Circle at salinity 33.92 indicates a Mn concentration below the detection limit of 1.4 nM.

5.3.17 Effect of sample storage on the detected metal concentrations

Table 2 shows the results for five seawater samples (salinity 32.19–32.79) (Liverpool Bay, June 2009). The average Zn concentration was 49 ± 26 nM and the average Mn concentration was 231 ± 86 nM. The samples were then stored at natural pH at 4 °C in the dark and reanalysed similarly after six months. Repeated analysis showed that the concentrations of Zn and Mn in the thus stored samples

had decreased significantly: Zn had decreased on average by 17 % and Mn by 93 %. The concentrations of Mn and Zn were nearly fully recovered after UV digestion (45 min) of sub-samples of the same bottles, at natural pH, with 95 % of the original Mn concentration recovered and 94 % of the original Zn concentration. This means that the conversion to non-labile Zn and Mn was not a result of bottle-wall adsorption. Conversion to non-labile metal is typically a result of inert complexation, a change into a non-reactive oxidation state, or association with particle surfaces with a very low rate of diffusion. In this case the large decrease in Mn was thought to be attributable to oxidation to electrochemically inert MnO_2, whereas the decrease in Zn was attributed to either adsorption on MnO_2 or other metal hydroxides, or because of organic complexation. The small, 5 %, non-recovered losses were attributed to adsorption on the Nalgene bottles, which had been stored at natural pH and kept unfrozen over an extended period of time.

Table 2. Effect of sample storage on labile concentrations (nM) of Mn and Zn in samples from Liverpool Bay, Irish Sea (June 2009)

Station	Salinity	Zn			Mn		
		Analysed immediately	6 months storage at 4 °C		Analysed immediately	6 months storage at 4 °C	
		Untreated	Untreated	UV digested	Untreated	Untreated	UV digested
1	32.62	30 ± 1	15 ± 1	29 ± 2	255 ± 23	27 ± 2	232 ± 11
8	32.28	67 ± 4	47 ± 2	65 ± 11	312 ± 19	62 ± 4	301 ± 21
14	32.8	35 ± 1	24 ± 2	31 ± 1	282 ± 17	35 ± 2	277 ± 14
22	32.79	31 ± 2	21 ± 1	26 ± 1	90 ± 8	14 ± 1	84 ± 9
35	32.19	40 ± 2	30 ± 2	39 ± 2	215 ± 17	28 ± 1	206 ± 15

Labile metal concentrations were determined immediately after sampling, and again after 6 months storage (refrigeration to 4 °C) with and without UV digestion (at pH 8)

The similarity of the concentrations found for labile (untreated samples, within a week) and total dissolved (after UV digestion after several months storage) metal concentrations suggests that the majority (>95 %) of the Mn and Zn in these samples was initially labile in the experimental conditions used here, and became oxidised or organically complexed upon extended storage. It is likely that the Mn and Zn were largely labile because of the large over-potential used in the deposition step on the VGME. This means that it is sufficient to determine labile metal concentrations without any sample treatment for the purpose of monitoring Mn and Zn in natural waters using this technique. Samples kept for long-term storage should be either acidified or kept frozen.

5.4 Conclusion

Most (95 %) of the Zn and Mn in untreated seawater is labile and quantifiable using the new ASV method. Measurement is at natural pH without the need for reagents apart from the removal of oxygen before the scan. These are important considerations for an in-situ detection method and facilitate an in-situ monitoring system.

References

[1] K.W. Bruland, J.R. Donat, D.A. Hutchins, Limnol Oceanogr, 36 (1991) 1555.
[2] G.P. Klinkhammer, Anal Chem, 52 (1980) 117.
[3] C.M.G. Van Den Berg, A.G.A. Merks, E.K. Duursma, Estuar Coast Shelf S, 24 (1987) 785.
[4] F.L.L. Muller, D.R. Kester, Mar Chem, 33 (1991) 71.
[5] M.J. Ellwood, C.M.G. van den Berg, Mar Chem, 68 (2000) 295.
[6] K.W. Bruland, Limnol Oceanogr, 34 (1989) 269.
[7] K.W. Bruland, G.A. Knauer, J.H. Martin, Nature, 271 (1978) 741.
[8] R.E. Laslett, Estuar Coast Shelf S, 40 (1995) 67.
[9] M.A. Saito, D.L. Schneider, Anal Chim Acta, 565 (2006) 222.
[10] G.P. Klinkhammer, Mar Chem, 47 (1994) 13.
[11] M.I. Abdullah, B.R. Berg, R. Klimek, Anal Chim Acta, 84 (1976) 307.
[12] L. Mart, H.-W. Nurnberg, D. Dyrssen, in: C. S. Wong, E. Boyle, K. W. Bruland, E. D. Goldberg (Eds.), Trace Metals in Sea Water, Plenum Press, New York, 1983, p. 113.
[13] R.W. Jakuba, J.W. Moffett, M.A. Saito, Anal Chim Acta, 614 (2008) 143.
[14] C.M.G. Van Den Berg, Talanta, 31 (1984) 1069.
[15] J. Wang, Electroanal, 17 (2005) 1341.
[16] C. Garnier, L. Lesven, G. Billon, A. Magnier, O. Mikkelsen, I. Pizeta, Anal Bioanal Chem, 386 (2006) 313.
[17] L. Lesven, S.M. Skogvold, O. Mikkelsen, G. Billon, Electroanal, 21 (2009) 274.
[18] I. Pizeta, G. Billon, J.C. Fischer, M. Wartel, Electroanal, 15 (2003) 1389.
[19] J.S. Roitz, K.W. Bruland, Anal Chim Acta, 344 (1997) 175.
[20] C.M. Welch, C.E. Banks, S. Komorsky-Lovric, R.G. Compton, Croat Chem Acta, 79 (2006) 27.
[21] A. Goodwin, A.L. Lawrence, C.E. Banks, F. Wantz, D. Omanovic, E. Komorsky-Lovric, R.G. Compton, Anal Chim Acta, 533 (2005) 141.
[22] G.W. Tindall, S.H. Cadle, Bruckenstein.S, J Am Chem Soc, 91 (1969) 2119.
[23] G. Herzog, D.W.M. Arrigan, Trac-Trend Anal Chem, 24 (2005) 208.
[24] P. Salaun, K. Gibbon-Walsh, C.M.G. van den Berg, Anal Chem, 83 (2011) 3848.
[25] P. Salaun, C.M.G. van den Berg, Anal Chem, 78 (2006) 5052.
[26] G. Billon, C.M.G. van den Berg, Electroanal, 16 (2004) 1583.
[27] P. Salaun, B. Planer-Friedrich, C.M.G. van den Berg, Anal Chim Acta, 585 (2007) 312.
[28] K. Gibbon-Walsh, P. Salaun, C.M.G. van den Berg, Anal Chim Acta, 662 (2010) 1.
[29] L. Nyholm, G. Wikmark, Analytica Chimica Acta, 257 (1992) 7.
[30] U. Oesch, J. Janata, Electrochim Acta, 28 (1983) 1237.
[31] G. Herzog, D.W.M. Arrigan, Electroanal, 17 (2005) 1816.
[32] G. Gillain, G. Duyckaerts, A. Disteche, Anal Chim Acta, 106 (1979) 23.
[33] R.J. O'Halloran, Anal Chim Acta, 140 (1982) 51.
[34] S. Taguchi, A. Aramata, J Electroanal Chem, 457 (1998) 73.
[35] C.M.G. van den Berg, Anal Chim Acta, 164 (1984) 195.
[36] P.W. Atkins, Shriver & Atkins' inorganic chemistry, Oxford University Press, Oxford, 2010.
[37] A.E. Martell, R.M. Smith, Critical stability constants, Plenum Press, New York ; London, 1974.
[38] R.J. Yang, C.M.G. van den Berg, Environ Sci Technol, 43 (2009) 7192.
[39] B. Cosovic, V. Vojvodic, Limnol Oceanogr, 27 (1982) 361.
[40] E.P. Achterberg, C. Colombo, C.M.G. van den Berg, Cont Shelf Res, 23 (2003) 611.
[41] D.J. Hydes, K. Kremling, Cont Shelf Res, 13 (1993) 1083.
[42] A.D. Tappin, D.J. Hydes, J.D. Burton, P.J. Statham, Cont Shelf Res, 13 (1993) 94.

6

Chapter 6
SCANNED STRIPPING VOLTAMMETRY OF COPPER AND ZINC AT A SOLID VIBRATING GOLD MICROWIRE ELCTRODE

6. SCANNED STRIPPING VOLTAMMETRY OF COPPER AND ZINC AT A SOLID VIBRATING GOLD MICROWIRE ELECTRODE

6.1 Introduction

Biogenic trace metals copper (Cu) and zinc (Zn) are essential micronutrients, serving as co-factors in a number of enzymes important for algal physiology [1]. Both Cu and Zn exist in seawater in the +II oxidation state, and Cu to some extent as Cu^{I} chloride [2]. Cu^{I} is increased by photochemical related reactions [3] and is stabilised by complexation with thiols [4]. In seawater, Cu^{II} is complexed up to 99 % with organic matter [5, 6], while organically bound Zn accounts for 98 % of its total metal concentration [7]. Knowing the distribution of a metal between its 'free' inorganic fraction and its organic complexed fraction (the metal speciation) is important as bioavailability is generally greatly increased when the metal occurs in the inorganic form [8] and greatly reduced when complexed to organic ligands [9], although this is a greatly simplified view.

The metal speciation can be determined by a combination of cathodic stripping voltammetry with ligand competition [10], or by anodic stripping voltammetry (ASV) [11]. The natural ligand concentration and its conditional stability constant are determined using complexometric titration techniques [12] in which the ligand is titrated with increasing amounts of metal, using ASV to detect the labile (as proxy for the free inorganic), or CSV to determine the metal bound by the competing ligand as a measure of the free metal ion concentration. In both cases the speciation in the original sample represents the first measurement, and the original speciation is computed from the ligand concentration and the conditional stability constant. Pseudopolarography (formally polarography using mercury electrodes) in which the response at each potential point is enhanced by a deposition step [13] is an alternative in which labile and inert species of metals are determined in the unmodified sample, without metal or ligand additions. Pseudopolarograms can be built up using scanned stripping techniques [14] in which labile and inert complexes of dissolved trace metals can be distinguished. Pseudopolarograms are constructed by obtaining a series of ASV [13] or stripping

chronopotentiometry (SC) [15, 16] scans at sequential changes of accumulation potential. The information gained from scanned stripping techniques is similar to that of classical polarography, but is achieved at a significantly lower metal concentration.

The half wave potential ($E_{1/2}$) of natural complexes and the limiting current are the main parameters derived from the pseudopolarograms. From the difference between the reduction potentials (estimated from $E_{1/2}$) of the inorganic metal and its inert organic complexes, the thermodynamic stability constant of the organic species can be calculated [17]. Reversible complexation causes a shift of the reduction wave of labile species of the metal towards more negative potentials [18] whereas inert species are separately reduced at increasingly more negative potentials [17]. Labile species are characterised by their dissociation in the diffusion layer, whereas inert species do not dissociate but are reduced at a potential related to the thermodynamic stability constant.

Previous work on scanned stripping techniques has used mercury-based electrodes:

a hanging mercury drop electrode (HMDE) [19], a mercury thin film electrode [20], and mercury hemisphere microelectrodes [21, 22]. Generally the metal concentration in the samples is increased to give the required voltammetric response. However there are examples of scanned stripping techniques applied to natural concentrations of Zn in seawater [23], Pb in sulfidic and oxic seawater [24], Cd in fresh water [25] and lead (Pb) in porewaters [22].

Thermodynamic stability constants of unknown inert metal complexes have been estimated for Cu and Zn in seawater [23, 26], Pb in oxic and sulfidic [24] seawater and Cd in freshwater [25] with calibration of the half-wave potentials against an experimentally established, operational 'chelate scale' of known complexing ligands.

Mercury is an excellent electrode material for several metals but not for copper, as its oxidation potential is close to that for mercury which increases the limit of detection and because of relatively poor solubility of copper in the mercury. Solid electrodes on the other hand can suffer from instability of response [22]. Here we describe the use of a vibrating gold microwire electrode (VGME)

for pseudopolarography of copper in seawater, with the advantage of better sensitivity sufficient for trace levels of copper. The response was stabilised by in-situ renewal of the electrode surface before each scan.

6.2 Experimental

6.2.1 Reagents

Water used to prepare reagents and preliminary working solutions was (resistivity 18 MΩ cm) deionised water (Millipore Elix 3 with Milli-Q gradient deioniser and UV). Standard solutions of Cu^{II} and Zn^{II} were prepared by appropriate dilution of stock solutions (1000 mg L^{-1} in nitric acid, atomic absorption standard solutions, purity 99.5 %, AnalaR BDH Chemicals Ltd, UK), acidified to pH 2 with HCl. Any unacidified stock solutions were prepared freshly for use. HCl was purified by sub-boiling distillation on a quartz condenser. 0.5 M H_2SO_4 used for electrode conditioning was from BDH (AnalaR grade). Humic acid and fulvic acid was "Suwannee river fulvic acid" from the International Humic Substances Society. HEPES buffer (purity 99 %, Acros organics, UK) contained 1 M (4-(2-hydroxyethyl)-1-piperazineethanesulfonic acid)4-(2-hydroxyethyl)-1-piperazineethanesulfonic acid (HEPES, Fisher scientific, UK) and had its pH adjusted to pH 7.85 using 0.5 M NaOH. POPSO buffer (purity 99 %, Acros organics, UK) contained 1 M Piperazine-1,4-bis-(2-hydroxy-propane-sulfonic acid) dihydrate and had its pH adjusted to pH 7.85 using NaOH. HEPPS buffer solution(purity 99 %, Acros organics, UK) contained 1 M (3-[4-(2-Hydroxyethyl)-1-piperazinyl]propanesulfonic acid and had its pH adjusted to pH 8 using NaOH.

The model ligands nitrilotriacetic acid (NTA, 99 %, Fluka, puriss p.a), 2-hydroxybenzaldehyde (Salicylaldoxime, Sigma, Germany), dodecane (99 %, Fisher scientific, UK), Dopamine hydrochloride (sigma, Germany), 3, 4-dihydroxy-DL-phenylalanine (DOPA, Sigma, Switzerland), n-nonane (>99 %, Acros organics), ethylenediaminetetraacetic acid (EDTA, BDH, analaR, Poole, UK), dimethylglyoxime (DMG, Sigma), L-cysteine (>99 %, Sigma), 1,2-cyclohexanedione dioxime (nioxime, Sigma),

ethylenediamine (>99.5 %, puriss p.a. absolute, Fluka), diethylenetriaminepentaacetic acid (DTPA, Acros organics), glutathione (>98 %, BDH, analaR, Poole, UK), 1,2-diaminocyclohexanetetraacetic acid (CDTA, >98 %, agross organics) and cyclen (97 %, Fisher scientific) were added to UV digested seawater buffered with HEPES (pH 7.85).

6.2.2 Sample collection and pre-treatment

Seawater used for optimisation experiments was collected from the Irish Sea, filtered (0.22 µm filtration cartridge) and stored in an acid rinsed 50 L polyethylene container. Individual seawater samples for on-board and laboratory analysis were collected (7 m depth) during a survey of the Irish Sea with the RV Prince Madog (June 2010) using a rosette-mounted, Niskin bottle (General Oceanics, 5 L), modified to obtain samples uncontaminated with metals (Teflon coated spring on the outside, no rubber inside). Samples to be analysed in the laboratory were filtered (0.22 µm Sartobran filtration cartridge) and transferred to 500 mL acid washed Nalgene low-density polyethylene bottles stored frozen on board the ship. A second bottle of each sample was acidified to pH ~ 2 using HCl for later metal analysis. A composite sample was made up from water samples collected in Liverpool Bay (March 2010), filtered and kept in an acid cleaned 50 L polyethylene container. This water was used for method development.

6.2.3 Instrumentation

Voltammetric instrumentation was a 696 VA electrode stand from Metrohm, Switzerland, connected via an interface (IME663, Autolab) to a µAutolab(III) (Metrohm, Switzerland) potentiostat. Data was processed with GPES 4.9 software. A 50 mL three-electrode cell (glass) was used containing the working electrode (WE) consisting of a gold microwire; a counter electrode (CE) consisting of a 200 µm iridium wire (from Goodfellow, UK); and a Ag/AgCl/KCl(3M)//KCl(3M) double junction reference electrode (RE). Both the WE and CE were heat-sealed in a propylene pipette tip, with 3 mm protruding as adapted from before [27-29], where the fitting was adapted to facilitate tip

replacement and vibration (patent applied for) [30]. The cell was PTFE for analyses and a separate, glass, cell was used for electrode preparation in 0.5 M H_2SO_4. The gold microwire (99.99 %, hard, Goodfellow) was fitted within a 100 µL polypropylene pipette tip (uncoloured). This tip was then fitted onto a 1 mL polypropylene pipette tip, which had a vibrator incorporated and a connecting electrical cable protruding ~1 cm at the bottom, which made contact with the WE. The vibrator was driven by a 1.5 V powersupply (home-built converter of 5 V to 1.5 V), which was interfaced to, and powered by, the IME (Autolab, Metrohm, Switzerland), and controlled by the stirrer on/off trigger in the software (GPES, Autolab). The diameter of the microwire electrode was 5 µM and the length approximately 0.5 mm, unless otherwise stated. For analysis conducted on board the Prince Madog (August 2010) the voltammetric cell was placed inside a Faraday cage (Windsor Scientific, UK) instead of the VA 696 stand.

Natural organic matter in seawater was destroyed, when required, by UV irradiation of seawater samples (30 mL) using a 125 W UV lamp. The quartz sample tubes were conditioned using neutral pH seawater prior to use to minimise adsorption, and irradiation was for 45 min. The surface of the WE was cleaned electrochemically by hydrogen generation at -2 V for 60 s in 0.5 M H_2SO_4, followed by cyclic voltammetry (5 scans) between 0 and 1.5 V (100 mV s^{-1}) to verify that the electrode response was without noise [31].

6.2.4 Determination of the length of the electrode

The total surface area and the geometric area were determined as previously described [31]. Briefly, an oxide monolayer was first formed at a positive potential in 0.5 M H_2SO_4 and its reduction charge used to calculate the total area, assuming a 450 µC cm^{-2} charge density for an oxide monolayer. The geometric area was obtained by fitting the diffusion-limited current in a solution of 10 mM ferricyanide (in 0.5 M KCl) to the theory. The length was the fitted parameter assuming a constant diameter of 5 µm (commercial specification and checked by scanning electron microscope) see Annex II and III.

6.2.5 Scanned stripping voltammetry parameters

Unless otherwise stated square-wave anodic stripping voltammetry (SWASV) was used to measure Zn and Cu in seawater. Optimisation of scanned stripping techniques on the VGME was conducted in seawater solutions (collected March 2010) before and after UV digestion (removal of organic complexation). 15 mL seawater was transferred to the voltammetric cell and buffered with 10 mM HEPES buffer in order to control the pH at the surface of the electrode. The solution was purged with N_2 for 15 min and a N_2 blanket maintained thereafter. A conditioning potential was used of +0.55 V (15 s), followed by a 60 s accumulation potential and a -1.2 V desorption potential (1 s), prior to the scan, to remove adsorbed organics and anions [31, 32]. A 3 s quiescence time was used and stripping scans were from -1 V to +0.5 V. A background scan, made after each analytical scan using the same parameters but no accumulation, was subtracted from the analytical scan. Scan parameters were square-wave mode, step: 8 mV, amplitude: 25 mV, frequency: 50 Hz. The derivative of the background corrected peak signal was used for quantification. The Zn peak was located at –0.55 V and the Cu peak at +0.2 V. Pseudopolarograms were constructed as a series of SWASV voltammograms with 25 mV step changes in the deposition potential. These measurements were carried out in a non-systematic manner to avoid introducing systematic errors finally giving a pseudopolarogram of 25 mV resolution.

6.3 Results

Preliminary experiments were carried out to optimise electrode and measurement stability. Cu measurement does not require degassing but as it is easy to include the peak for Zn in each scan, and as its peak is affected by that of dissolved oxygen (DO), solutions were N_2-purged. The purging also minimises any changes in the pH at the electrode surface which might affect the speciation, albeit only over a short time span of a few ms when the solution is in the diffusion layer during the deposition step. The use of pH buffers was tested to eliminate pH change during deposition at

potentials <-1 V when hydrogen generation could play a role. Measurement stability was optimised by making use of a desorption potential, and memory effects were eliminated by using an oxidation potential to re-oxidise any plated metals between measurements.

6.3.1 Choice of buffer

Buffer solutions were tested in UV digested seawater for interference with the voltammetric scans. 10 mM POPSO (pH = 7.85) and HEPPS (pH = 8) added to UV digested seawater (UV-SW) were found to interfere by causing suppression of the pseudopolarogram in the shape of a irreversible wave, indicating the formation of a mixture of poorly reversible Cu complexes. No interference was caused by 10 mM HEPES (pH = 7.85), which was the reason it was chosen for optimisation experiments. Pseudopolarography of Cu in UV-SW with and without added 10 mM HEPES buffer gave the same curve suggesting that pseudopolarography can be applied in seawater without the need for external buffering.

6.3.2 Desorption potential

Adsorption of anions on the surface of the gold electrode causes the sensitivity for Cu in seawater to vary [31]. Application of a desorption potential prior to the scan causes the sensitivity to increase and stabilise. Use of this desorption potential was found to be paramount in obtaining a well shaped peak in the scans used for the pseudopolarograms. Without this desorption step, the Cu peak was small and irregularly shaped, especially after deposition at a relatively high (positive) deposition potential (figure 1). Voltammetric scans using the mercury drop electrode are similarly improved by a desorption step used to remove adsorbed surface-active substances (SAS) [32, 33]. The influence of using a desorption potential (E_{des}) on scanned stripping voltammetry of Cu at trace levels in seawater with and without UV-digestion (figure 1A) in the range -0.2 to -1.5 V was studied. The deposition potential was -0.2 V for 60 s and the desorption time was 1 s. For both UV and non UV seawater the peak intensity increased at more negative desorption potential, reaching a maximum

when E_{des} = -1.4 V. The Cu peak strongly decreased when E_{des} was ≤-1.6 V (figure 1A) possibly due to the reduction of sodium [34]. The increase in response at deposition potentials <-0.5 V in UV-SW indicates that the desorption potential removes, or at least strongly diminishes, the negative influence of adsorbed anions during the stripping process. However the increased influence of the desorption potential on non-UV-SW, suggests a possible organic influence at the surface of the electrode, also reduced by the use of a more negative desorption potential, the 19 fold increase in peak intensity by the desorption potential at E_{des}=-1.4 V in non-UV-SW (see inset figure 1A) highlights the paramount importance of this desorption potential that should be considered for any ASV method.

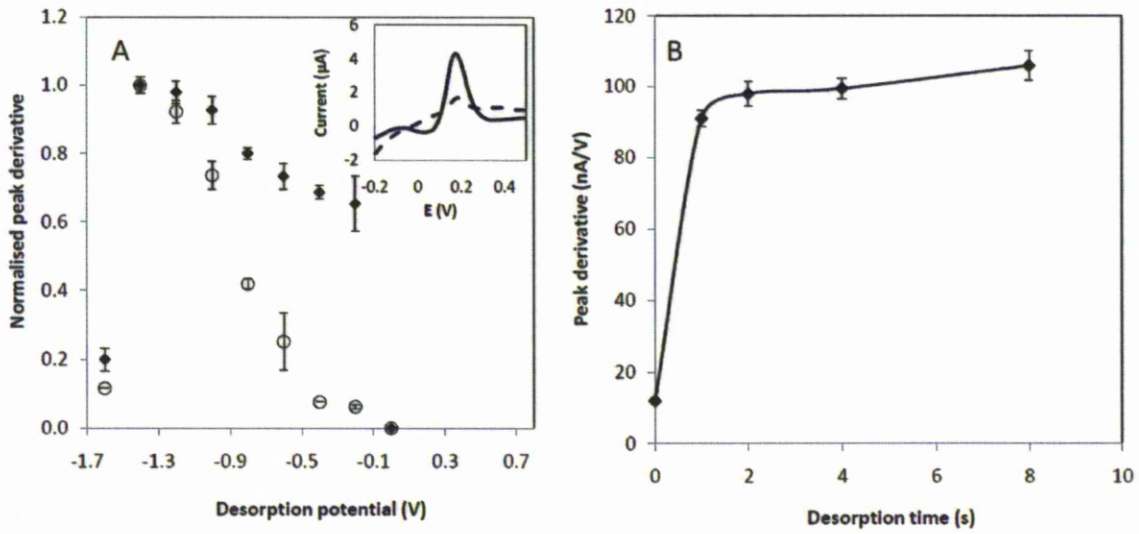

Figure 1. The desorption potential is applied between deposition at -0.2 V for 60 s and the scan **A)** Cu signal intensity determined at varied 1 s desorption potentials in seawater (empty circles) and UV digested seawater (full diamonds) both containing 10 mM HEPES, pH 7.85. **B)** The effect on Cu signal intensity of -1.2 V desorption potential applied for increased periods of time before the scan.

The desorption time (E_{des} = -1.4 V) was varied from 0 s to 8 s after a constant deposition time of 60 s in non-UV-digested seawater. The desorption effect was found to be completed within 1 s after which no further improvement in the peak height was obtained (figure 1B). A desorption potential of -1.2 V for 1 s was employed in all voltammetric analyses.

6.3.3 *Memory effects*

A hysteresis was found to occur between pseudopolarograms carried out in a forward (increasing negative deposition potentials) and negative potential direction. Repeated measurements after deposition at various potentials showed that this hysteresis was caused by an accumulated charge with more negative deposition potential, due to the accumulation of anions at the surface of the electrode. Such effects do not occur on mercury drop electrodes due to the formation of a new drop before each measurement [35], but these effects are typical for solid electrodes which always require some sort of cleaning step between scans. In this case the hysteresis was the cause of a bias in the half-wave potentials determined and for this reason experiments were conducted to negate the memory effects on the gold wire electrode.

As the hysteresis was caused by reversible changes of the electrode during the sequence of voltammograms, it was attempted to return the electrode to a constant initial state, without deposited metal, prior to each subsequent voltammogram. Hysteresis was reduced by using 10 preliminary voltammograms from a fixed deposition potential (the best results were obtained with E_{dep} = -1.4 V, but others were tried too) before each subsequent voltammogram in the pseudopolarogram, although this significantly decreased hysteresis, it did not completely remove the memory effects.

In several experiments a conditioning procedure was optimised with the following final conditions: -1.4 V, 30 s followed by 0.55 V for 60 s. This procedure was found to create a consistent electrode surface before each scan, by first removing anions with a negative potential, followed by re-absorbing them to a controlled degree at a positive potential. Just a conditioning at 0.55 V was not found to be effective and so both potentials were required in this 2:1 ratio. Other ratios of these potentials were tested, but did not have the same effect. 30 s followed by 60 s was also found to be the minimum time necessary for this conditioning interval to work, with lesser times proving less effective. The memory effect of the scans was completely removed by this conditioning interval

between each voltammetric scan. This interval was found to be suitable relevant for accumulation periods of up to 300 s with no need for further optimisation. The conditioning procedure was found to work equally well for gold microwires of diameters, 5, 10 and 25 μm, however a 100 μm wire was found to require longer periods of conditioning: -1.4 V, 90 s followed by 0.55V for 180 s.

As a result of the electrode stability pseudopolarograms could be constructed from voltammetric scans either in a systematic or randomised order without causing significant change in the shape of the final pseudopolarogram, causing reliable measurement of half-wave potentials of complex species. To prevent the possibility of experimental bias, pseudopolarograms were constructed 4-fold, with 100 mV difference between sequential scans to build up a full pseudopolarogram, first in a forward direction, the second in a backward direction offset by 25 mV, etc. The final pseudopolarogram had a 25 mV resolution without systematic bias. This iterative procedure was easier to programme than a completely randomised version.

6.3.4 Estimation of half-wave potentials ($E_{1/2}$) of the pseudopolarograms

Values for $E_{1/2}$ were determined using a modified Lingane equation [26, 36, 37] valid for reversible and irreversible systems:

$$\log(i_{max}-i/i) = (\alpha nF/RT)(E_{dep}-E_{1/2}) = (\alpha n/0.059)(E_{dep}-E_{1/2}) \quad (1)$$

where i_{max} is the diffusion-limited current of copper at deposition potentials E_{dep} below the half-wave potential $E_{1/2}$ of the relevant species, i is the current at each E_{dep}, α is the transfer coefficient, n is the number of exchanged electrons, $F = 96500$ C, $R = 8.314$ J mol^{-1} K^{-1}, and $T = 293$ K. By plotting $\log(i_{max} - i)/i$ vs E_{dep}, $E_{1/2}$ is obtained at the potential where the log-term is zero ($i = i_{max}/2$) [23]. The value for $E_{1/2}$ is independent of the transfer coefficient, α, as it is in the slope. The slope equals the product of α with the number of electrons of the electrode reaction.

6.3.5 *Effect of oxygen*

SSV waves were constructed in real seawater sample in the presence of oxygen and after purging for 15 minutes with N_2 (g). Oxygen had no interference on the Cu SSV waves due to it being more positive (+0.2 V) than the oxygen wave present on the gold electrode (-0.3 V) in SWASV [31]. Zn however occurs under the oxygen wave and so for SSV waves for Zn to be constructed purging the solution with N_2 (g) was necessary.

6.3.6 *Stability of Cu signal*

The Cu response was measured in a 400 mL seawater sample containing 17 nM Cu, at -1 V once an hour for 72 h in a 500 mL Nalgene bottle showing an 8.4 % (n = 72) decrease over this period. The original signal was recovered after cyclic conditioning in 0.5 M H_2SO_4. The result shows that the Cu signal and the electrode work well over a period of several days in the same solution. This decrease was due to fouling at the surface of the electrode as the calibrated sensitivity of the electrode in seawater was recovered only after the electrode was conditioned in H_2SO_4. The stability of response indicates that the gold wire electrode can be used for extended on-site, or in-situ, analysis, with only intermittent calibration.

Desorption potentials are important when dealing with real water samples such as seawater, adsorption of surface active substances (SAS), which forms a major fraction of present natural organic matter (NOM), can interfere with the voltammetric signal of Cu on mercury based electrodes [33].

6.3.7 *Pseudopolarography of Cu(EDTA)*

The $E_{1/2}$ for Cu(EDTA) was estimated 5x in UV-SW containing 1 µM EDTA, and compared to the $E_{1/2}$ for inorganic Cu in UV-SW without EDTA, but containing 10 mM HEPES buffer, fnal pH = 7.85. With the electrode conditioned in 0.5 M H_2SO_4 between pseudopolarograms. The half-wave potential of inorganic copper was 90 ± 10 mV (n=5).

In the presence of EDTA (figure 2A), the wave was shifted towards a more negative half-wave potential of $E_{1/2}$ = -970 ± 15 mV. The 15 mV standard deviation of $E_{1/2\ (CuEDTA)}$ translates into a standard error of ~0.3 in a log K of ~18.

The shift in $E_{1/2(CuEDTA)}$ is much greater than expected (expected shift for log K=18 is 18 x 30 mV = 540 mV instead of the actual shift of ~1100 mV), and is much greater than found previously using a HMDE ($E_{1/2}$ = -0.46 V, a negative shift of 0.21 V) [26] where the shift was much less than expected.

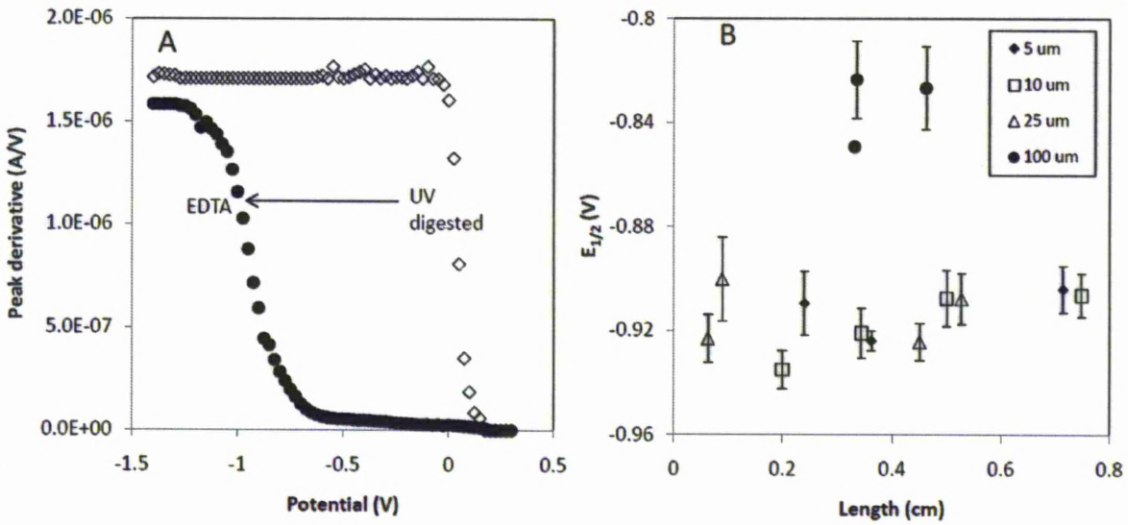

Figure 2. A) ~ 1 V shift of $E_{1/2}$ for a single wave of +0.1 V in UV digested seawater, to 0.9 V after addition of 200 µM EDTA (a strong copper complexing ligand, LogK' = 17.94). **B)** The effect of the length of the microwire electrode on the Cu(EDTA) half wave potential for wires of 5, 10, 25 and 100 µm diameter.

The half-wave potential for inorganic copper ($E_{1/2}$ = 0.09 V) in UV-SW is much more positive than that found using the HMDE (-0.2 V) [26]. The oxidation of copper to Cu^{II} in seawater is a two-step process (Cu(0) → Cu(I) → Cu(II)) due to stabilization of Cu^{I} by complexation with chloride [2]. High stability of these chloride species causes a predicted negative shift of the Cu(0)/Cu(I) couple of about 0.25 V, causing a peak potential for Cu of about -0.2 V using the HMDE in seawater, equal to the $E_{1/2}$ found using the HMDE by pseudopolarography [26]. The Cu(I)/Cu(II) peak cannot be seen using the HMDE as it is masked by the oxidation of Hg. Using the gold electrode also only one peak is apparent for Cu which is that for Cu(0)/Cu(II) which has been shifted to +0.2 V from an expected 0 V due to

adsorption stabilization on the gold, which is the cause for the well known process of under-potential stabilization [38]. The half-wave potential for inorganic Cu found here using the gold microwire electrode equals the peak potential found with this electrode, similar to that found using the HMDE. In each case therefore, for the HMDE and for the gold electrode, the experimental $E_{1/2}$ for inorganic Cu differs from that expected, although in different potential directions. In each case there is also a problem with the $E_{1/2}$ found for Cu(EDTA): the $E_{1/2}$ being more positive than expected using the HMDE and more negative using the gold electrode. The large negative shift on the gold may have been caused by irreversibility in the reduction of the Cu(EDTA) species. The reason for the more positive potential on the HMDE is not known.

In diffusion limited conditions (E_{dep} = -1.4 V), the current for Cu with EDTA was 10% lower than without EDTA (figure 2A), in general agreement with a lower diffusion coefficient for Cu(EDTA) than for inorganic Cu [39].

The peak potential for Cu on each SWASV scan was not affected by the presence of EDTA, because the copper concentration in the diffusion layer can be expected to be much greater than that of EDTA because of the electrochemical pre-concentration step prior to the scan, coupled with slow rate of complex formation compared to the fast rate of Cu oxidation during the square-wave modulation of the scan.

6.3.8 Square wave anodic stripping voltammetry versus stripping chronoamperometry

The SWASV scanning method was compared to anodic stripping chronoamperometry (ASC) for the construction of the Cu pseudopolarograms in UV-SW, with and without 200 µM EDTA. The relevant potentials for deposition, desorption and conditioning were kept the same so that only the stripping methods differed, with a 50 nA oxidising current used in chronoamperometry. The peak area was used for quantification in ASC, but this had to be measured manually to avoid misreading of the baseline. The peak derivative was measured automatically in the SWASV method. The $E_{1/2}$ values obtained for SSV and SSC for UV-SW with EDTA were 0.91 V and 0.89 V respectively within 20 mV of

eachother, whilst for UV-SW they were 0.09 V and 0.11 V respectively within 10 mV of each other, which is in line with expectation for 25 mV pulses of the SWASV method. The voltammetric stripping method was chosen for this work as it was facilitated by the automation of the peak measurement.

6.3.9 Effect of varying microwire length and diameter

Experiments were conducted to assess the effect of microwire size (length and diameter) on the $E_{1/2}$ for the EDTA wave in UV-SW containing 200 µM EDTA and 10 mM HEPES buffer (pH 7.85). 14 gold electrode tips were prepared, 4 of diameter 10 and 25 µm and 3 of diameter 5 and 100 µm. The $E_{1/2}$ of Cu(EDTA) averaged -0.91 ± 0.01 V (n =11), showing no effect of different electrode diameter in the range of 5 – 25 µm. Electrode length was also not found to have an effect. A 90 mV shift was found using thicker electrodes of 100 µm diameter, with $E_{1/2}$ averaging -0.83 ± 0.01 V (n =3). 5 µm electrodes were used for the remainder of this work.

6.3.10 Effect of varying the ligand concentration

In case of a labile complex ML which dissociates before reduction of the metal, the half wave potential is strongly dependent on the concentration of the ligand. This potential shift can be used for the determination of stability constant using the Deford and Hume theory, if the reversibility of the reaction is not affected by the addition of ligand [18]. On the other hand, when an inert complex is directly reduced at the electrode surface without prior dissociation of the complex, the half wave potential is only dependent on the thermodynamic stability constant of ML and not on the ligand concentration [17]. We tested this theory by measuring the effect of the ligand concentration on $E_{1/2}$ of Cu(EDTA) in UV-SW containing 17 nM Cu, 10 mM HEPES buffer and varying concentrations of EDTA of 1, 10, 100 and 1000 µM. In agreement with the theory for irreversible systems, the $E_{1/2}$ was found to be independent of the EDTA concentration.

6.3.11 Effect of variation of the metal concentration

The effect of variation in the Cu concentration on $E_{1/2}$ was tested for the Cu(EDTA) species in UV-SW containing 17 nM Cu, 200 µM EDTA and 10 mM HEPES buffer (pH 7.85). The diffusion limited current was found to increase as expected with the increased Cu concentrations. The increase in Cu concentration gave a negative shift in the EDTA $E_{1/2}$, initially of 2.4 mV nM^{-1}, which began to level off after 15 nM Cu was added with a 26 mV shift over the 50 nM of Cu added. This behaviour was the same as that observed on the HMDE where there is also no shift in $E_{1/2}$ for increasing metal concentration [35].

6.3.12 Effect of varying the deposition time

The effect of varying the deposition time on $E_{1/2}$ for the labile Cu wave in UV digested seawater containing 17 nM Cu and 10 mM HEPES buffer (pH 7.85). After normalisation a negative shift in $E_{1/2}$ is observed with increasing deposition time. For a reversible electrode reaction such as this the difference between $E_{1/2}$ for two different accumulation times is given by the equation [35]:

$$E_{1/2,2} - E_{1/2,1} = 0.059 \times \log(t_{acc,1}/t_{acc,2})/n \quad (2)$$

Linearity between the difference of the half wave potentials and the logarithm of the accumulation times has a slope of 57.1 mV. This slope represents $59/n$ mV, where n represents the number of electrons transferred, which is 1 and as Cu is reduced in seawater via a one-electron charge transfer. This represents a good agreement between the theoretically predicted value for a reversible one-electron charge transfer and the empirical result on the VGME.

The effect of varying deposition time on $E_{1/2}$ for Cu(EDTA) in UV-SW containing 17 nM Cu^{II} and 10 mM HEPES buffer (pH 7.85). After normalisation the $E_{1/2}$ was found to shift in a negative direction with increasing deposition time. Cu(EDTA) is expected to exhibit irreversible behaviour, i.e. no shift with deposition time on the HMDE [40] however a shift was obtained with the VGME, with a linear calibration with a slope of 28.3 mV indicating that the Cu(EDTA) complex is displaying

quasi-reversible properties with a two-electron charge transfer, which is in line with the expectation for the Cu^{II}(EDTA) species, however unexpected.

6.3.13 Effect of pH on pseudopolarograms of EDTA

Pseudopolarograms of UV-SW, containing 17 nM Cu, were carried out at 2 pH values: buffered at pH 7.85 with 10 mM HEPES, pH 5.8 with 10 mM acetate buffer. No change was observed in $E_{1/2(CuEDTA)}$ suggesting that the half wave potential is independent of pH in this range for irreversible Cu-organic ligand complexes.

6.3.14 Effect of pH on pseudopolarograms of seawater

Pseudopolarograms of seawater containing 17 nM Cu, were carried out at 3 pH values: buffered at pH 7.85 with 10 mM HEPES, pH 5.8 with 10 mM acetate buffer and acidified to pH 3 with HCl and left to equilibrate for 24 h. No difference was apparent in the pseudopolarograms at pH 7.85 or 5.8, except for a 3 % increase in the limiting current (E_{dep} = -1.4 V) at pH 5.8. There was a much larger effect at pH 3, as the labile fraction was much increased as a large proportion of the Cu, causing a 50 % increase in the labile wave, a 400 mV positive shift in the major Cu-organic ligand wave from -0.8 V to -0.4 V and a 5 % increase in the final limiting current. The redistribution of the organic fraction of Cu complexes to inorganic species is as expected due to the competition between Cu^{2+} and H^{+} for ligand binding sites. The redistribution of the organic fraction of Cu complexes to inorganic forms during acidification to pH 3 is due to the competition between Cu^{2+} and H^{+} for ligand binding sites. The large difference between pH 5.8 and pH 3 could be explained by the average pKa of the carboxylic-like sites present in dissolved organic matter (DOM) in seawater being 4.5 [41].

6.3.15 Effect of humic substances

Suwannee river (SR) humic acid (HA) and fulvic acid (FA) were added to UV-SW containing 12 nM Cu and 10 mM HEPES buffer (pH 7.85). Pseudopolarograms for this seawater with additions of 0, 0.5, 1,

2 and 4 mg/L HA are shown in figure 3A. The wave for Cu(HA) was found to be located in the labile potential region (within 0.2 V of inorganic Cu), in spite of the known strong stability of Cu with HA [42]. In line with expectation for a labile species, the $E_{1/2}$ was found to shift in a negative direction with increasing concentrations of HA, (figure 3B). The diffusion limited current became smaller as a result of the slower diffusion of the Cu(HA) species and as seen before for FA [43]. Addition of FA to UV seawater (figure 3C) shows less pronounced, but analogous behaviour to that of HA, also showing a negative shift in $E_{1/2}$, shown in figure 3D. This could also be the result of the kinetic effects of competition with other metals in solution.

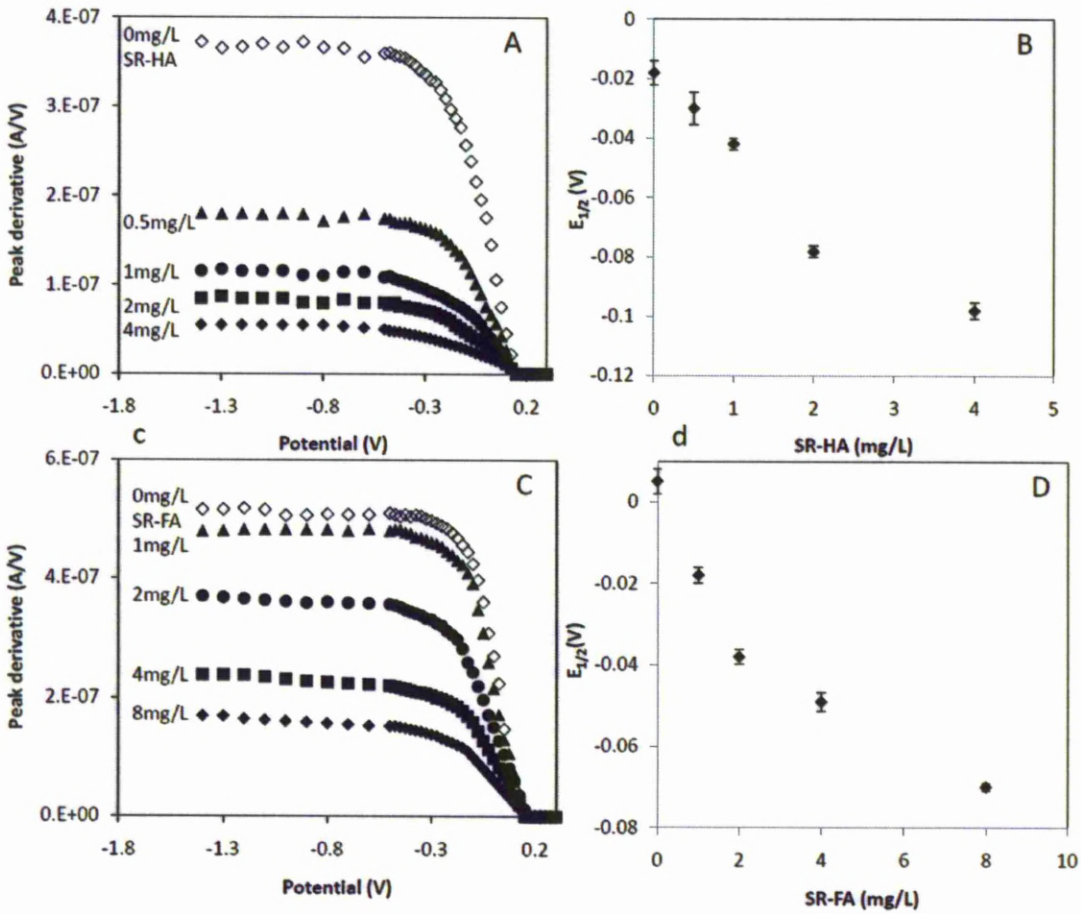

Figure 3. Pseudopolarograms are constructed for UV digested seawater containing 12 nM Cu, **A)** with increasing concentrations of Suwannee river humic acid **C)** with increasing concentrations of Suwannee river fulvic acid **B)** The shift in the half wave potential for increasing concentrations of SR-HA. **D)** The shift in the half wave potential for increasing concentrations of SR-FA.

6.3.16 Pseudopolarograms of model ligands

All experiments with model ligands were carried out in seawater from Liverpool Bay (March 2010). The seawater was UV-digested (UV-SW) and 10 mM HEPES was added giving a final pH of 7.85. The Cu concentration was 17 nM and model complexing ligands were added in large excess of the Cu. The model ligands were selected to cover a broad range of functionality and range of complex stabilities and most have been used in pseudopolarography of Cu previously [26]. Thermodynamic stability constants for the complexes (log K* values) ranged from 12.4 for $Cu(NTA)^-$ to 26.5 for Cu(cydam).

Table 1 summarizes the results of the laboratory experiments with the model organic ligands. The half-wave potentials ranged from 0.01 V for $Cu(NTA)^-$ to -1.05 V for Cu(CDTA). No wave is seen for Cu(cydam) (the highest logK* complex), as the complex must be so strong as to mean the complex cannot be reduced even at -1.4 V, compared to a mercury electrode which has a more negative potential range [26].

The experimentally determined shifts in $E_{1/2}$ on the VGME are plotted against previously determined literature values for LogK* to derive a 'chelate scale', shown in figure 3. This has been utilised previously for mercury based electrodes for iron (Fe) [44], Cu [26], Cd [25], Pb [24] and Zn [23]. The 'chelate scale' allows an estimation to be made of the thermodynamic stability constants of unknown metal binding ligands in natural waters, such as copper-organic ligand complexes in seawater samples using the equation:

$$\log K^*_{CuL} = -11.19\ (\pm 1.64)\, E'_{1/2} + 8.95\ (\pm 1.23) \qquad (3)$$

This equation is derived from the operational chelate scale (figure 4) and allows LogK* to be estimated from the half waves of unknown metal-organic ligand complexes in natural samples.

Figure 4 shows the chelate scale constructed from the experimentally derived half wave potential data for Cu with model ligands on the VGME, shown in table 1. Figure 3 also shows similar data

constructed using the hanging mercury drop electrode (HMDE) [26]. The data from the VGME is more scattered, than that derived from the HMDE previously [26], however the reasons for this remain unclear. The modelled trend lines through the experimental data using equation (1) give an α of 0.38 and 0.76, and an $E_{1/2Cu}$ of 0.62 and 0.21 for the VGME and HMDE respectively. This is a positive shift of 400 mV from the expected potentials for $E_{1/2Cu}$ on both electrodes.

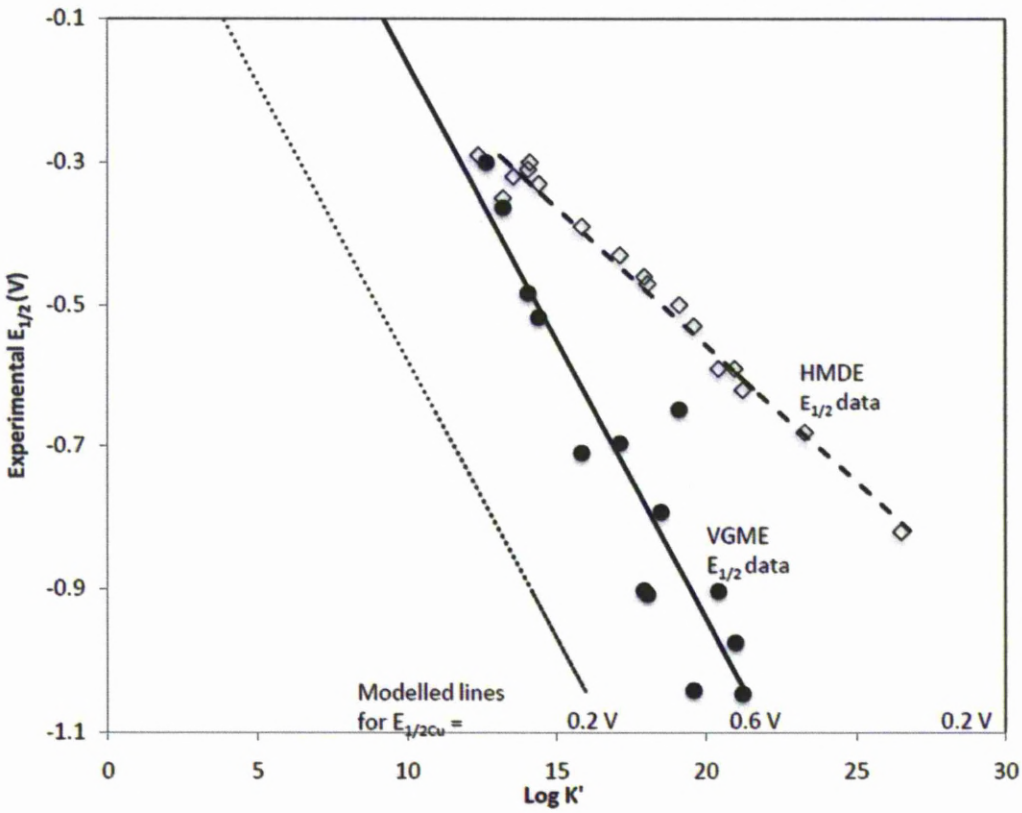

Figure 4. 'Chelate scale' - plot of thermodynamic stability constants, log K' vs. experimentally derived half-wave potentials ($E'_{1/2}$) for the complexation of Cu^{II} in UV digested seawater with selected organic ligands at pH 7.85. Dotted line represents experimentally derived half-wave potentials vs. Log K' calculated using equation (1), where $E_{1/2Cu}$ equals the peak potential for Cu of gold (0.2 V). The full circles are the experimental half wave potentials (derived on the VGME) vs. literature LogK' values, the full trend line represents a modelled line where $E_{1/2Cu}$ = 0.66 V. The empty diamonds are the experimental half wave potentials (derived on the HMDE[26]) vs. literature LogK' values, the dashed trend line represents a modelled line where $E_{1/2Cu}$ = 0.21 V.

Table 1. Experimentally derived half-wave potentials ($E'_{1/2}$) and thermodynamic stability constants for copper-ligand complexes with selected 'model' ligands in seawater at pH 7.85 (10 mM HEPES buffer)

Organic ligand	[L]	Functional group	Log (imax-i/i) vs E (V)	experimental $E'_{1/2}$	literature log K*
UV seawater		Cl_2	0.07	0.03	
NTA(1:1)	5μM	COOH-NH_2	0.07	0.01	12.37
Salicylaldoxime	50 μM	CN(OH)	0.4	-0.30	12.64
Dodecane	100 μM	–NH	0.43	-0.36	13.2
Dopamine	100 μM	–C(OH)–NH2	0.06	-0.48	14.04
DOPA	100 μM	–C(OH)–COOH–NH2	0.14	-0.52	14.4
n-Nonane	10 μM	–NH	0.16	-0.71	15.84
NTA(1:2)	2mM	COOH-NH_2	0.31	-0.70	17.13
EDTA	200 μM	COOH-NH_2	0.46	-0.90	17.94
DMG	500 μM	CN(OH)	0.44	-0.91	18.05
Cysteine	100 μM	–SH	0.27	-0.79	18.5
Nioxime(1:2)	200 μM	CN(OH)	0.09	-0.65	19.11
Ethylenediamine(1:2)	25 μM	NH2	0.37	-1.04	19.6
DTPA	200 μM	COOH-N	0.15	-0.90	20.43
Glutathione	50 μM	–SH	0.24	-0.97	21
CDTA	100 μM	COOH-N	0.21	-1.05	21.24

6.3.17 Scanned stripping voltammetry of Cu and Zn in seawater

Scanned stripping voltammetry was conducted a seawater sample from Liverpool Bay (station 1, March 2010). The sample contained a total Cu concentration of 17 nM and a total zinc concentration of 13 nM. Figure 5A shows the peak potentials of Cu at +0.2 V and Zn at -0.5 V in the same seawater sample after being accumulated for 60 s at -1.4 V.

The shape of the pseudopolarogram for Cu in seawater (figure 5B) shows an initial wave at +0.2 V which corresponds to the free/labile copper species on the VGME. At more negative accumulation potentials two more distinct waves at -0.35 V and -0.8 V can be separated and depend on metal complexes having different thermodynamic stability constants, which can be estimated using the chelate scale to be ~13 and 18 respectively (table 2), before the Cu signal begins to plateau at -1 V.

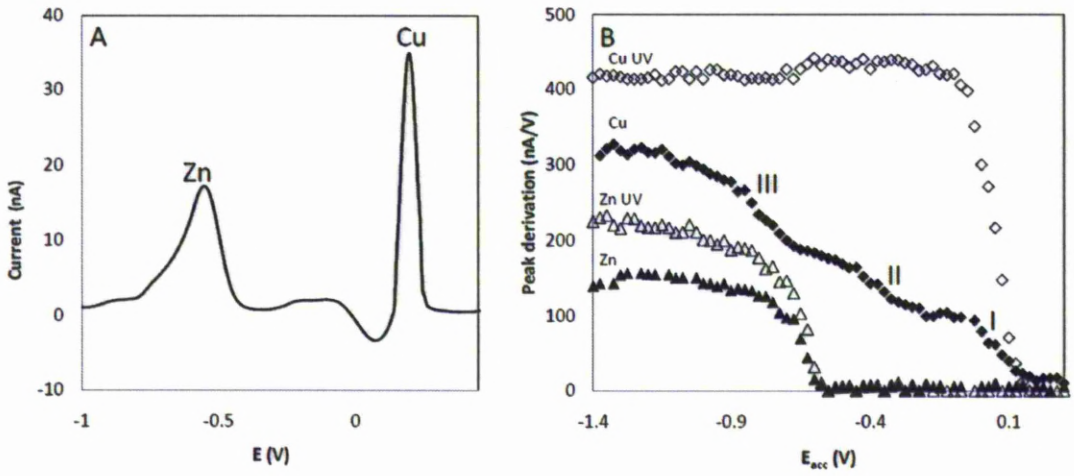

Figure 5. A) Square wave ASV scan in purged seawater (station 1) with 10 mM HEPES, pH 7.85, E_{dep} = -1.4 V, t_{dep}=60 s, E_{des}=-1.2 V, t_{des}=1 s, t_{equ}=2 s. **B)** Pseudopolarograms for Cu and Zn in purged seawater (station 1) with 10 mM HEPES buffer, pH 7.85 before and after UV digestion. Numerals relate to waves for Cu seawater, the half wave potentials for Cu in station 1 are given in table 2.

UV digestion of the sample leads to the redistribution of the organic Cu fraction to inorganic forms and so only the free Cu is present, shown by the large wave at +0.2 V followed by a plateau in Cu signal. It is also worth noting that the maximum Cu signal after UV was 12 % greater than that in the seawater sample, suggesting that accumulation potentials of -1.4 V on the gold electrode were not sufficient to reduce all inert Cu complexes in solution.

SSV of Zn was conducted during the same experiments as those for Cu. In contrast to SSV for Cu, there is only one wave which corresponds to the free/labile Zn at -0.5 V, which is steep and quickly plateaus. After UV digestion the same shaped wave occurs, however with a higher overall intensity.

The potential and half width ($W_{1/2}$) of the peaks as a function of the changing accumulation potential can provide additional information about the sample. The peak potential for both Cu and Zn Shifts towards more negative potentials as the accumulation potential reaches the peak potential, due to strong complexing ligands concentrating at the surface of the electrode [22, 45]. At further negative potentials the relationship is very stable for both metals. $W_{1/2}$ relationship with accumulation potential can indicate two closely overlapped peaks occurring through adsorption processes [41] and so can be of interest. $W_{1/2}$ for Cu was stable at around 70 mV, however for Zn there is a significant

change in $W_{1/2}$ with changing accumulation potentials as the signal increases with potentials more negative than -0.5 V, reaching a plateau at -0.8 V before decreasing again at -1.2 V.

Table 2. $E'_{1/2}$ and log K* values derived from pseudopolarograms for organic Cu species in Irish Sea water using equation (3).

	Wave	$E_{1/2}$	SD ($E_{1/2}$)	LogK*	
Station 1	*I*	0.067	0.003		*labile wave*
(March 2010)	*II*	-0.349	0.004	12.9	
	III	-0.797	0.005	17.9	
	Wave				
Station 27	*I*	0.004	0.002		*labile wave*
(August 2010)	*II*	-0.441	0.001	13.9	
	III	-0.99	0.02	20.0	

6.3.18 On-site analysis of coastal waters Liverpool Bay (Irish sea)

Figure 6 shows three SSV waves of Cu for a seawater sample from Liverpool Bay, UK (August 2010) which was collected and analysed by SSV on-board the Prince Madog. Of the 400 mL unaltered seawater collected, 200 mL was filtered (0.22 µm) and 200 mL was left unfiltered. The unfiltered sample was analysed in the presence of oxygen and its resulting SSV constructed. The filtered sample was then analysed in the presence of oxygen and then after purging with N_2 (g) to remove all oxygen. Only minor variations between waves result from a filtered deoxygenated sample and the same sample analysed without purging or filtration. As expected the bioavailable fraction was shown to be in the dissolved phase. This result shows that the VGME can be utilised for SSV without the need for sample preparation.

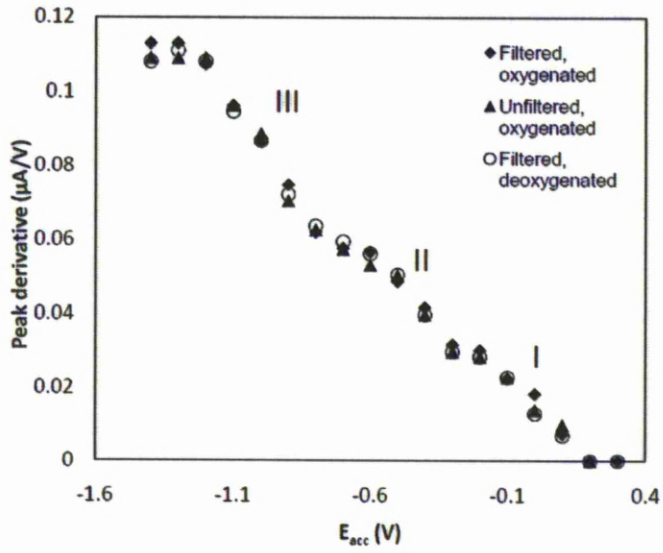

Figure 6. Three pseudopolarograms constructed in unaltered seawater (station 27, Liverpool Bay) on-board the RV Prince Madog: without filtration; after filtration and after filtration and purging. Numerals relate to waves for Cu seawater for the unfiltered, oxygenated pseudopolarogram, the half wave potentials for Cu in station 27 are given in table 2.

Similarly to the sample collected in March (figure 5B), the Sample has three distinct waves (table 2) corresponding to three separate classes of ligand; free + labile Cu complexes shown by wave I ($E_{1/2}$ =0.004 V) and two more strongly bound ligand classes at II ($E_{1/2}$ =-0.44) and III ($E_{1/2}$ =-0.99), using the chelate scale the LogK* of these Cu–ligand complexes is ~14 and 20 respectively. Thus in August although the shape of the pseudopolarogram is the same there could be more strongly binding ligands present. On-site analysis of unaltered seawater in parallel with stability of the electrode and the VGME's ability to measure natural levels indicates the potential of the VGME to perform scanned stripping analysis in-situ.

6.4 Conclusions

Scanned stripping voltammetry was developed and optimised for use for the first time on a solid electrode, the VGME. This is a new sensitive and portable technique for the speciation of Cu and Zn in seawater. The method was optimised and a desorption potential and conditioning interval used to improve the electrodes reproducibility. Model ligands, including EDTA, humic acids and glutathione

were analysed in order to estimate the class of ligands complexing with the Cu in Liverpool Bay using an experimentally derived operational 'chelate scale'. On-site speciation of Cu was successfully carried out in unaltered seawater from Liverpool Bay.

References

[1] W. Stumm, J.J. Morgan, Aquatic chemistry : chemical equilibria and rates in natural waters, Wiley, New York ; Chichester, 1996.
[2] A. Nelson, R.F.C. Mantoura, J Electroanal Chem, 164 (1984) 237.
[3] J.W. Moffett, R.G. Zika, Mar Chem, 13 (1983) 239.
[4] M.F.C. Leal, C.M.G. Van den Berg, Aquat Geochem, 4 (1998) 49.
[5] L.M. Laglera, C.M.G. van den Berg, Mar Chem, 82 (2003) 71.
[6] K.N. Buck, K.W. Bruland, Mar Chem, 96 (2005) 185.
[7] K.W. Bruland, Limnol Oceanogr, 34 (1989) 269.
[8] K.S. Jackson, G.B. Skippen, J Geochem Explor, 10 (1978) 117.
[9] D.A. Hansell, C.A. Carlson, Y. Suzuki, Global Biogeochem Cy, 16 (2002).
[10] J.R. Donat, C.M.G. van den Berg, Abstr Pap Am Chem S, 201 (1991) 44.
[11] T.M. Florence, Analyst, 117 (1992) 551.
[12] C.M.G. Vandenberg, Mar Chem, 15 (1984) 1.
[13] M. Branica, D.M. Novak, S. Bubic, Croat Chem Acta, 49 (1977) 539.
[14] R.M. Town, H.P. van Leeuwen, Croat Chem Acta, 79 (2006) 15.
[15] H.P. van Leeuwen, R.M. Town, J Electroanal Chem, 536 (2002) 129.
[16] H.P. van Leeuwen, R.M. Town, J Electroanal Chem, 523 (2002) 16.
[17] G. Branica, M. Lovric, Electrochim Acta, 42 (1997) 1247.
[18] D. Omanovic, Croat Chem Acta, 79 (2006) 67.
[19] A. Zirino, S.P. Kounaves, Anal Chem, 49 (1977) 56.
[20] M. Lovric, Electroanal, 10 (1998) 1022.
[21] S.P. Kounaves, Anal Chem, 64 (1992) 2998.
[22] I. Pizeta, G. Billon, D. Omanovic, V. Cuculic, C. Garnier, J.C. Fischer, Anal Chim Acta, 551 (2005) 65.
[23] B.L. Lewis, G.W. Luther, H. Lane, T.M. Church, Electroanal, 7 (1995) 166.
[24] T.F. Rozan, G.W. Luther, D. Ridge, S. Robinson, Environ Sci Technol, 37 (2003) 3845.
[25] J.J. Tsang, T.F. Rozan, H. Hsu-Kim, K.M. Mullaugh, G.W. Luther, Environ Sci Technol, 40 (2006) 5388.
[26] P.L. Croot, J.W. Moffett, G.W. Luther, Mar Chem, 67 (1999) 219.
[27] G. Billon, C.M.G. van den Berg, Electroanal, 16 (2004) 1583.
[28] P. Salaun, K. Gibbon-Walsh, C.M.G. van den Berg, Anal Chem, 83 (2011) 3848.
[29] L. Nyholm, G. Wikmark, Anal Chim Acta, 257 (1992) 7.
[30] C.S. Chapman, C.M.G. van den Berg, Electroanal, 19 (2007) 1347.
[31] P. Salaun, C.M.G. van den Berg, Anal Chem, 78 (2006) 5052.
[32] Y. Louis, P. Cmuk, D. Omanovic, C. Garnier, V. Lenoble, S. Mounier, I. Pizeta, Anal Chim Acta, 606 (2008) 37.
[33] G. Scarano, E. Bramanti, Anal Chim Acta, 277 (1993) 137.
[34] P. Salaun, B. Planer-Friedrich, C.M.G. van den Berg, Anal Chim Acta, 585 (2007) 312.
[35] D. Omanovic, M. Branica, J Electroanal Chem, 543 (2003) 83.
[36] D.R. Turner, M.S. Varney, M. Whitfield, R.F.C. Mantoura, J.P. Riley, Sci Total Environ, 60 (1987) 17.
[37] M.S. Shuman, J.L. Cromer, Anal Chem, 51 (1979) 1546.
[38] Y. Bonfil, M. Brand, E. Kirowa-Eisner, Anal Chim Acta, 387 (1999) 85.
[39] D.G. Leaist, L. Hao, J Chem Soc Faraday T, 90 (1994) 133.
[40] D. Omanovic, M. Branica, J Electroanal Chem, 565 (2004) 37.
[41] R. Nicolau, Y. Louis, D. Omanovic, C. Garnier, S. Mounier, I. Pizeta, Anal Chim Acta, 618 (2008) 35.
[42] M.B. Kogut, B.M. Voelker, Environ Sci Technol, 35 (2001) 1149.

[43] C.L. Chakrabarti, P. Chakraborty, I.I. Fasfous, J. Murimboh, Anal Bioanal Chem, 388 (2007) 463.

[44] B.L. Lewis, P.D. Holt, S.W. Taylor, S.W. Wilhelm, C.G. Trick, A. Butler, G.W. Luther, Mar Chem, 50 (1995) 179.

[45] R.M. Town, M. Filella, J Electroanal Chem, 488 (2000) 1.

7

Chapter 7
GENERAL CONCLUSIONS & FUTURE PERSPECTIVES

7. GENERAL CONCLUSIONS AND FUTURE PERSPECTIVES

This thesis has achieved many of its initial motivations through the continued development of the vibrating gold microwire electrode (VGME); a sensitive solid electrode alternative to the hanging mercury drop electrode (HMDE) for trace element speciation. As well as not having to work with a very toxic mercury electrode material, it has a number of other important advantages:

1. the relatively easy application for on-site analysis;
2. An improved sensitivity for Cu;
3. The potential to measure As;
4. It is Cheap and relatively easy to prepare and maintain.

The VGME is used to analyse the speciation of several metals (Cu, Mn and Zn) and the metalloid (As) in natural waters at unaltered trace concentrations (nM) with very good sensitivity due to its small diffusion layer (~0.8 µm for a 5 µm gold wire). This also allows access to a different kinetic window from many comparable dynamic techniques, such as the HMDE and the diffusion gradients in thin-film gels (DGT). So in collaboration with such techniques this could help to give a greater understanding of the speciation and thus the potentially bioavailable fraction of an element. The comparison of the VGME to similar dynamic speciation techniques could be interesting. Keeping in mind, which organisms may equate to which technique, based on the similarities in the diffusion layer thickness. For example a direct comparison could be made between scanned stripping techniques on the VGME and the HMDE. In this example, one could expect to observe a larger labile fraction on the HMDE due to its larger diffusion layer, whilst also seeing some of the stronger metal-organic ligand complexes.

Another advancement made during this work was the simple implementation of detachable tips, which made for a very rapid preparation time (minutes) for each new electrode (allowing each one to be easily tested). The detachable tips also give the potential to attach varied electrode materials (as a wire or a disk for example) to the vibrating device very easily. This could be of interest to

determine cadmium and lead, for example in natural waters using a mercury film electrode, as these metals are not easily resolved from one another using the VGME. The detachable tip has also proved to be very useful in the field; where due to circumstances (unknown matrix, equipment failure) electrodes (pseudo reference, working or counter) may be lost, therefore replacing the need to bring heavy cables with just a small box of detachable electrodes.

Methods developed for speciation of As in the groundwaters of West Bengal and As, Zn, Mn and Cu in seawater have all been measured on-site in real water samples. This is possible due to the minimal reagents necessary for each speciation method (EDTA was required in the groundwaters of West Bengal due to the high Fe and Mn concentrations present and Mn was required to measure As^{V} at neutral pH) and the portability of the voltammetric system. This is preferential as it maintains as much of the original speciation as possible. The idea of working on-site with a solid electrode and minimal reagents I expect will be explored much further in the future. I believe (due to the preliminary results collected over previous years) that the VGME is applicable for in-situ analysis and this could allow it to be used to study changes in an aquatic systems trace element speciation through long term monitoring although further work is necessary for the in-situ removal of oxygen interference.

In-situ analysis could be of particular use to measure As in the groundwaters of West Bengal, where reactive As^{III} seems to be the dominant species, due to reductive conditions. However West Bengal is still only one of many regions all over the world that suffers from As pollution. Therefore the VGME could also be used to assess other As release mechanisms. for example in Argentina where the groundwaters are predominantly oxidizing (therefore predominantly As^{V}) with low dissolved Fe and Mn concentrations and high alkalinity, although no doubt there will be new interferences to overcome in such cases. It is my hope that portable systems such as the VGME could be found to be reliable enough to be simply operated by indigenous, non experts to give a reading of their local drinking water supply for pollutants, such as As or Mn to aid the overall mitigation process.

The material problems facing solid electrodes, such as stability and reproducibility were addressed and can be illuminated best by the use of the VGME for scanned stripping voltammetry (SSV). SSV shows the signal stability and the reproducibility of the VGME over a large number of scans due to the introduction of an in-situ conditioning interal and a desorption potential. Surface fouling over longer periods is an issue that will become more apparent only with further testing of the VGME in-situ.

The VGME should of course also be capable of trace element speciation in many samples other than the natural waters samples in this thesis. I'm sure it would be of interest to the food industry, who must meet regulations for many trace elements, which could be sensitively determined using this approach.

Overall I feel that the VGME is a powerful electroanalytical tool with the capability to become a useful and important part of many electrochemists arsenal of analytical techniques.

ANNEX

ANNEX I. Detailed fabrication of the VGME

The vibrating gold microwire electrode consists of a microwire electrode sealed in a pipette tip, which can then be attached and detached to a vibrating device. Together they take no more than 5 minutes to make and are inexpensive and robust.

To fabricate the attachable microwire electrodes of 5, 10 or 25 µm (figure IA):

1) 5 cm length of 100 µm copper wire is passed through a clear 200 µL pipette tip (polyethylene, fisher scientific, UK). The end of the Cu wire is then dipped in a conductive silver resin (Leitsilber L100, Maplin, UK), which had been freshly agitated and acted as conductive adhesive used to create a conection between the gold microwire and Cu wire. The copper wire is attached to a 0.5 cm length of gold microwire by gently touching them flat on a clean white piece of paper (be careful with direction of breathing at this point). The copper wire is then carefully pulled through the pipette tip until the Au microwire and Cu wire connection is at the tip of the pipette.
2) The microwire and the Cu wire are sealed together in the tip by holding it for several seconds in the top of the oven (400 °C), this may need to be repeated, make sure that the seal is complete (figure IB). The Cu wire must be well sealed so that the electrode can be detached from the vibrator without losing its source of electrical contact (figure IA).

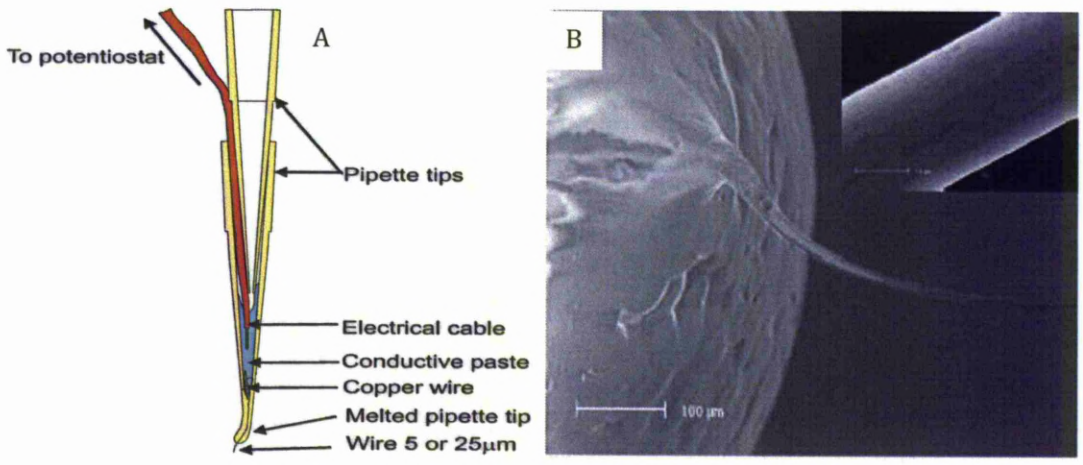

Figure I. (A) microwire electrode, (B) SEM of melted pipette tip with sealed gold wire.

To fabricate the vibrating section of the VGME:

1) The microelectrode can then be fitted onto a 1 mL polypropylene pipette tip with a 1 cm length of connecting electrical cable protruding at the bottom, which makes contact with the microwire electrode shown in figure 1A.
2) The vibrator is incorporated at the top of the 1 mL pipette tip and is driven by a 1.5 V power supply (home-built converter of 5 V to 1.5 V), which is interfaced to, and powered by, the IME (Autolab, Metrohm, Switzerland), and controlled by the stirrer on/off trigger in the software interface (GPES, Autolab).

The main advantage of such a system with a detachable microwire electrode is that the time taken to test electrodes is greatly reduced as they can be so easily replaced if they do not work optimally and reattached if testing with a number of electrodes.

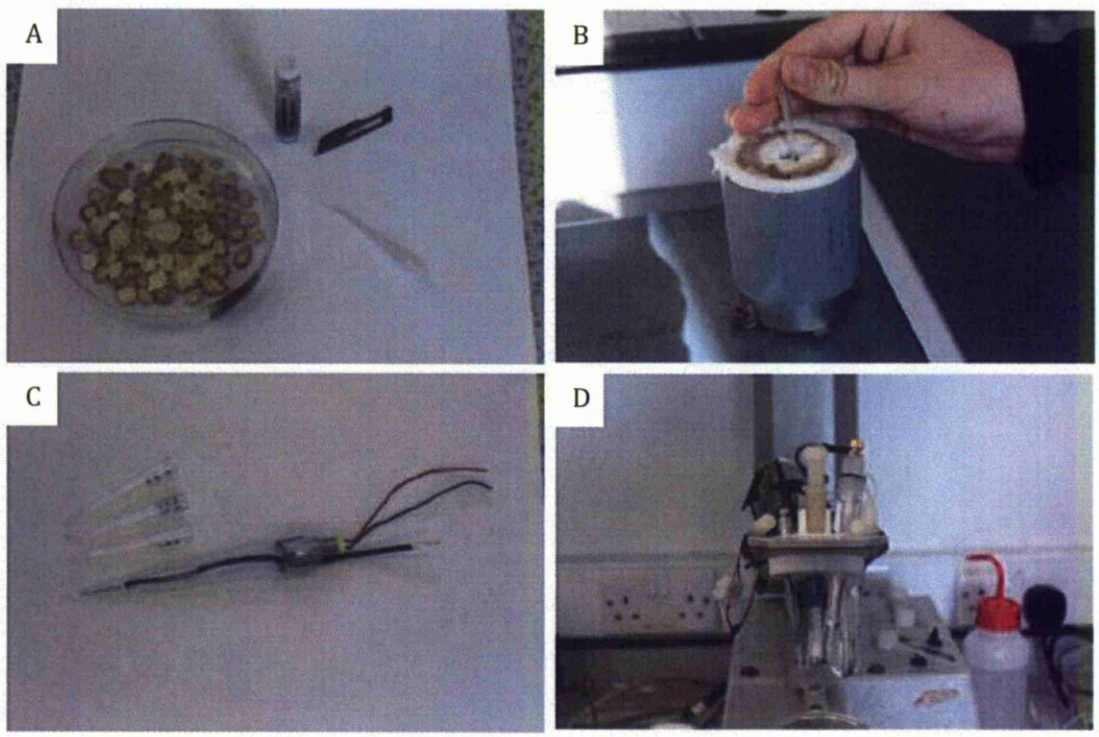

Figure II. (A) Attaching the Cu wire to Au microwire electrode with silver epoxy (B) Sealing Au and Cu connection in pipette tip (C) VGME with replaceable microwire electrodes (D) Voltammetric cell setup.

ANNEX II. Electrode conditioning and measurement of the electrode surface area.

Figure III shows a typical cydic voltammogram of a 5 µm gold electrode in 0.5 M H_2SO_4. The gold is oxidized at potentials of >0.9 V and the oxidation current reaches a maximum at 1.11 V (point A) and then went through a minimum at 1.36 V (point B) before increasing again due to further oxidation of the gold and possible evolution of oxygen[1]. On the reverse, cathodic scan, the peak (C) corresponds to the reduction of the previously formed gold oxide. The anodic peak (at A) is known to depend on the solution composition and on the crystallographic properties of the gold, and the minimum (B) is thought to indicate the completion of monolayer coverage of the gold surface with oxide[2].

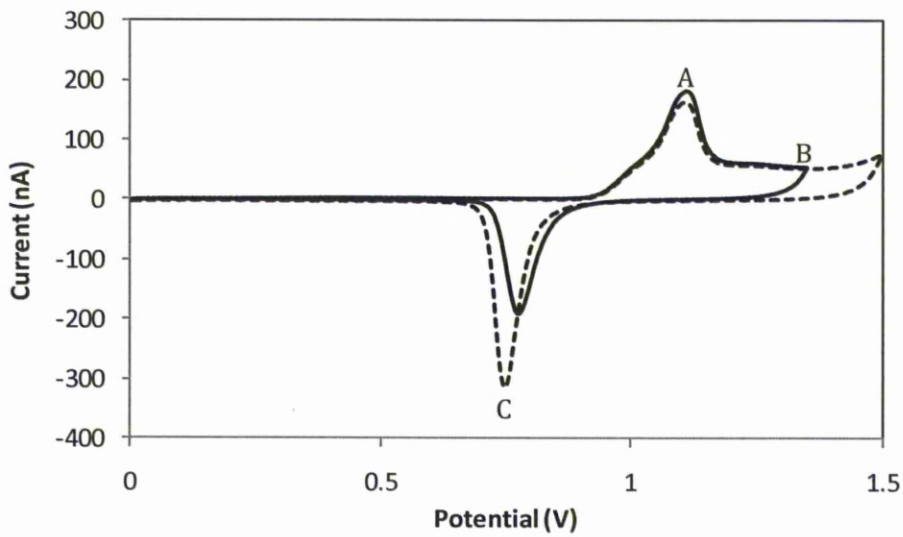

Figure III. Cyclic voltammogram in 0.5 M H_2SO_4 between 0 V and E_a, scan rate 10 mV/s. E_a = 1.36 V (solid line) and E_a = 1.45 V (dashed line); (A–C) see text.

The area of peak C gives a charge, this charge taken from the reduction peak of the completion of monolayer coverage of the gold surface with oxide (solid line, figure III) at 1.36 V corresponds to the real surface area of the electrode taking into account the electrodes roughness. This can indicate the electrodes stability over time if determined regularly.

The effect of prolonged and repeated anodic polarization of a gold electrode is apparent in SEM pictures of a 25 µm wire before (A) and after (B) one week of intensive use in 0.6 M NaCl, where a conditioning potential of 0.85 V was applied for each measurement (Figure IV). In agreement with the low roughness value, the gold surface was smooth before use. After use, the diameter had decreased to 16 µm, and the roughness had increased. Care should therefore be taken in the choice of the conditioning potentials, especially in chloride media where the oxidation of gold starts at lower potentials due to the formation of gold chloride complexes. In some conditions, the gold chloride species can also precipitate, leading to a partial or complete blocking of the electrode[1].

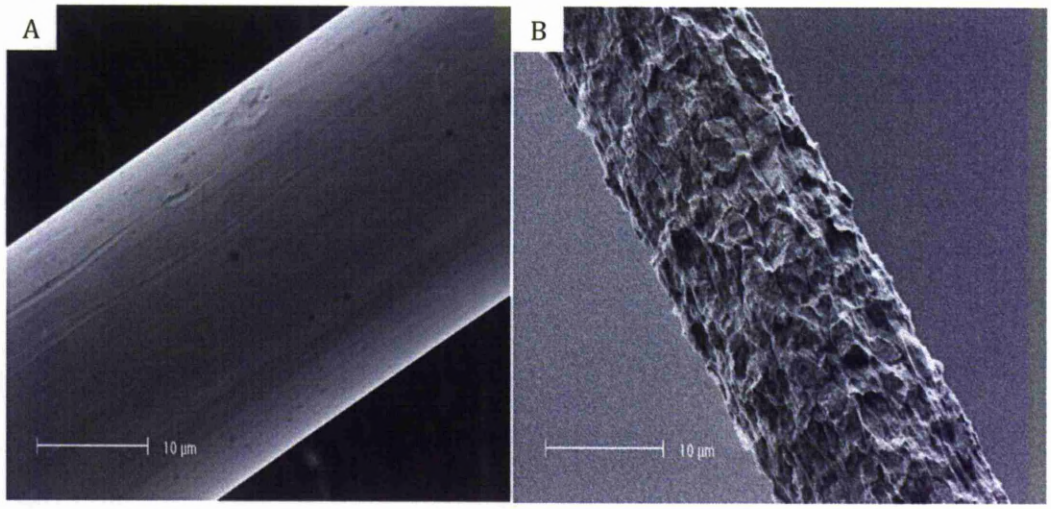

Figure IV. A) SEM pictures of a 25-µm gold wire before use **B)** and after 1 week of intensive use with a high, oxidizing, conditioning potential (0.9 V in 0.6 M NaCl) (right).

Annex III. Current density and diffusion layer thickness at microwire electrodes.

The theoretical diffusion-limited current density at a microwire electrode of length *l* and radius r° ($l \gg r^\circ$ so that end effects are negligible) is given by equation 1:

$$I(t) = 2\pi n l F D C_b \left\{ \frac{e^{-0.1\sqrt{\frac{\pi Dt}{r^2}}}}{\sqrt{\frac{\pi Dt}{r^2}}} + \left[\ln\left(5.2945 + 1.4986\sqrt{\frac{\pi Dt}{r^2}} \right) \right]^{-1} \right\} \quad (1)$$

Where n is the number of electrons involved, F is the Faraday constant (96,500 $C.mol^{-1}$), D is the diffusion coefficient ($cm^2.s^{-1}$), t is the electrolysis time (s), and C_b is the bulk concentration ($mol.cm^{-3}$).

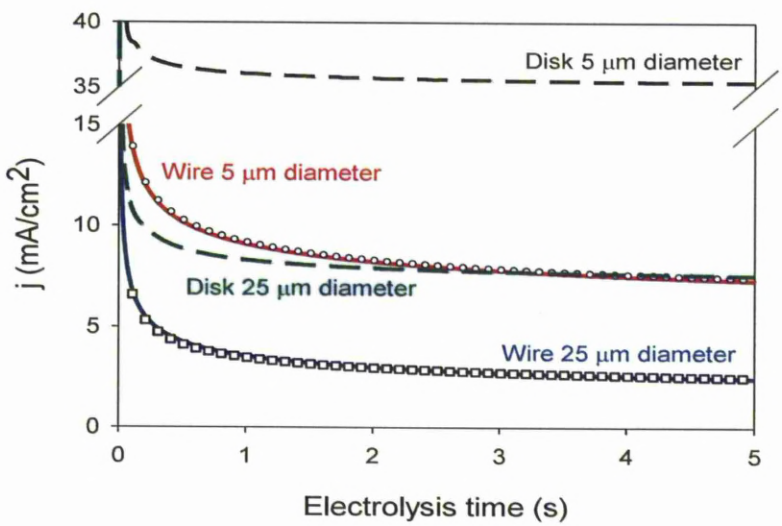

Figure V. Diffusion-limited current density as a function of the electrolysis time. Comparison of experiment and theory for wire and disk microelectrodes.

Figure V shows the experimental diffusion limited current density determined in a 10 mM ferrous cyanide solution ($Fe(CN)_6^{3-}$) also containing 0.5 M KCl for 5 and 25 μm diameter microwire electrodes as a function of time and the theoretical diffusion-limited current density calculated using equation 1. In this medium, the diffusion coefficient of $Fe(CN)_6^{3-}$ is 7.17 $cm^2\ s^{-1}$. The diameter of the wire used was that given by the manufacturer and was the same as that measured by SEM.

Wire lengths can be determined from the variation of the diffusion-limited current within the first 5 s (Figure 3) and calculated using equation 1.

Experimental data are shown as data points (circle and square) and the theoretical data as a solid line (microwire) or dashed line (disk) for the first 5 s. Experimental parameters: electrodes of 5- and 25-µm diameter; 10 mM $K_3Fe(CN)_6$ in 0.5 M KCl. $D = 7.17\ 10^{-6}$ $cm^2 \cdot s^{-1}$ and $E = -0.3$ V.

ANNEX IV. A typical seawater scan by square wave voltammetry and the need for background subtraction

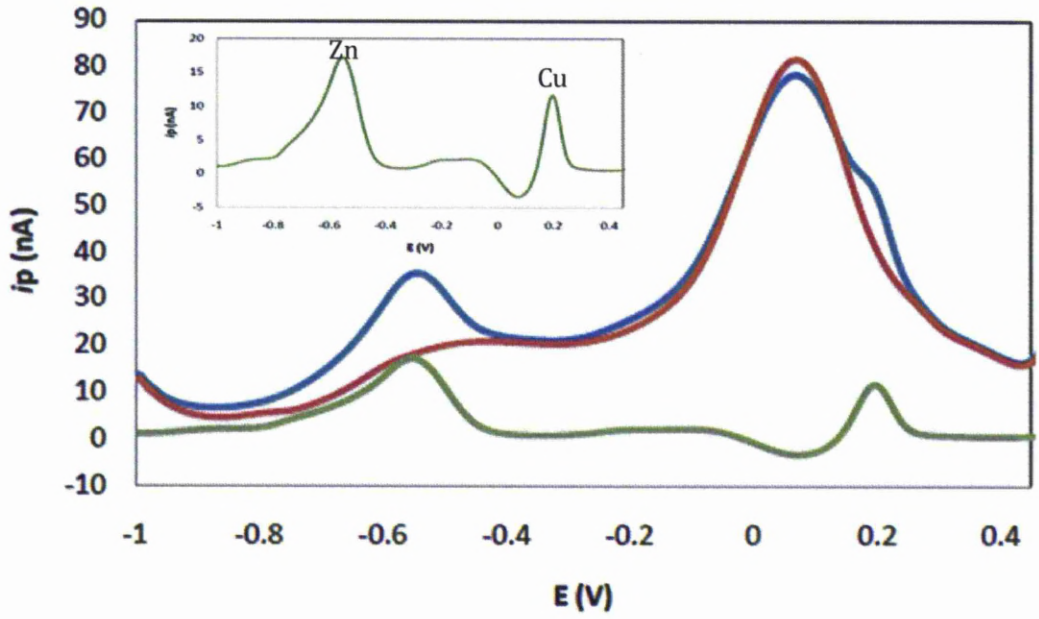

Figure VI. Analytical (blue), background (red) and subtracted (green) scans in typical seawater sample containing 15 nM Cu and 20 nM Zn, inset shows background subtraction of a seawater sample.

Analytical scan parameters: E_{dep}=-1.2 V, t_{dep}= 61 s, E_{des}=-1 V, t_{des}=1 s, scan -1 to 0.5 V, f=50Hz, Amp=25 mV, step=4 mV.

Background scan parameters: E_{dep}=-1.2 V, t_{dep}= 1 s, E_{des}=-1 V, t_{des}=1 s, scan -1 to 0.5 V, f=50Hz, Amp=25 mV, step=4 mV.

Background subtraction is required when using the VGME in seawater. Figure I shows a typical square wave anodic stripping voltammetric (SWASV) scan in a purged (oxygen wave would be seen between -0.8 V and -0.2 V) seawater sample. In the analytical scan (blue line) the copper peak occurs on the shoulder of the halide wave between -0.2 V and +0.2 V in seawater. Arsenic if present on this scan would occur on the negative shoulder of the halide wave and so also benefit from background subtraction. Background subtraction can be automated using the autolab and Palmsens software interface.

ANNEX V. Nalgene bottle sterilization procedure and clean working for trace metal work

In laboratory

1. Soak bottles in soapy hot tap water (for new bottles and unknown samples) for 1 week. Afterwards empty the bottles and rinse thoroughly with milli-Q water (MQ) 5 times or until no soap residue remains. Skip this step if the bottles are pre-used for seawater sampling.
2. Wearing full safety protection (Goggles, gloves and labcoat) transfer the bottles to a 0.5 M HCl solution in a large polyethylene container and leave to soak for 1 week.
3. Empty the bottles back into the container and transfers to a 0.1 M HCl bath (wearing full protective gear) and leave to soak for 1 week. After which (wearing polyethylene gloves), empty the bottles and rinse thoroughly with MQ 3 times.
4. Leave the bottles to stand in clean pH 2 acid and MQ water until transport, (use polyethylene gloves and avoid the neck of the bottle) and seal the bottles in individual polyethylene bags and then 4 into a larger sealed polyethylene bag.
5. *Before transport* empty the bottle until only a small amount (50 mL of clean acid solution remains) and reseal them in their bags *making sure to use* polyethylene gloves and avoid the neck of the bottle.

Onboard/on-site

1. Deploy acid cleaned Niskin bottle without trigger to condition it to the seawater.
2. After collecting seawater sample in the Niskin bottle, pump any remaining seawater from the tubing. Then allow seawater to run through the tubing then add the filter and allow seawater to run though filter also.
3. Rinse the Nalgene bottles with the filtered sea water sample for collection 3 times under fumehood.
4. Collect sample leaving enough room for freezing capacity (2/3 full) and re-seal in two well labelled bags (label with sample preparation, date and location).

References

[1] P. Salaun, C.M.G. van den Berg, Anal Chem, 78 (2006) 5052.
[2] U. Oesch, J. Janata, Electrochim Acta, 28 (1983) 1237.